Plant-fungus interactions and their implications for nutrient cycling and biomass growth:

Insights from modelling arbuscular mycorrhizal fungi in a heterogeneous environment

**Dissertation zur Erlangung des
Doktorgrades der Naturwissenschaften (Dr. rer. nat.)
am Fachbereich Mathematik und Informatik der Universität Osnabrück**

vorgelegt von Joachim Ulrich Kleinmann

aus Tübingen

Osnabrück 2016

Für meine Kinder

Abstract

A continuously growing world population with a projected size of more than 9 billion inhabitants in the year 2040 requires huge efforts in food production while concurrently avoiding adverse side effects such as the use of pesticides or fertilizers. Among them phosphorus (P) is an important mineral fertilizer for which only few renewable sources exist and which is becoming increasingly scarce. Therefore, methods to reduce P fertilization or enhance fertilization efficiency are urgently needed. One idea is to look how plants in natural ecosystems cope with the problem of nutrient limitation. A strategy, found in almost all plant species is interaction with mycorrhizal fungi. Plants usually deliver carbohydrates (C) to the fungi and get nutrients, like phosphorus (P), in exchange. In natural ecosystems, plants usually interact with multiple fungi, which perform differently in their P delivery.

However, in agro-ecosystems not all these fungi are helpful. Fungi which are carbon demanding but deliver just few P, might even result in lower plant growth. Therefore a deep knowledge of the mechanisms driving the P and C dynamics is necessary. This can be gained by a computer simulation model, which is possible to examine the influence of different nutrient exchange strategies in detail and make prediction how they perform.

In this PhD thesis, a spatially explicit simulation model of arbuscular mycorrhizal fungi (AMF) was developed and specific laboratory experiments have been conducted and used for model calibration. This model has been used to evaluate the performance of different nutrient exchange strategies by the emerging maximum achievable fungal biomass, the C uptake rate from the plant and the P delivery rate to the plant. On this basis, three functional types could be identified: parasitic type, intermediate type, mutualistic type.

In further steps these functional types have been used to investigate their performance to smooth temporal P pulses (i.e., by transforming them into a continuous P flux delivered to the plant) and to take up spatially heterogeneously distributed P. In both cases, the mutualistic type was found to perform worst and parasitic type best. Two key mechanisms for efficient resource use in spatiotemporally heterogeneous environments could be identified. By the ability of quick fungal biomass growth, AMF can efficiently explore space and store P inside the fungal mycelium. By the creation of spores that do not need C for

maintenance, AMF can use the saved C to grow new hypha for further spatial exploration. Through these two mechanisms AMF are able to adapt their mycelium to the spatial and temporal conditions of the P distribution and thus have the potential to largely enhance P-use efficiency. This finally might reduce the application of P fertilizers.

Contents

Chapter 1: General Introduction

1.1 Phosphorus scarcity as a global problem

A projected world population of more than 9 billion humans in 2040 (UN Populations division 2015) retrieves a huge challenge for agriculturalists to produce enough food for this population. This challenge has been faced in the past decades, by mechanization of agriculture. Since this 'green revolution' in the 1960s, agricultural yields are less receptive of soil, crop rotation and weather, but very much depend on the use of fertilizers, plant protection products and soil cultivation. This led to a strong dependency of agriculture on mineral and organic fertilizer. While organic fertilizers tend to eutophicate ground- and surface waters because of their excess supply from livestock breeding, mineral fertilizers are often rare. Phosphorus (P) as a mineral fertilizer e.g. is mostly a mined product for which merely few renewable sources exist and which is becoming increasingly scarce. Therefore, methods to reduce P fertilization are crucially needed (Cordell et al. 2009). Only about 45% of all applied P fertilizers are nowadays taken up by their intended plants (Tilman et al. 2002). This implies a large potential for efficiency improvement.

This means, the 'green revolution' is urgently needed to be further developed to keep pace with population growth and produce food for more and more humans. Additionally, possibilities to reduce the impact of agriculture on nature and to improve the efficiency of mineral fertilizers like P are needed.

Since P is not only a important and scarce nutrient in intensive agriculture, but also in natural ecosystems, natural mitigation strategies to cope with limiting nutrient availability suggest itself as strategy to investigate. One strategy, found in almost all plant families, is concentrated in the term mycorrhiza.

1.2 Mycorrhiza as a natural key factor to cope with nutrient scarcity

Mycorrhiza are one of the most common and important symbioses between two species of different taxonomic kingdoms: plants and fungi. Mycorrhizal fungi and the roots of vascular plants interact in this symbiosis in a way that is beneficial for both partners. Fungi deliver

inorganic nutrients like phosphorus (P), nitrogen (N), potassium (K) sulfur (S), calcium (Ca), iron (Fe), copper (Cu) and zinc (ZN) to the plant and gain carbohydrates, mainly glucose and sucrose in exchange (Smith and Read 2008, Marschner, 2012). Plants benefit, as the fungal mycelium has very thin and flexible hyphae, which can quickly respond to nutrient changes. Furthermore, there is some evidence that plants are protected from toxicants, diseases and droughts by the symbiotic fungi (Newsham et al. 1995). Fungi profit, because they can use photosynthetic products of the plant without investing themselves in green tissue for photosynthesis.

There are two generally different forms of mycorrhiza: endo- and ectomycorrhiza. While in ectomycorrhiza, the nutrient exchange takes place in the extracellular space, and fungi do not penetrate individual cells, endomycorrhizal fungi grow directly into cell walls of plant roots for nutrient exchange (Moore et al. 2011). Endomycorrhiza can be further divided into ericoid, orchid and arbuscular mycorrhiza. Like the name says, ericoid and orchid mycorrhizae are specialized to ericaceae and orchids, respectively. However, arbuscular mycorrhiza can be found in a large variety of plants, i.e. about 80 % of all vascular plant families, among which are several crop species (e.g. wheat (*Tritium aestivum*), barley (*Horteum vulgare*), etc.) are known to build arbuscular mycorrhiza (Moore et al. 2011).

Arbuscular mycorrhizal fungi (AMF) belong to the very old phylum of Glomeromycota (Schüßler et al. 2001). Molecular techniques gave evidence that arbuscular mycorrhiza originated at least 400 Million years ago and played a crucial role in the land colonization of plants (Wang and Qiu, 2006). In this symbiosis, fungi penetrate the parenchyma cortex of plant cells and build highly branched structures, called arbuscules, which are relevant for the nutrient exchange between the plant and the fungus and gave the name to this type of mycorrhiza (Moore et al. 2011).

The extraradical mycelium of AMF shows some more characteristic morphologic preferences. Runner hyphae are fast growing, long hyphae, which are mainly relevant for intracellular nutrient transport (Friese and Allen 1991). Minerals are transported into the direction of the plant roots, carbohydrates are distributed in the whole mycelium. From this runner hyphae, highly branched, tree like structures branch off. These branched absorbing structures (BAS) are relevant for the uptake of nutrients from soil (Bago et al. 1998). If they are not used anymore, because of e.g. nutrient depletions in the surrounding soil, spores are

built at those BAS before they are detached from the corresponding runner hypha (Bago et al. 1998). AMF are obligate symbionts, which means, with no other energy source, they depend on photosynthesis products of their plant partners (Moore et al. 2011). This led to many research projects addressing the type of this symbiosis and the mycorrhizal growth response (MGR) to plants (e.g. Hetrick et al. 1992, 1996, Ravnskov and Jakobsen 1995, Graham and Abbot 2000, Li et al. 2008).

1.3 Type of interaction between plant and mycorrhiza and implications on the C-P dynamics

There is a large and ongoing discourse about the question whether the interaction between AMF and plants is always a mutualistic symbiosis or whether AMF can be seen as parasites in some cases (see Feddermann et al. 2010). Evidence for a mutualistic interaction was found by Marschner and Dell (1994) when they determined the phosphorus (P) depletion zone around mycorrhized and non-mycorrhized plants. Since P is very immobile in soil, P depletion zones form around root hairs and root P uptake quickly declines over time. For non-mycorrhized roots, this depletion zone was strongly related to root length, however, for mycorrhized roots, the depletion zone largely exceeded root distribution. However, it was also possible to construct conditions under which mycorrhized plants developed worse than plants without AMF that means the costs exceeded the plants benefits. Additionally, different strains of AMF were found to perform better in nutrient delivery than others (Johnson et al. 1997, Jansa et al. 2005, Avio et al. 2006). Since there is evidence that AMF and plants work together since the land colonization of plants, it seems clear that AMF are no pure parasites. Furthermore, Eckardt (2005) discovered that plants prepare for colonization when they sense AMF. This means plants play a key role in the infection process (Bucher 2007). More recent studies also found evidence that even though AMF penetrate host cells, plants have mechanisms to adapt their carbohydrate deliveries to the fungus to the amount of arriving fungal nutrients (Steward et al. 2006). Since a significant proportion of photosynthetically produced carbon is delivered from the plant to the fungus (Jakobsen and Rosendahl 1990, Wright et al. 1998) plants would suffer largely from an omnipresent parasite. This carbon delivery to AMF results in a carbon sink in the plants roots. The

strength of this sink determines the carbon production by photosynthesis and enlarges the plants photosynthetically active organs (Wright et al. 1998.). Plants can influence the strength of this sink by allowing a higher or lower degree of colonization depending on their nutrient and status (Burleigh et al. 2002, Smith et al. 2003) and their carbon production capacity (Johnson et al. 1997). This means, plants allow a larger colonization when nutrient availability is poor, but reduce fungal colonization under limiting light conditions to save carbon. However, Bücking and Shachar-Hill (2005) found that the uptake of P by the fungus from soil and its transfer to the plant is stimulated by the plants C supply. This means both partners have methods to limit their deliveries to their partner.

To completely understand this interaction between plants and AMF and solve the question of parasitism or mutualism and its consequences for AMF growth and the coupled P-C-dynamics, the mechanisms driving nutrient exchange need to be completely understood. With this understanding, the functional consequences of such plant-fungus interactions for natural ecosystems can be investigated. In particular, it is unclear how different (mutualistic or parasitic) nutrient exchange strategies impact the dynamics of fungal biomass growth and the nutrient fluxes of P and C in a spatially and temporally variable environment. Can AMF increase the efficiency of resource use for the plant? Can AMF attenuate or even equalize spatiotemporal resource pulses and turn them into a steady flow to their plant partners? Could these fungi even prevent nutrient leaching into groundwater by quickly taking up resource pulses in a way in which they are no more subject to water percolation? Looking on the use in agricultural processes, in conventional agriculture, common soil cultivation prevents the development of a healthy soil micro flora such that AMF usually play nowadays a minor role (Gosling et al 2006). In organic agriculture, however, there are methods to cultivate AMF and use them to reduce fertilization (Gosling et al. 2006). This means even for agricultural systems these results can be very relevant. A primary question would be whether AMF can help crops to exploit spatially heterogeneously distributed soil nutrient resources more efficiently? If yes, is it possible to group AMF into different functional types to typify and establish an optimal fungal fauna for crop fertilization? The grouping of species into functional types is common in ecological literature (see e.g. Köhler et al. 2000, Picard et al. 2012, Kazmierczak et al. 2015), because it allows to break down the vast number of species into a small number of groups sharing a common feature which is under

investigation. This means, the identification of functional types could be a starting point to find an optimal fungal fauna for a specific habitat and to investigate the different C-P dynamics resulting from these functional types.

However, for functional grouping of AMF, a deeper understanding of the complex mechanisms driving the plant-fungus interaction is necessary. Uptake, transport and exchange of different nutrients (e.g., P and C) between two species (e.g., AMF and plants) exhibit a complex system of many coupled processes and addresses two mayor disciplines of ecological research: community ecology, which deals with biodiversity and interspecific interactions and ecosystem ecology, which deals with material and energy flows in and between systems. In the AMF-plant system, community ecology focuses on the growth and performance of fungi and plants, their type of interaction and why there are different fungal strains performing differently in nutrient delivery. Ecosystem ecology, however, studies the uptake and transport of nutrients and their exchange, without a detailed look on the differently performing species governing these processes. Merging of these two disciplines was proposed by Loreau (2010) and characterized as one major challenge of ecological research. It requires combining knowledge, theories and processes of both disciplines resulting in a highly complex interdisciplinary framework. The large number and different types of processes interacting with each other make it difficult or even impossible to draw valid conclusions for the emerging structural and functional dynamics and the potential impacts on natural and agricultural systems, without using a simulation model.

1.4 AMF Modelling

Few models for the simulation of fungal growth and even less for AMF exist. In existing models fungal growth usually depends only on carbohydrates and the extraradical mycelium of AMF is usually not modelled spatially explicitly but as hyphae density. First simulation models for fungal growth came up in 1979 by Prosser and Trinci with their model for hyphal growth and branching. This model was very simple but fungal growth was artificial and did not depend on nutrients. Boswell et al. (2003) developed a more complex model of fungal growth. In this model, fungal growth depended on nutrients, which had to be taken up from the surrounding medium. However, hypha were not modelled spatially explicitly but as

hypha density. In 2007, they extended their model to simulate fungal growth in complex environments and included spatially explicit growth of fungal hypha. However, they did not simulate AMF and considered only two spatial dimensions. A third dimension in modelling of fungal growth was introduced by Meskauskas et al. (2004). This model was very flexible in building different fungal types, but did not include internal transport of nutrients and was not suitable for AMF. A further spatially explicit three-dimensional model for fungal growth was developed by Knudsen et al. (2006). They included nutrient transport in the hypha, but did not consider AMF. A first model to simulate AMF was developed by Schnepf et al. (2008). However, they did not consider nutrient exchange between fungi and plants or transport in the hypha and used density distributions for fungal mycelium. In a following study (Schnepf et al. 2011), they developed a mathematical model to simulate nutrient uptake by a single hypha in soil. All these models address interesting questions and help to get further understanding of fungi in general and AMF in special, but cannot fully address the questions described above.

1.5 This PhD thesis

We therefore developed a spatially explicit simulation model, which simulates fungal growth in three spatial dimensions depending on the availability of carbohydrates and phosphorus. Whereas fungi are able to take up phosphorus by themselves, they can only access carbohydrates in exchange for phosphorus at the plant-fungus-interface. Thus, plant and fungus interact in the simulation model via nutrient exchange with implications for biomass growth and nutrient cycling.

The development of the model and this whole PhD thesis took place in a cooperation project of two different disciplines: laboratory work and ecological modelling. Laboratory studies were conducted by our cooperation partner (T. Fester) to quantify the C and P dynamics resulting from the interplay of plant root and AMF in a petri dish experiment. The results of these experiments have been used to parameterize the nutrient processes in the simulation model.

The PhD thesis is divided into 6 Chapters. After this General Introduction, Chapter 2 is dedicated to the development of the model, the detailed explanation of the laboratory

experiments and the parameterization of the model. In Chapter 3 to 5, the model is applied to answer three important questions on the AMF-mediated plant-fungus interactions and their implications for AMF growth and the coupled C- and P-dynamics. Chapter 3 investigates the biomass growth of AMF and the related nutrient dynamics as a function of the nutrient (P and C) exchange strategy between AMF and plant. From these dynamics, characteristics to grouping AMF into different functional types are identified, and how these types influence the C- and P-dynamics emerging from the interplay of AMF and plants. Chapter 4 relaxes the assumption of homogenous environments and uses the different AMF functional types to address their ability to equalize the impacts of P-pulses. Here, AMF growth is simulated under temporally varying nutrient conditions and it is investigated whether, and under which conditions the individual AMF functional types are able to utilize P-pulses and transform them into a steady flow to the plant. Mechanisms for equalizing P-pulses by AMF are identified. Chapter 5 investigates how AMF can exploit P-sources in spatially heterogeneous environments. It studies which functional types perform best under different spatially heterogeneous P- distributions and finite diffusion rate of nutrients and in which scenarios plants can profit from AMF. Mechanisms for efficient spatial resource use by AMF are identified. The thesis finishes with Chapter 6 that synthesizes the outcomes of the different chapters from the point of view of the mentioned questions on the AMF and their functional implications, the interplay of the organismal and matter flux aspects highlighted by Loreau (2010) and methodological conclusions on the modeling approach used.

1.6 References

Avio, L., Pellegrino, E., Bonari, E. and Giovannetti, M. 2006 Functional diversity of arbuscular mycorrhizal fungal isolates in relation to extraradical mycelial networks. New Phytologist 172: 347-357.

Bago, B., Azcón-Aguilar, C., Goulet, A. and Piché, Y. 1998 Branched Absorbing Structures (BAS): a feature of the extraradical mycelium of symbiotic arbuscular mycorrhizal fungi. New Phytologist 139: 375-388.

Boswell, G.P., Jacobs, H., Davidson, F.A., Gadd, G.M. and Ritz, K. 2003 Growth and Function of Fungal Mycelia in Heterogeneous Environments. Bulletin of Mathematical Biology 65: 447-477.

Boswell, G.P., Jacobs, H., Ritz, K., Gadd, G.M., and Davidson, F.A. 2007 The Development of Fungal Networks in Complex Environments. Bulletin of Mathematical Biology 69: 605-634.

Bucher, M. 2007 Functional Biology of plant phosphate uptake at root and mycorrhiza interfaces. New Phytologist 173: 11-26.

Bücking; H. and Shachar-Hill, Y. 2005. Phosphate uptake, transport and transfer by the arbuscular mycorrhizal fungus Glomus intraradices is stimulated by increased carbohydrate availability. New Phytologist 165: 899–911.

Burleigh, S.H. Cavagnaro, T. and Jakobsen, I. 2002. Functional diversity of arbuscular mycorrhizas extends to the expression of plant genes involved in P nutrition. Journal of Experimental Botany 53: 1593-1601.

Cordell, D., Drangert, J.-O. and White, S. 2009 The Story of phosphorus: Global food security and food for thought. Global Environmental Change 19: 292-305.

Eckardt, N.A. 2005 Insights into plant cellular mechanisms: of phosphate transporters and arbuscular mycorrhizal infection. The Plant Cell 17: 3213–3216.

Feddermann, N., Finlay, R., Boller, T. and Elfstrand, M. 2010. Functional diversity in arbuscular mycorrhiza – the role of gene expression, phosphorus nutrition and symbiotic efficiency. Fungal Ecology 3: 1-8.

Friese, C.F. and Allen, M.F. 1991 The Spread of VA Mycorrhizal Fungal Hyphae in the Soil: Inoculum Types and External Hyphal Architecture. Mycologia 83: 409-418.

Gosling, P., Hodge, A., Goodlass, G. and Bending, G.D. 2006 Arbuscular Mycorrhizal fungi and organic farming. Agriculture, Ecosystems&Environment 113: 17-35.

Graham, J.H. and Abbott, L.K. 2000 Wheat responses to aggressive and nonaggressive arbuscular mycorrhizal fungi. Plant and Soil 220: 207–218.

Hetrick, B.A.D., Wilson, G.W.T. and Cox, T.S. 1992 Mycorrhizal dependence of moder wheat cultivars and ancestors: a synthesis. Canadian Journal of Botany 71: 512- 518.

Hetrick, B.A.D., Wilson, G.W.T. and Todd, T.C. 1996 Mycorrhizal response in wheat cultivars: relationship to phosphorus. Canadian Journal of Botany 74: 19-25.

Jakobsen, I. and Rosendahl, L. 1990. Carbon flow into soil and external hypae from roots of mycorrhizal cucumber plants. New Phytologist 115: 77–83.

Jansa, J., Mozafar, Ahmad and Frossard, E. 2005 Phosphorus acquisition strategies within arbuscular mycorrhizal fungal community of a single field site. Plant and Soil 276: 163-176.

Johnson, N.C., Graham, J.H. and Smith, F.A. 1997 Functioning of mycorrhizal associations along the mutualism–parasitism continuum. New Phytologist 135: 575–585.

Kazmierczak, M., Johst, K., and Huth, A. 2015. Conservatives and Gamblers: Interpreting plant functional response to water stress in terms of a single indicator. Ideas in Ecology and Evolution 8:29-41.

Knudsen, G.R., Stack, J.P., Schuhmann, S.O., Orr, K. and LaPaglia, C. 2006 Individual-Based Approach to Modeling Hyphal Growth of a Biocontrol Fungus in Soil. Phytopathology 96: 1108-1115.

Köhler, P., Ditzer, T. and Huth, A. 2000. Concepts for the aggregation of tropical tree species into functional types and the application on Sabah's dipterocarp lowland rain forests. Journal of Tropical Ecology 16:591-602.

Li, H., Smith, F.A., Dickson, S., Holloway, R.E. and Smith, S.E. 2008 Plant growth depressions in arbuscular mycorrhizal symbiosis: not just caused by carbon drain? New Phytologist 178: 852–862.

Loreau, M. 2010 Linking biodiversity and ecosystems: towards a unifying ecological theory. Philosophical Transactions of the Royal Society B 365: 49-60.

Marschner, H. and Dell, B. 1994. Nutrient uptake in mycorrhizal symbiosis. Plant and Soil 159: 89-102.

Marschner, P. 2012 Mineral nutrition of higher plants, 3rd ed. San Diego, USA: Academic Press. 651p.

Meskauskas, A., Fricker, M.D. and Moore, D. 2004. Simulating Colonial growth with the Neighbour-Sensing modelof hyphal growth. Mycological research 108: 1241- 1256.

Moore, D., Robinson, G.D., Trince, A.P.J. 2011 21st Century Guidbook to Fungi. Cambridge University Press. 639pp.

Newsham, K.K., Fitter, A.H. and Watkinson, A.R. 1995 Multi-functionality and biodiversity in arbuscular mycorrhizas. Trends in Ecology and Evolution 10: 407–411.

Picard, N., Köhler, P., Mortier, F. and Gourlet-Fleury, S. 2012. A comparison of five classifications of species into functional groups in tropical forests of French Guiana. Ecological Complexity 11: 75-83.

Prosser, J.I. and Trinci, A.P.J. 1979. A Model for Hyphal Growth and Branching. Journal of General Microbiology 111, 153-164.

Ravnskov, S. and Jakobsen, I. 1995 Functional compatibility in arbuscular mycorrhizas measured as hyphal P transport to the plant. New Phytologist 129: 611–618.

Schnepf, A., Roose, T. and Schweiger, P. 2008 Impact of growth and uptake patterns of arbuscular mycorrhizal fungi on plant phosphorus uptake – a modelling study. Plant Soil 312: 85-99.

Schnepf, A., Jones, D. and Roose, T. 2011 Modelling Nutrient Uptake by Individual Hyphae of Arbuscular Mycorrhizal Fungi: Temporal and Spatial Scales for an Experimental Design. Bulletin of Mathematical Biology 73: 2175-2200.

Schüßler, A., Schwarzott, D. and Walker, C. 2001 A new phylum, the Glomeromycota: phylogeny and evolution. Mycological Research 105: 1413-1421.

Smith, S.E., Smith, F.A. and Jakobsen, I. 2003. Mycorrhizal fungi can dominate phosphate supply to plants irrespective of growth responses. Plant Physiology 133: 16–20.

Smith, S.E. and Read, D.J. 2008 Mycorrhizal symbiosis, 3rd ed. San Diego, USA: Academic Press. 800p.

Stewart, L.I., Jabaji-Hare, S. and Driscoll, B.T. 2006 Effects of external phosphate concentration on glucose-6-phosphate dehydrogenase gene expression in the arbuscular mycorrhizal fungus Glomus intraradices. Canadian Journal of Microbiology 52: 823-830.

Tilman, D., Cassman, K.G., Matson, P.A., Naylor, R and Polasky, S. 2002 Agricultural sustainability and intensive production practices. Nature 418: 671-677.

United Nations, Department of Economic and Social Affairs, Population Division. 2015. World Population Prospects: The 2015 Revision, Key Findings and Advance Tables. Working Paper No. ESA/P/WP.241

Wang, B. and Qiu, Y.-L. 2006 Phylogenetic Distribution and evolution of mycorrhizas in land plants. Mycorrhiza 16: 299-363.

Wright, D.P., Read, D.J. and Scholes, J.D. 1998. Mycorrhizal sink strength influences whole plant carbon balance of *Trifolium repens* L. Plant, Cell and Environment 21: 881–891.

Chapter 2: Ecological system and modelling framework

2.1 Introduction to mycorrhiza

One of the, if not the, most common and important symbiosis between two species of different kingdoms is that of plants and mycorrhiza. Fungi and roots of vascular plants interact in this symbiosis in a way from which usually both profit. Fungi deliver mostly inorganic nutrients like phosphorus (P), nitrogen (N), potassium (K) sulfur (S), calcium (Ca), iron (Fe), copper (Cu) and zinc (ZN) to the plant and gain carbohydrates (C), mostly glucose and sucrose in exchange (Smith and Read 2008, Marschner, 2012). Furthermore there is some evidence that plants get protected from toxicants, diseases and droughts by the symbiotic fungi (Newsham et al. 1995). Fungi profit, because they can use photosynthetic products of the plant without investing energy and nutrients in green tissue. Plants benefit, from a fungal mycelium with very thin and flexible hypha which can quickly respond to nutrient changes.

There are two different forms of mycorrhiza: endo- and ectomycorrhiza. While in ectomycorrhiza the nutrient exchange takes place in the extracellular space, and fungi do not penetrate individual cells, endomycorrhizal fungi grow directly into cell walls of plant roots for nutrient exchange (Moore et al. 2011). Endomycorrhiza can be further divided into ericoid, orchid and arbuscular mycorrhiza. Like the name says, ericoid and orchid mycorrhizae are specialized to ericaceae and orchids, respectively. However, arbuscular mycorrhiza can be found in a large variety of plants. About 80 % of all vascular plant families, among which are several crop species (e.g. wheat (*Tritium aestivum*), barley (*Horteum vulgare*), etc.) are known to build arbuscular mycorrhiza (Moore et al. 2011).

Arbuscular mycorrhizal fungi (AMF) belong to the phylum of Glomeromycota which is a very old phylum (Schüßler et al. 2001). Molecular techniques gave evidence that arbuscular mycorrhiza originated at least 400 Million years ago and played a crucial role in the land colonization of plants (Wang and Qiu, 2006). In this symbiosis, fungi penetrate the parenchyma cortex of plant cells and build highly branched structures, called arbuscules, which are relevant for the nutrient exchange between the plant and the fungus and gave the name to this type of mycorrhiza (Moore et al. 2011).

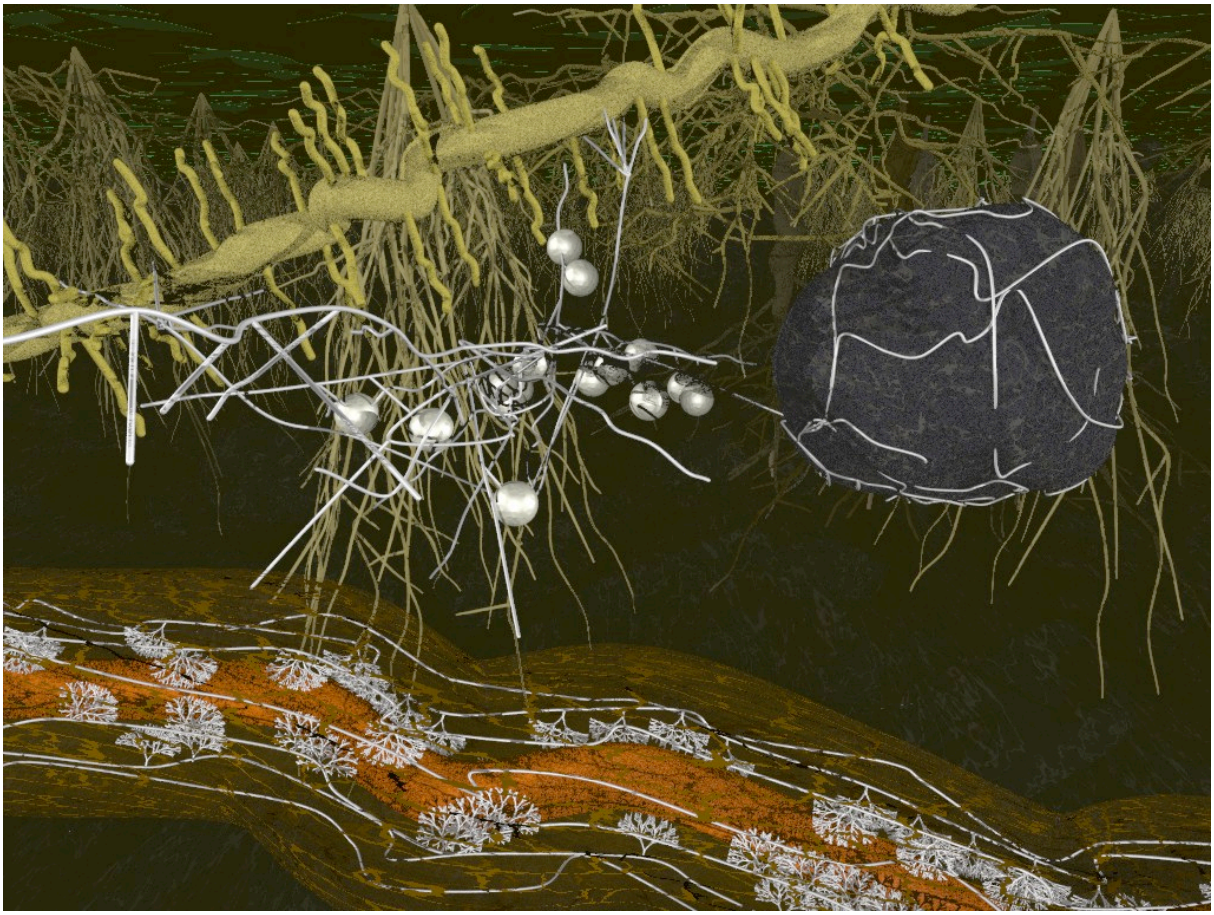

Figure 2-1. Arbuscular mycorrhizal fungi (white structures) interacting with plant routes (large brown structures). Grey spheres show spores. Illustrated by Thomas Fester.

The extraradical mycelium of AMF shows some more characteristic morphologic preferences. Runner hyphae are fast growing, long hyphae which are mainly relevant for intracellular nutrient transport (Friese and Allen 1991). Minerals are transported into the direction of the plant roots, carbohydrates are distributed in the whole mycelium. From this runner hyphae, highly branched, tree like structures branch off. These branched absorbing structures (BAS) are relevant for the uptake of nutrients from soil (Bago et al. 1998). If they are not used anymore, e.g. because of nutrient depletions in the surrounding soil, then spores are built at the BAS before they are detached from the corresponding runner hypha (Bago et al. 1998). AMF are obligate symbionts, that is they depend on photosynthesis products of their plant partners (Moore et al. 2011). An illustration of AMF growing in soil together with plant routes can be seen in Figure 2-1.

2.2 Laboratory experiments

2.2.1 Laboratory experiments

This dissertation is a cooperation project combining theory, modelling and experiments. Laboratory experiments were conducted by Thomas Fester and Frank Zielinsky from the Department of Environmental Microbiology of the Helmholtz Centre for Environmental research. Two different laboratory experiments were conducted to study the dynamics of P and C in combination with the growth of AMF and thus to support the modelling work.

We cultivated the arbuscular mycorrhizal fungus *Glomus intraradices* in a closed system on Petri dishes of 12 cm diameter which were divided equally by a closed plastic barrier into two compartments (see Figure 2-2). The medium in the first compartment (R+F), contained carbon and phosphorus. That in the second compartment (F), contained only phosphorus.

We inoculated the compartment *R+F* with Ri T-DNA transformed *Daucus carota* roots which were mycorrhized by *G. intraradices*. *D. carota* was manually prevented to grow over the barrier between the two compartments. However, *G. intraradices* was able to overgrow it and to occupy the compartment (F). This second compartment was used to measure the carbon content of the fungal biomass and the phosphorus content in the surrounding medium. Since *G. intraradices* is an obligate symbiont and cannot take up carbon directly from the medium, any carbon found in the fungal mycelium must have been obtained from the plant, which provides us with the carbon uptake rate of *G. intraradices*. Moreover, since the fungal mycelium is the only phosphorus sink in F, the loss of P in the medium provides a direct measure of the fungal P uptake.

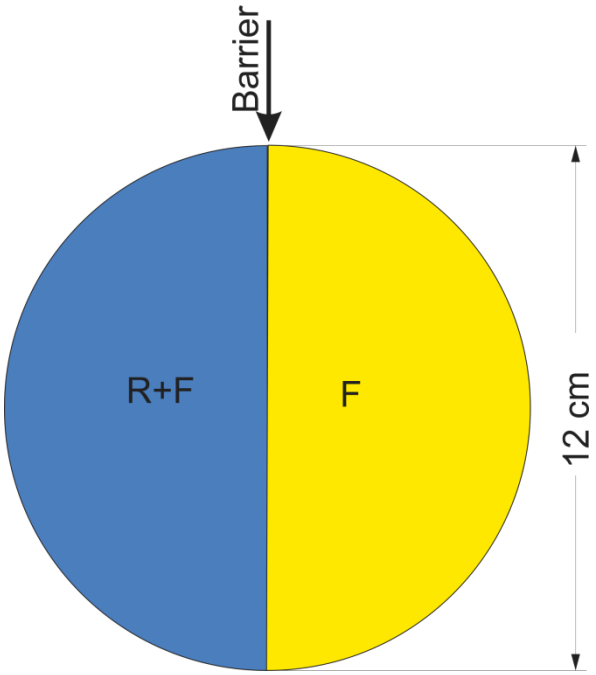

Figure 2-2: Petri dish system. Blue compartment (R+F) was inoculated with plant roots of Daucus carota and arbuscular mycorrhizal fungi Glomus intraradices. Yellow compartment (F) was colonized by G. intraradices after growth through the barrier.

This led to the following protocol for designing and observing the experiments. We monitored when the fungus first managed to overgrow the barrier into compartment F and defined this as $T_0 = 0$ [days], which was the beginning of the experiments.

Experiment 1 – Measurement of growth speed and branching activity

The first experiment was conducted by myself. At time steps, (T_0-T_2), the growth speed [*mm* d^{-1}] and branching activity of fungal hyphae [*branches* d^{-1}] were investigated on 8 petri dishes by measuring several hyphae each day and counting of the branching events of these hyphae. Figure 2-3 shows an example of a petri dish with the measured lengths of individual hyphae.

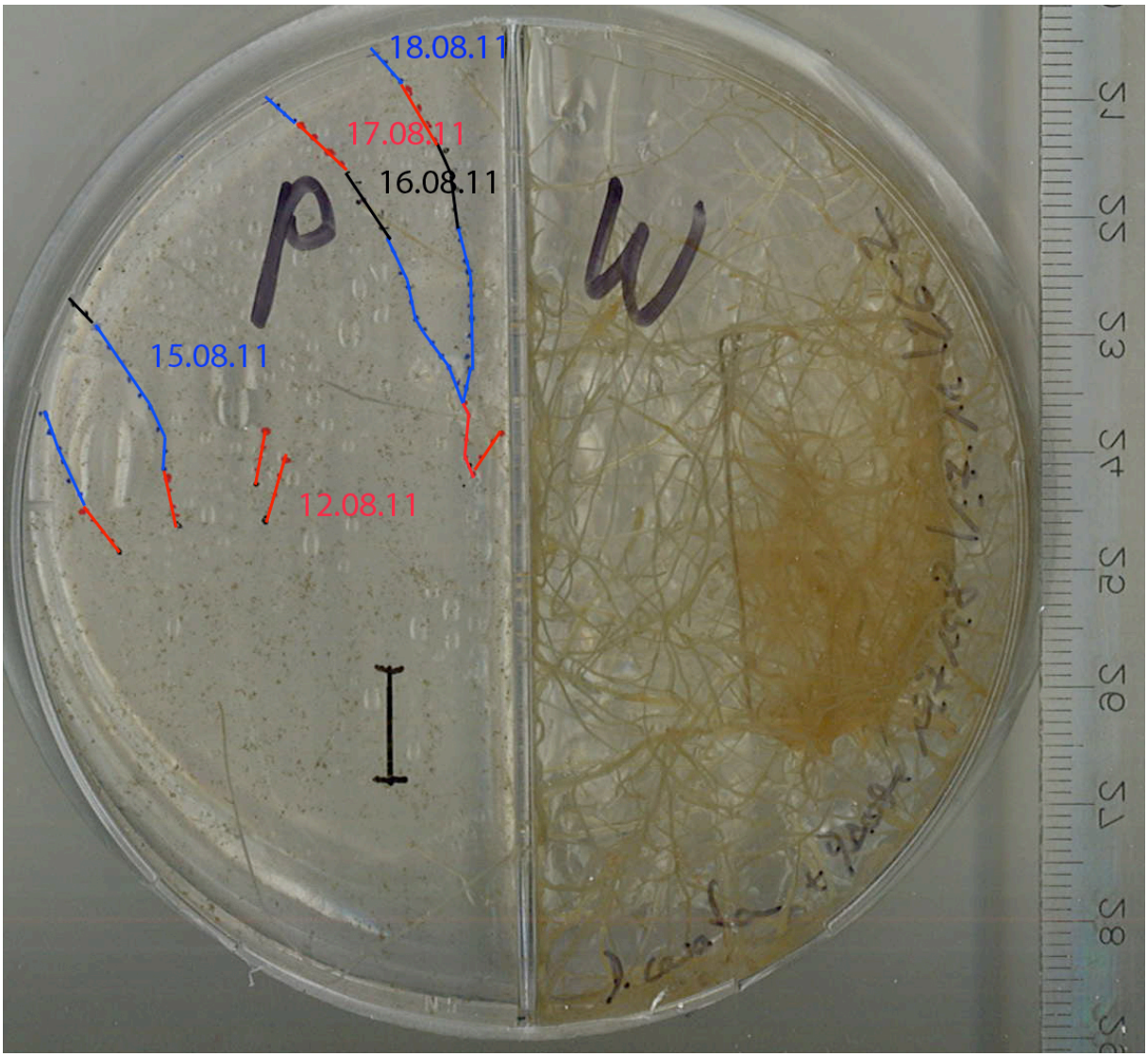

Figure 2-3.Example of a petri dish, used to measure daily growth of individual hypha. On the right-hand side (marked with a "W") plant roots and mycorrhiza were inoculated and could grow together. On the left (marked with an "P") only the fungus could grow.

These parameters were measured at the beginning of the experiments under high amounts of phosphorus and carbon to obtain their maximum values in absence of nutrient limitation. This made a total mean growth speed of 0.6 cm per day with a standard deviation of 0.3 cm as well as a mean of 0.09 branches per day.

Experiment 2 – Measurement of the P and C Dynamics

Thereupon, we measured the total amount of C in the fungal mycelium and P in the medium in compartment F at four different points in time (T_1-T_4, Table 2-1). Since the system had to be destroyed for each measurement, we performed several replicate experiments for each

point in time. We did three replicates for T_0 and seven replicates for T_1-T_4 respectively. P analytic was done by using inductively coupled plasma optical emission spectrometry, carbon measurement by dry combustion in an oxygen stream at 950°C using an automated CHN elemental analyser (Vario El III, Elementar, Hanau, Germany).

Additionally, we performed control experiments with *D. carota* inoculated in the R+F compartment as before, but without mycorrhization of *G. intraradices*. These control experiments were performed in three replicates for each point in time T_1-T_4 (Table 2-1).

Table 2-1: Overview of the experiments performed for observing the carbon and phosphorus contents in compartment F, in presence of plant roots and AMF (Fungal growth), and in presence of plant roots only (Control)

Point in time	Time	Number of replicates – Fungal growth	Number of replicates – Control
T_0	0d	3	-
T_1	+3d	7	3
T_2	+10d	7	3
T_3	+17d	7	3
T_4	+24d	7	3

This experiment was done by Dr. Frank Zielinski from the Department of Environmental Microbiology; P analytics were done by Dr. Sybille Mothes from the Department of Analytical Chemistry, C analytics by Dr. Elke Schulz from the Department of Soil Microbiology.

The resulting P and C dynamics are shown in Figure 2-4.

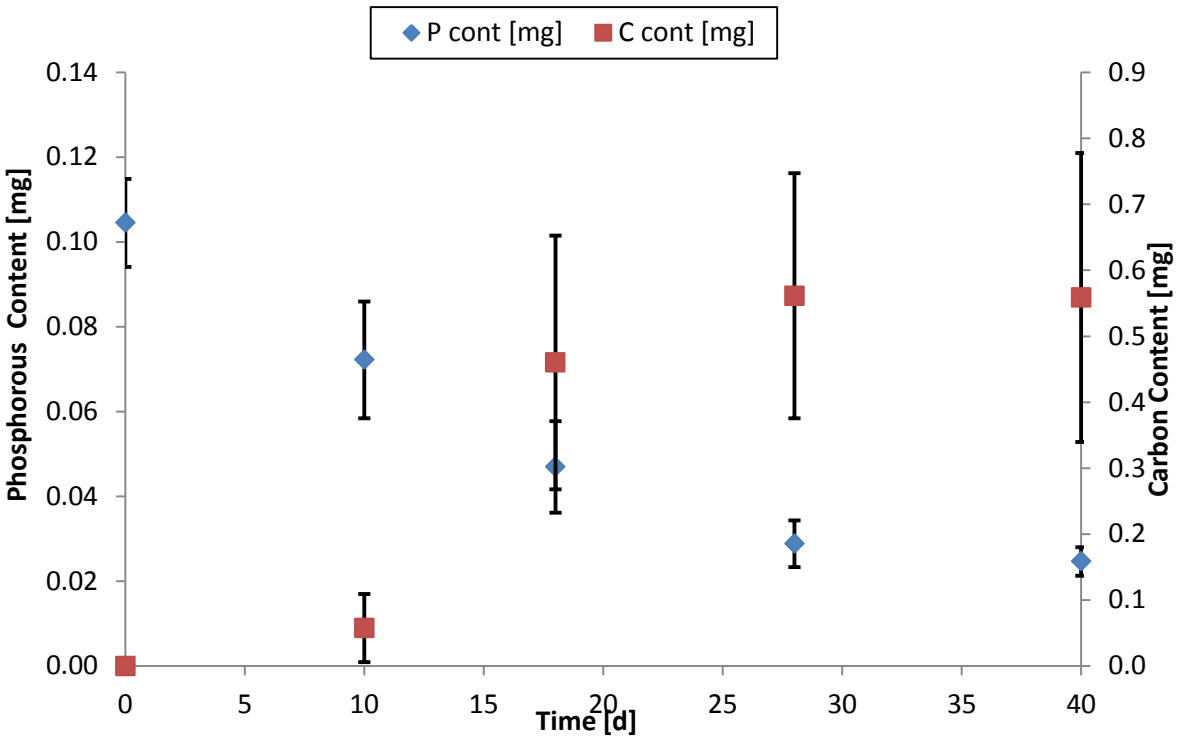

Figure 2-4. Phosphorus and carbon content measured in the F compartment at different time steps.

Like expected, the carbon content in the investigated compartment F was rising, whereas the phosphorus content was decreasing. Since the only possible carbon source in the compartment F was the mycorrhizal fungus, these dynamics verify that the fungus uptakes carbon from the plant roots in the compartment R+F ,and transports it to the compartment F to grow . The same applies for the P dynamics. The only P sink in the compartment F is the mycorrhizal fungus which uptakes and transports it to the plant. Therefore, the measured P dynamics are an indication for the fungus' phosphorus uptake and transport capacity.

2.2.2 Relevant outcome for modelling

The growth speed, resulting from experiment 1 was directly used to parameterize the growth speed of the AMF without limitation of C and P in the model. The decline of the P concentration in the medium and the rising amount of fungal C of compartment (F) in experiment 2 was taken to parameterize all other processes.

2.3 Model description

We developed a spatially explicit simulation model for the growth of arbuscular mycorrhizal fungi (AMF) in dependence on resource uptake and resource exchange with a plant. The model explicitly describes the uptake of the inorganic nutrient phosphorus from soil, the subsequent fungal hypha growth processes, and the exchange of phosphorus for carbon with the plant. Model parameterization is based on experimental results of AMF growth in Petri dishes (see section 1.1).

The spatial model for AMF growth and nutrient transport is based on a model for fungal growth developed by Boswell et al. (2007). This model describes fungal growth on a two-dimensional grid with hexagonal grid cells depending on one single nutrient which is taken up by the fungus (P in our case). We expanded this model in multiple directions. First, we consider a second nutrient (C) which cannot be taken up directly from the soil but via the plant in exchange for P. Second, we introduce a third spatial dimension to consider vertical (height) layers. These were necessary to avoid unrealistically large rates of anastomoses. Third, we include several additional internal processes which are important for the uptake, transport, and exchange of the two nutrients (such as BAS, Sporulation, different directions of the internal transport of the different nutrients). .

The model is able to study different plant-fungus nutrient exchange strategies, ranging from parasitic to mutualistic interactions. This is modeled via the amount of phosphorus the fungus has to deliver to receive a certain amount of carbon from the plant. If much phosphorus is required we call it ‘mutualistic’ interaction, if just a small amount of phosphorus is required to receive the same amount of carbon, we call it ‘parasitic’ interaction.

The model is also able to study different spatiotemporally heterogeneous distributions of resource P. We investigated first spatiotemporally homogeneous distributions with infinite diffusion rates, second spatially homogeneous but temporally heterogeneous distributions in form of resource pulses and third spatiotemporally heterogeneous resource distributions with finite diffusion rate.

2.3.1 Purpose of the Model

The model is aimed at the general understanding of the interaction between mycorrhizal fungi and plant roots via different nutrient exchange strategies. This functional view allows us to get new insights in the resulting nutrient dynamics of C and P. The model considers processes such as fungal growth, nutrient exchange with the plant and sporulation. It is based on laboratory experiments and investigates the role of arbuscular mycorrhizal fungi for the coupled dynamics of C and P and its implications for plant growth. In particular, we want to investigate to what extent arbuscular mycorrhizal fungi may buffer spatially and/or temporally varying resource fluxes emerging from spatially and/or temporally heterogeneous distributions of P in soil. Furthermore, we analyze the dependence of the buffering effect on the type of nutrient exchange strategy, i.e. whether the plant-fungus interactions are parasitic or mutualistic. Therefore, the model elucidates the role of plant-fungus interactions for the functional stability of this system i.e. the tolerance of plants to spatiotemporally heterogeneous resource supply with the help of fungi.

A schematic representation of the simulation model's processes is given in Figure 2-5.

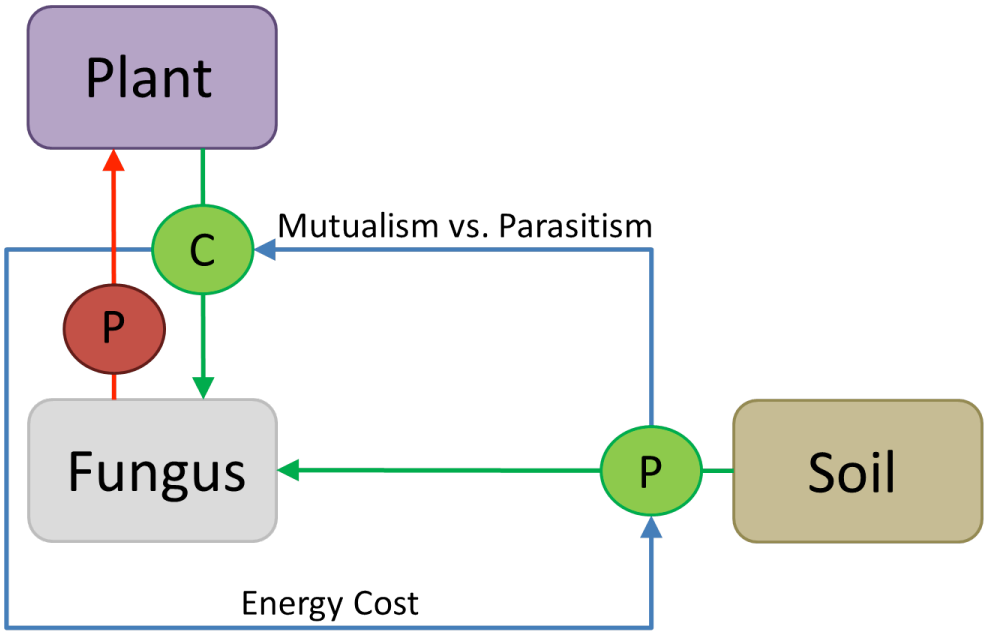

Figure 2-5: Scheme of the processes involved in the simulation model. Green arrows show nutrient fluxes to the fungus. Red arrows show nutrient fluxes leaving the fungus. Blue arrows indicate feedbacks. The "Mutualism versus Parasitism" arrow characterises how much P the fungus has to uptake from soil and to deliver to the plant to get back a certain amount of C. The "Energy cost" arrow visualizes that the fungus needs energy for uptaking P from the soil which has to be taken from C.

2.3.2 Overview

The model is based on laboratory experiments in which a system of arbuscular mycorrhiza is growing on Petri dishes (cf. section 2.2.1). Therefore, the model's simulation area consists of a two-dimensional hexagonal grid, which has the same extent as the Petri dishes, i.e. a diameter of 12 cm. The choice of grid cell resolution presents a trade-off between sufficient precision for capturing the details relevant for the modelled dynamics and sufficient computation efficiency, since simulation time drastically increases with the number of grid cells. With regard to this trade-off, we selected the diameter Δx = 0.5 mm for each grid cell. We used discrete time steps Δt *[d]* for all processes. The time step length was not fixed, but is adjusted after each time step for the next, as a function of the nutrient-dependent growth probabilities (section 2.3.3) and, if simulated, the external nutrient fluxes (section 2.3.9).

Grid cells contain external phosphorus P_{ext} *[mg]*, and can be unoccupied or occupied by fungal mycelia of three kinds: plant-fungus interface, fungal tip, or parts of fungal hypha. All

three kinds of mycelium share the following attributes: They transform P_{ext} by phosphorus uptake P_{upt} *[mg]* (section 2.3.5) to internal phosphorus P_{int} *[mg]*, which is used for growth (section 2.3.3) transported against the fungal growth direction (section 2.3.8) and exchanged at the plant-fungus interface to internal carbon C_{int} *[mg]* (section 2.3.6), which is transported in the fungal growth direction and used for growth, phosphorus uptake and maintenance processes (section 2.3.7). They have a certain number of branched absorbing structures (*BAS*) (section 2.3.4) which are relevant for phosphorus uptake. BAS are converted to spores (*SP*) that store C_{int} and P_{int}, if the uptake rate of P drops below a certain value (section 2.3.10).

Fungal tips can grow new hyphae (section 2.3.3). To allow tips to grow below or above already present parts of the fungal mycelium, we introduced ten height layers, on which the fungi grow. A grid cell's total amount of P_{ext} is accessible from all height layers of the corresponding grid cell. This results in a quicker drop of external phosphorus in the cell; the more height layers of a grid cell are occupied. Hence, the three-dimensional model of the fungal mycelium is projected on a two-dimensional model of external phosphorus. New fungal tips emerge from branching events (section 2.3.4).

The plant-fungus interface is the starting point of the first fungal tip at simulation begin. Moreover, at this interface phosphorus and carbon are exchanged (see section 2.3.6).

Fungal hyphae can be seen as individual tubes, the fungal mycelium as a system of connected tubes. The hexagonal grid allows us to address parts of the tube system with the length of the diameter of one grid cell. If more than one tube crosses a grid cell, the height layers allow us to distinguish them. These parts of tubes (i.e. parts of fungal hypha) in the different height layers contain their individual amounts of P_{int}, C_{int}, and their individual numbers of branched absorbing structures and spores. So grid cells can address up to ten individual parts of fungal hypha with their own state variables and characteristics. Unless otherwise specified, all processes take place on the level of individual parts of hypha.

2.3.3 Growth of fungal mycelium via movement of fungal tips and the creation of branched absorbing structures (BAS)

Fungi are known to grow only by the tips of their hyphae, so fungal growth takes place by the tips moving through the hexagonal grid depending on their internal amounts of growth

limiting nutrients, C and P. Therefore, a fungal tip's probability of jumping to a neighboring grid cell accords to following rules: Without limitation of nutrients, this probability is equal to one. With limitation, for the time step length Δt, and the grid cell diameter Δx (i.e. the length of fungal growth), a growth reduction factor is calculated for each nutrient, and the stronger limitation is selected:

$$Gr(i,t) = \min\left(\frac{P_{int}(i,t)}{k_P + P_{int}(i,t)}, \frac{C_{int}(i,t)}{k_C + C_{int}(i,t)}\right), \qquad \textit{Equation 1}$$

where i indicates the grid cell of the fungal tip, k_P is the amount of phosphorus, where the P limitation factor is equal to 0.5, and k_C is the corresponding quantity for carbon.

In the hexagonal grid with usually six neighbor grid cells (except for boundary grid cells), growth is possible into three directions (Figure 2-6), since growth into the directions straight backwards, sharp left and sharp right have not been observed in nature.

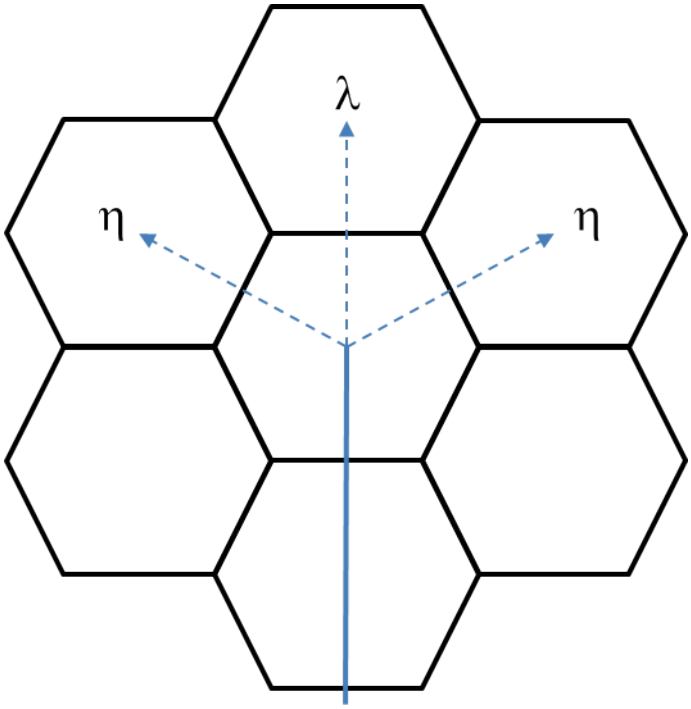

Figure 2-6: Fungal growth directions in a hexagonal grid. Straight blue: fungal hypha, broken blue: possible growth directions and their probabilities.

The corresponding growth probabilities are λ for straightforward and η for slight left and slight right movement of the fungal tip, respectively. On Petri dishes, fungi were observed to grow straightforward with rare random changes to left and right. Incorporated in the simulation model, these biological observations translate to directed movement with

random deviations, which can be mathematically described by convection for the directed part (Equation 2) and diffusion for the random deviations (Equation 3). The probabilities for directed movement *Conv* and for random movement *Diff*, depend on the growth reduction factor *Gr(i)*, the time step length Δt, the movement distance Δx, and the convection parameter *v* and the diffusion parameter *D*, respectively:

$$Conv(i,t) = v\frac{\Delta t}{\Delta x} \cdot Gr(i,t) \qquad \textit{Equation 2}$$

$$Diff(i,t) = D\frac{\Delta t}{\Delta x^2} \cdot Gr(i,t) \qquad \textit{Equation 3}$$

Consequently, the directed movement probability applies to the straight forward direction, and the random movement probability applies to all three possible growth directions in our system (Equation 4 and Equation 5).

$$P_{i,t}(\lambda) = Conv(i,t) + Diff(i,t) \qquad \textit{Equation 4}$$

$$P_{i,t}(\eta) = Diff(i,t) \qquad \textit{Equation 5}$$

The sum of the movement probabilities to all three directions $P(\lambda) + 2P(\eta)$ for one fungal tip at time *t* must not exceed 1. If this constraint is not met, the time step length Δt is reduced until it becomes equal to or smaller than 1. Note that if it is smaller than 1, the remaining fraction determines the probability for the tip to stay in its current grid cell.

If a fungal tip moves to a grid cell that is already occupied by another part of a fungal mycelium, an anastomosis is built. Anastomoses can short-circuit or build endless loops of internal nutrient fluxes. To limit the amount of anastomoses to a biologically realistic value preventing the enrichment of nutrients via endless loops, we introduced ten height layers for each grid cell (cf. section 1.2.1).

If a fungal tip moves to a neighboring grid cell, it arrives either one layer above or below, or at the same height layer as in the original grid cell, with each of the three options having the same probability. (For fungal tips in the top or bottom height layer, only two options remain, both with the same probability.) The first fungal tip starts at the fifth height layer in the beginning of the simulations (cf. section 1.2.1). Thus, anastomoses are built only if a fungal tip moves to a height layer that is already occupied by fungal mycelium in the respective grid cell. The building of anastomoses results in the destruction of the respective fungal tip.

If a fungal tip has moved, the respective height layer in grid cell left behind changes its state to fungal hypha. Therefore, each movement of a fungal tip produces new fungal hypha and so biomass. Naturally, this consumes nutrients to be converted to organic material and, thus, become unavailable for other processes. The required amounts of phosphorus g_P and carbon g_C to grow 1 mm of fungal biomass reduce the internal nutrients during on time step:

$$P_{int}(t+\Delta t) = P_{int}(t) - g_p \cdot \Delta x \cdot \Delta BM,$$

Equation 6

$$C_{int}(t+\Delta t) = C_{int}(t) - g_C \cdot \Delta x \cdot \Delta BM,$$

Equation 7

where ΔBM are all in this time step new grown hypha.

Another characteristic of AMF is the creation of branched absorbing structures (BAS). As these tree-like structures are smaller than a single grid cell, they are not modeled explicitly. Instead, we incorporated them implicitly by assigning higher P uptake rates to the hypha in grid cells containing BAS, because the main function of these structures is nutrient uptake. The attribute of increased P uptake is assigned randomly to each new grown hypha such that it corresponds to the experimental measured mean of 10 BAS per centimeter hypha. This results for our grid size in 1 or no BAS per hypha of length *ΔX* with the same probability for both options. A height layer with hypha and one BAS has twice the biomass of a height layer only with hypha. BAS are transformed to spores, when the uptake rate of their corresponding hypha drops below a minimum uptake rate (see section 2.3.10).

2.3.4 Growth of fungal mycelium via branching

Branching is the creation of a new fungal tip. Branching can occur after each movement event of a fungal tip into a certain grid cell (cf. section 1.2.2). To calculate the probability of a branching event *P(branch)* during time step Δt, the basic branching probability *b* [d^{-1}] (which would apply without nutrient limitations) is reduced by the growth reduction factor *Gr(i, t)* according to the amounts of internal carbon and phosphorus of the fungal tip (cf. Eq. 1):

$$P_i(branch) = b \cdot \Delta t \cdot Gr(i,t),$$

Equation 8

According to this probability P_i(branch), an additional fungal tip is created in one of the remaining two grid cells to which the fungal tip could have moved during growth (cf. section

1.2.2, Fig. 2). The respective grid cell is chosen randomly with equal probability for both options, the choice of the height layer is done according to the rules of tip movement (section 2.3.3). The nutrients remaining inside the original fungal tip after movement and branching are divided equally between both fungal tips.

2.3.5 Fungal uptake of phosphorus

The fungus takes up P with its entire mycelium, that is, in each occupied grid cell. Active uptake of P_{ext} requires energy in form of C_{int}, and the required amount of C_{int} increases with decreasing P_{ext} available in the grid cell. Therefore the P-uptake during time step Δt (Equation 9) depends on the amount of C_{int} in the fungal hypha, the amount of $P_{ext,}$ the number of BAS *nBAS* in grid the cell and a factor α. Equation 10 calculates the energy cost for the uptake.

$$P_{upt}(i,t) = \alpha \cdot C_{int}(i,t) \cdot P_{ext}(i,t) \cdot \Delta t \cdot nBAS(i) \qquad \textit{Equation 9}$$

$$C_{cost}(i,t) = k \cdot \frac{1}{P_{ext}(i,t)} \cdot P_{upt}(i,t) \qquad \textit{Equation 10}$$

If C_{cost} is larger than C_{int}, the entire internal carbon is used for the uptake of phosphorus. This means, the dependency of P_{upt} and C_{cost} turns around. The maximum uptake rate P_{upt} for the available carbon C_{int} is calculated and C_{cost} equals C_{int}. If in one grid cell, more than one height layer is occupied, C_{int} is the sum of internal carbon of all height layers. After calculation of the P_{upt}, every height layer gets its share of P. k is a linear scaling factor.

2.3.6 Exchange of carbon and phosphorus between fungus and plant

The plant provides carbon to the fungus via the plant-fungus interface. This is the sole carbon and so energy source for the AM fungus. In exchange, the fungus provides phosphorus as a nutrient to the plant. To simulate the exchange, we calculate the rate of carbon C_{upt} that the fungus receives for the delivered rate of phosphorus P_{del} from the plant:

$$C_{upt}(t) = min\left(0.7\ C_{max},\ C_{min} + (C_{max} - C_{min}) \cdot \frac{P_{del}(t)}{K_m + P_{del}(t)}\right). \qquad \textit{Equation 11}$$

Here, C_{min} is the minimum carbon uptake rate of the fungus, which is always realized even without delivery of phosphorus (i.e. if P_{del} = 0). C_{max} is a theoretical maximum carbon uptake rate, reflecting the plant's carbon limitation and the transport capacity of the plant-fungus

interface. This restricts the exchange depending on the amount of delivered phosphorus P_{del} and results in a Michaelis-Menten like kinetic equation, where K_m is the half-saturation constant of phosphorus. As a consequence of these kinetics, the additional carbon gains for the fungus when delivering more phosphorus to the plant are decreasing to almost zero for high values of P_{del}. Therefore, the exchange is additionally restricted to 70% of $C_{max.}$ When this carbon uptake rate is reached, the corresponding phosphorus is delivered to the plant and the surplus is stored as internal phosphorus P_{int} in the fungus.

It is important to note that the half-saturation constant K_m provides the means to characterize the nutrient exchange strategy between the plant and the fungus. At low K_m values, the fungus profits most from this symbiosis, as it receives relatively high amounts of carbon for the phosphorus delivered. In the extreme case with K_m equal to zero, the fungus acts as a parasite, because it receives the possible maximum amount of carbon without delivering phosphorus to the plant. Contrarily, at high K_m values, the plant profits more, as the fungus receives relatively low amounts of carbon for the phosphorus delivered. However, since the plant is the sole energy source for the fungus, pure parasitism of the plant is impossible. So below a certain limit C_{min}, the fungus cannot grow anymore and the system will collapse.
Thus, the parameters C_{min} and K_m can be systematically varied to study all possible nutrient exchange strategies and their impacts on the resulting nutrient and fungal biomass dynamics.

2.3.7 Maintenance of fungal biomass

The amount of carbon required for maintenance is directly related to the fungal biomass. Therefore, we calculated the maintenance rate MR for each occupied height layer of each grid cell as a linear function of the sum of hyphal biomass *hBM,* the number of branched absorbing structures *nBAS* on this height layer and a factor a (Equation 12). This rate reduces the internal carbon in each time step for each occupied height layer of each grid cell (Equation 13).

$$MR(i,t) = a \cdot (hBM(i,t) + nBAS(i,t)),$$

Equation 12

$$C_{int}(i, t + \Delta t) = C_{int}(i, t) - MR(i, t) \qquad \textit{Equation 13}$$

If the maintenance rate cannot be paid fully, all available C_{int} is paid instead.

2.3.8 Internal Transport of the two nutrients P and C (inside the fungus)

Carbon is taken up only at the plant-fungus interface, but needed in the tips for growth (sections 2.3.3 and 2.3.4) and in the whole mycelium for maintenance (section 2.3.7) and phosphorus uptake (section 2.3.5). Therefore, the internal carbon is transported passively Tr_{dif} via diffusion according to its concentration gradient (Equation 14), and actively towards the fungal tips via convection Tr_{conv} according to its concentration (Equation 15).

Phosphorus is, in contrast, taken up in all grid cells of the whole mycelium, but used at the fungal tips for growth (sections 2.3.3 and 2.3.4) and towards the plant-fungus interface to be exchanged for carbon (section 2.3.6). This leads to a convective transport Tr_{conv} directed to the plant-fungus interface (Equation 14). Additionally to the directed convective transport, diffusion provides the fungal tip with phosphorus, when it moved to P depleted areas. This is incorporated by using Equation 15 as diffusion equation.

$$Tr_{conv}(h, t) = v_s \cdot S_{int}(h, t) \cdot \frac{\Delta t}{\Delta x}, \qquad \textit{Equation 14}$$

$$Tr_{dif}(h, t) = D_s \cdot \left(S_{int}(h, t) - S_{int}(h + 1, t)\right) \cdot \frac{\Delta t}{\Delta x^2}, \qquad \textit{Equation 15}$$

Transport takes place in the fungal hypha, so the equations describe nutrient fluxes between connected parts of hypha. Indices *h* and *h+1* indicate height layers of neighboring cells which are connected by fungal mycelium. S_{int} stands in this place for P_{int} and C_{int} respectively depending on the calculated nutrient flux, v_s is the convection coefficient and D_s the diffusion coefficient for P and C respectively. Tr_{conv} and Tr_{dif} are calculated for all fungal connections on all occupied layers of all grid cells. Looking at a fungal hypha of one height layer, convective transport is only directed in one direction, or two in branching points. Fluxes in branching points sum up, or are equally divided. Diffusion can have more directions, so all connected hyphae are examined at the same point. When all fluxes in and out of the observed cell are calculated, C_{int} and P_{int} of that cell is updated.

2.3.9 External Transport of P (outside the fungus)

The external P in the grid cells is subject to diffusion. We used a module analogous to the internal diffusion (Equation 15) for calculating the amounts of phosphorus that change between neighboring grid cells in the two-dimensional simulation environment (cf. section 1.2.1). In this module, all six (except for border cells) neighboring cells are examined at the same time.

2.3.10 Sporulation

The main function of branched absorbing structures (BAS) is the uptake of phosphorus. However, when the amount of external phosphorus in the grid cell of BAS drops, this function cannot be provided anymore at some point, but the BAS still require carbon for maintenance (cf. section 1.2.6). Therefore, a BAS converts into a spore *SP* if the phosphorus uptake rate of its corresponding hypha decreases below a threshold $minP_{upt}$. Contrary to the BAS, these spores do not increase the fungal phosphorus uptake rate, but store nutrients. Internal carbon and phosphorus from the fungal mycelium is transported to and stored in them. To this end, the corresponding fluxes of C and P from the hypha into the spore are calculated depending on the ratio of the respective nutrient concentrations within the fungus and the spore (Equation 16):

$$S_{flux}(i,t) = D_{spore,s} \cdot \frac{S_{int}(i,t)}{S_{spore}(i,t)}, \qquad \textit{Equation 16}$$

where *S* stands for the respective nutrient *P* or *C and* $D_{spore,S}$ is the corresponding transport coefficient. The hyphas state variables P_{int} and C_{int} change by Equation 17, the spore's state variables C_{spore} and P_{spore} by Equation 18.

$$S_{int}(i,t+\Delta t) = S_{int}(i,t) - S_{flux}(i,t), \qquad \textit{Equation 17}$$

$$S_{spore}(i,t+\Delta t) = S_{spore}(i,t) + S_{flux}(i,t), \qquad \textit{Equation 18}$$

When $S_{flux}(i,t)$ drops below a threshold $minS_{flux}$, the spore is full and becomes decoupled from the mycelium, meaning that no further nutrients are transported into the spore.

2.3.11 Model parameterization

Since for most parameters no values could be obtained from literature, the model was parameterized on the basis of the laboratory experiments on growth speed of individual fungal hypha and the dynamics of carbon and phosphorus in the system. This was done using the method of pattern oriented modelling (Grimm et al, 1996). Since with growth speed of individual hypha and the C-P dynamics only two pattern were available, and the signals from these pattern were weak (few data points, high standard deviation), a stepwise approach was followed. This approach allowed us to parametrize the simulation model with sufficient accurateness for describing fungal growth and resulting P and C dynamics (compare Figure 2-7).

In a first step, according to the design of experiment 1, it was assumed that growth speed was measured during a phase, in which neither carbon nor phosphorus but metabolic processes were limiting fungal growth. Therefore, processes describing the impact of nutrient limitation in the model were not considered in this step. As a result, only the probabilities to grow from one cell to another due to convection (V) and diffusion (D) were left as parameters influencing growth speed. They were chosen to result in the growth speed measured in experiment 1.

In the second step, according to the design of experiment 2, nutrient limitation processes were included into the model, and parameters relevant for nutrient exchange, transport and sporulation (see Table 2-2) were chosen to result in a dynamics which fit to that measured in experiment 2. The dynamics resulting from the parametrized simulation model together with the measured dynamics are shown in Figure 2-7.

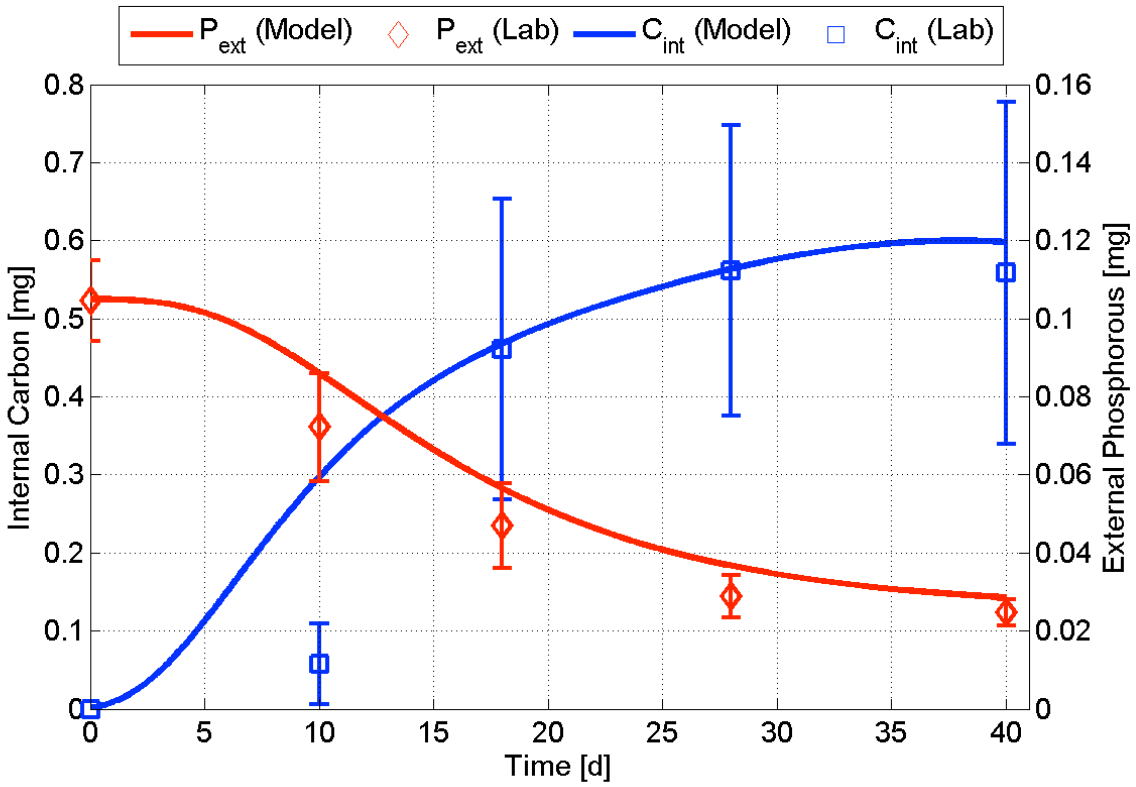

Figure 2-7.Measured and simulated dynamics of carbon and phosphorus.

Since external diffusion of phosphorus and fungal growth were found to take place on different time scales in the experimental system, external diffusion coefficients for P could not be calibrated by means of the measured nutrient dynamics without dramatically decreasing time steps and thus unacceptably long simulation time. Thus, for parameterization the external diffusion of phosphorus was not spatially explicitly considered but an infinite diffusion rate was assumed. This means, all fungal hypha had access to the whole amount of external phosphorus. Thus, the spatial explicitness of the fungal mycelium had no effect on model calibration. The impact of this assumption was studied in chapter 3 considering the consequences of finite external diffusion rates and spatially heterogeneous distribution of external P.

Table 2-2: Parameters with units, calibrated values and calibration method

Parameter	Unit	Calibration method	Value
Δx	[mm]		0.5
α	[-]	Calibrated on experimental data Ex2	0.1
a	[mg mm^{-1}]	Calibrated on experimental data Ex2	1.00E-06
b	[d^{-1}]	Calibrated on experimental data Ex1	0.09
C_{int}	[mg]	Initial Value	1.00E-03
C_{max}	[mg]	Calibrated on experimental data Ex2	2.00E+03
C_{min}	[mg]	Calibrated on experimental data Ex2	3.00E-04
D	[mm^2 d^{-1}]	Calibrated on experimental data Ex 1	0.01
D_C	[mm^2 d^{-1}]	Calibrated on experimental data Ex2	1.00E-03
D_{ext}	[mm^2 d^{-1}]	Infinite on experimental data Ex2	∞
D_P	[mm^2 d^{-1}]	Calibrated on experimental data Ex2	1.00E-03
$D_{spore,C}$	[mg]	Calibrated on experimental data Ex2	1.00E-05
$D_{spore,P}$	[mg]	Calibrated on experimental data Ex2	1.00E-05
g_c	[mg mm^{-1}]	Calibrated on experimental data Ex2	1.00E-06
g_p	[mg mm^{-1}]	Calibrated on experimental data Ex2	1.00E-08
k	[mg]	Calibrated on experimental data Ex2	2.50E-09
k_c	[mg]	Calibrated on experimental data Ex2	1.00E-29
k_P	[mg]	Calibrated on experimental data Ex2	1.00E-30
K_m	[mg]	Calibrated on experimental data Ex2	5.00E-05
$maxC_{spore}$	[mg]	Calibrated on experimental data Ex2	1.00E-05
$maxP_{spore}$	[mg]	Calibrated on experimental data Ex2	1.00E-06
$minP_{upt}$	[mg]	Calibrated on experimental data Ex2	1.00E-09
P_{ext}	[mg]	Initial Value	0.08
P_{int}	[mg]	Initial Value	1.00E-07
V	[mm d^{-1}]	Calibrated on experimental data Ex 1	0.9
v_C	[mm d^{-1}]	Calibrated on experimental data Ex2	0.4
v_P	[mm d^{-1}]	Calibrated on experimental data Ex2	0.4

2.4 References

Bago, B., Azcón-Aguilar, C., Goulet, A. and Piché, Y. 1998 Branched Absorbing Structures (BAS): a feature of the extraradical mycelium of symbiotic arbuscular mycorrhizal fungi. New Phytologist 139: 375-388.

Boswell, G.P., Jacobs, H., Ritz, K., Gadd, G.M., and Davidson, F.A. 2007 The Development of Fungal Networks in Complex Environments. Bulletin of Mathematical Biology 69: 605-634.

Friese, C.F. and Allen, M.F. 1991 The Spread of VA Mycorrhizal Fungal Hyphae in the Soil: Inoculum Types and External Hyphal Architecture. Mycologia 83: 409-418.

Grimm, V., Frank, K., Jeltsch, F., Brandl, R., Uchmański, J. and Wissel, C. 1996. Pattern-oriented modelling in population ecology. Science of the total environment 183: 151-166.

Marschner, P. 2012 Mineral nutrition of higher plants, 3rd ed. San Diego, USA: Academic Press. 651p.

Moore, D., Robinson, G.D., Trince, A.P.J. 2011 21st Century Guidbook to Fungi. Cambridge University Press. 639pp.

Newsham, K.K., Fitter, A.H. and Watkinson, A.R. 1995 Multi-functionality and biodiversity in arbuscular mycorrhizas. Trends in Ecology and Evolution 10: 407–411.

Schüßler, A., Schwarzott, D. and Walker, C. 2001 A new phylum, the Glomeromycota: phylogeny and evolution. Mycological Research 105: 1413-1421.

Smith, S.E. and Read, D.J. 2008 Mycorrhizal symbiosis, 3rd ed. San Diego, USA: Academic Press. 800p.

Wang, B. and Qiu, Y.-L. 2006 Phylogenetic Distribution and evolution of mycorrhizas in land plants. Mycorrhiza 16: 299-363.

Chapter 3: Identification of AMF functional types in a plant-fungus interaction system

3.1 Introduction

In multiple studies, strains of arbuscular mycorrhizal fungi (AMF) have been shown to interact very differently with their plant partner (Johnson et al. 1997, Jansa et al. 2005, Avio et al. 2006). On a scale from parasitic to strongly mutualistic interactions, all forms of symbiosis could be observed. This resulted in a great discussion about the benefits and harms of AMF to their plant partners.

Marschner and Dell (1994), for instance, highlighted that AMF may be beneficial for their host plants by improving their phosphorus (P)-supply. They concluded this from the observation that P was depleted to a much larger extent around plant roots which were mycorrhized than in control plant systems without mycorrhiza. Since P is key resource for plant growth and P fertilizers are mostly produced from fossil resources which become scarce, an efficient P use gets more and more important. In contrast, Abott et al. (1984) found that mycorrhized subterranean clover developed worse than unmycorrhized controls in conditions where P was not limiting. However, in conditions of P scarcity, mycorrhized plants performed better. This implicated that AMF may not always be beneficial for plants. Although this is not very surprising, because AMF get carbohydrates from the plants, these results brought up different questions.

Under what conditions are AMF beneficial for plants in the sense of enhanced supply with P as key resource and biomass development? To what extent and how is the plant-fungus interaction altering/influencing the dynamics of the two key resources P and C?

Due to the complexity of these processes, it is unclear how the resulting dynamics of the two nutrients P and C depend on the fungal nutrient exchange strategy and how this strategy is influencing the fungal biomass growth. Since these questions can only be investigated by coupling matter flux aspects (P-dynamics) with organismic aspects (plant-fungus-interaction), it addresses also the linkage of biotic and abiotic processes by feedbacks in ecological systems which is a major upcoming challenge in ecology (Loreau, 2010).

The simulation model developed in Chapter 2 explicitly considers fungal nutrient uptake, transport inside the hyphae, and exchange with the plant as processes affecting fungal growth. Evidently, it has the appropriate structure to enable studies of the growth of fungal biomass resulting from a certain fungal nutrient exchange strategy. Therefore, using the simulation model, we study the performance of a variety of nutrient exchange strategies of artificial AMF ranging from strongly parasitic to strongly mutualistic. Using systematic parameter variation, we uncover functional types of AMF by exploring, classifying and characterizing three processes: the resulting dynamics of the two key nutrients P and C, and the resulting AMF biomass growth dynamics.

3.2 Methods

The simulation model developed in this thesis is used to simulate fungal growth as a result of nutrient exchange between the fungus and its plant partner (see Chapter 2). Spatial simulation area is the petri dish system of our lab experiments. Simulations run over 2000 h, 50 replicates are performed to minimize random artefacts. To investigate the role of different nutrient exchange strategies, parameters K_m and C_{min} of the plant-fungus interface (see eq. 11 of Chapter 2), which are responsible for nutrient exchange between the fungus and its plant partner, are varied. To give an impression, Figure 3-1 shows the representations of the functional response mediated by two fungal nutrient exchange strategies of different ends of the investigated range.

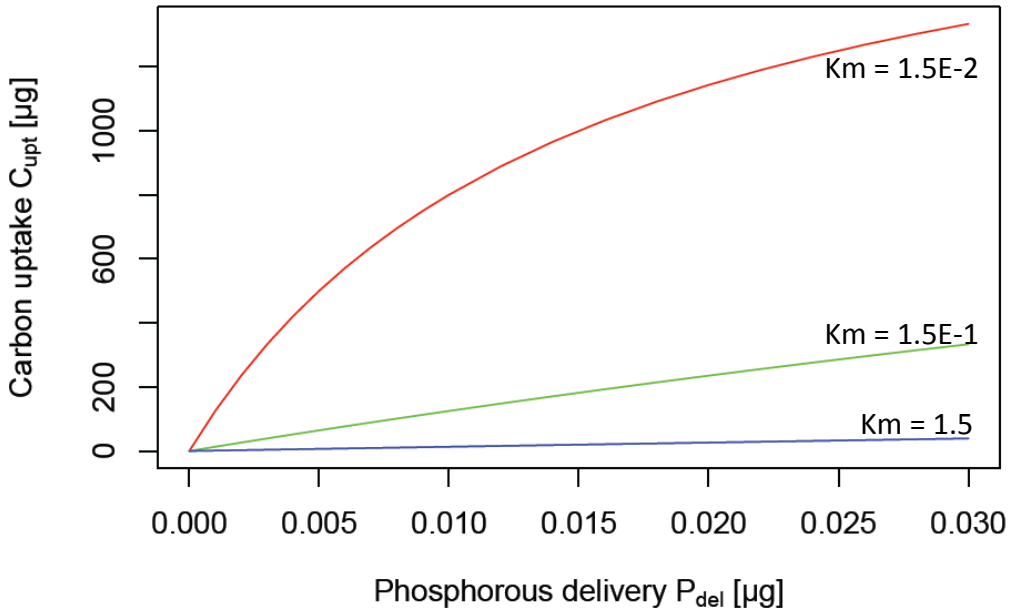

Figure 3-1. C uptake versus P delivery for two different fungal nutrient exchange strategies. The red curve (resulting from K_m = 1.5E-2 mg) exhibits a strongly parasitic nutrient exchange strategy (fungus gets much C for little P delivered),the green curve (resulting from K_m = 1.5E-1 µg) belongs to a intermediate type, while the blue curve (resulting from K_m = 1.5 µg) a strongly mutualistic nutrient exchange strategy (fungus gets little C for much P delivered). C_{min} was 3.0E-4 for all curves.

The parameter K_m directly indicates the type of symbiosis, where low values refer to parasitic and high values to mutualistic fungal nutrient exchange strategies. C_{min} is the minimum C delivery to the fungus, even without P delivery. Table **3-1** shows the values of C_{min} and K_m for the examined exchange strategies. As P-pool available to the fungus at the beginning of the simulation, an amount of 0.08 mg P is homogenously distributed over the whole simulated area. Substrate diffusion is set to an infinite speed, since laboratory experiments (see calibration section) showed that substrate diffusion was much faster than fungal growth. The simulation model simulates only the compartment of the petry dish in which the fungus grows alone, therefore simulations start at the time point of the laboratory experiment, where one fungal hypha manages to overgrow the barrier between the PF compartment and the F compartment (see Figure 2-2 in Chapter 2).

Table 3-1: Simulated nutrient exchange strategies. Codes indicate the simulated scenarios with varied K_m value [µg] and minimum C uptake rate C_{min} [µg].

	C_{min}[µg]			
K_m [µg]	**0.1**	**0.15**	**0.2**	**0.3**
1.5E-2	A1	A2	A3	A4
3.5E-2	B1	B2	B3	B4
8.5E-2	C1	C2	C3	C4
1.5E-1	D1	D2	D3	D4
3.5E-1	E1	E2	E3	E4
8.5E-1	F1	F2	F3	F4
1.5E0	G1	G2	G3	G4
3.5E0	H1	H2	H3	H4
8.5E0	I1	I2	I3	I4

3.3 Results

The first process to distinguish between the simulated fungal nutrient exchange strategies of artificial AMF and to evaluate their performance is fungal biomass growth. Figure 3-2 shows fungal biomass over time for all strategies. K_m is varied within each graph indicated by the different colors of the curves; C_{min} is varied between the graphs. As can be seen, biomass increases in time saturating at a maximum biomass that is inversely related to the value of K_m. Increasing C_{min} values have generally less influence. They lead to a slight increase in maximum biomass for nutrient exchange strategies with higher K_m. Thus, in terms of fungal biomass growth, high performance is achieved for exchange strategies with low K_m and high C_{min}.

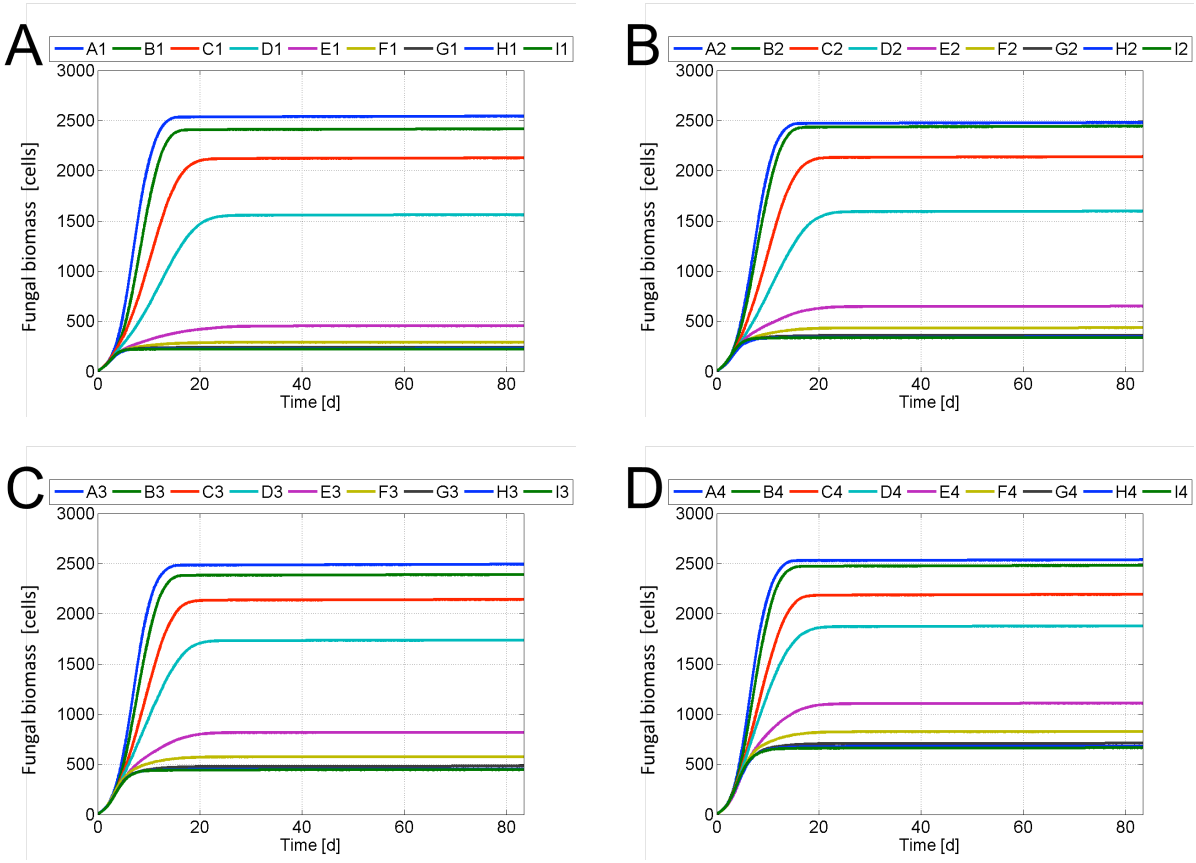

Figure 3-2: Fungal biomass [cells] over time [d] for all simulated nutrient exchange strategies (see Table 1). A: C_{min} = 0.1 µg, B: C_{min} = 0.15 µg, C: C_{min} = 0.2µg and D: C_{min} = 0.3 µg.

To get a better overview over all simulated strategies, Figure 3-3 shows the maximum fungal biomasses over the simulated K_m values for all C_{min} values. Figure 3-3 confirms the results of Figure 3-2: rising K_m values result in declining maximum fungal biomass for all C_{min}. C_{min} variations show almost no differences in maximum fungal biomass for low and medium K_m values, but start getting more important for higher K_m. Above a threshold of K_m = 3 µg, rising K_m values do not affect maximum biomass anymore, whereas rising C_{min} values increase the maximum fungal biomass.

This can be explained by looking at the mechanism behind the varied parameters. K_m directly influences the value of P units to be supplied to get one unit of C and therefore directly indicates the nutrient exchange strategy of the fungus. Very low K_m values imply that the fungus gets much C for little P (Fig. 1). Because of the infinite P diffusion rate assumed in the simulated scenarios, the fungus can always deliver P to the plant and so C delivery never drops to the minimum C_{min}. With higher K_m values, the fungus gets less C for its P and the C

delivery rates drop down to the corresponding minimum C_{min}, which explains the rising relevance of C_{min} with increasing K_m.

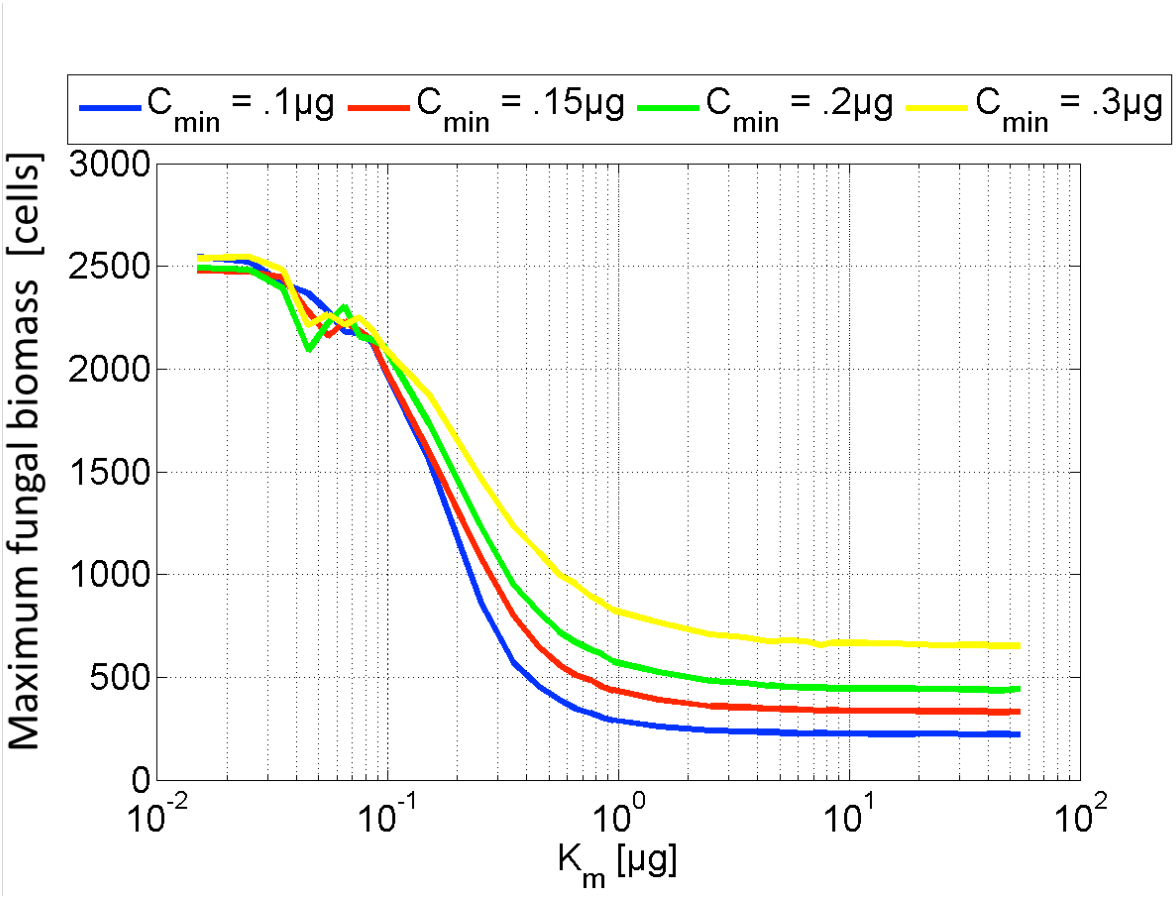

Figure 3-3: Maximum fungal biomass [cells] over K_m [µg] for all simulated C_{min} [µg] values. To show the minimum maximum fungal biomass for all simulated C_{min}, the range of simulated K_m values was extended to a maximum K_m of 5.5E2 for this graph.

To manifest this explanation, Figure *3-4* shows the resulting fungal C uptake rate over time for all simulated nutrient exchange strategies. Evidently, C uptake over time is unimodal. Starting from the initial value C_{min} (the minimum C uptake rate), it first increases with time, reaches a peak resp. plateau, and then decreases again to a minimum uptake that does not change anymore. The value of K_m affects the unimodal shape of the C uptake curve including the height and width of the peak resp. plateau, whereas C_{min} affects the long-term minimum value of C uptake. All strategies show the peak of C uptake in the first third of the simulation period. Comparing this with the biomass time series (Figure 3-1), this peak and the quick decrease correspond with the growth period of fungal biomass. The peaks of strategies A

and B reach the maximum possible C uptake rate ($C_{max,}$ see Chapter 2) that causes the formation of a temporal plateau. The corresponding fungi, therefore, become able to store P and use this surplus to maintain higher C uptake after the growth phase. On closer inspection, the long-term minimum value of C uptake corresponds to the C_{min} value or, for strategies A and B, the double of the C_{min} value. The explanation for this picture is that all strategies except A and B are too mutualistic (get too little C for their P). Therefore, they can never reach their maximum C uptake rate and are thus not able to store P in their mycelium. C uptake rates begin to decrease when all external P is taken up by the fungus. This also stops fungal growth (also for the parasitic strategies A and B) since P is stored near the plant-fungus interface and not at the fungal tips, where growth takes place. When P is depleted and P uptake decreases at the fungal tip, fungal growth stops.

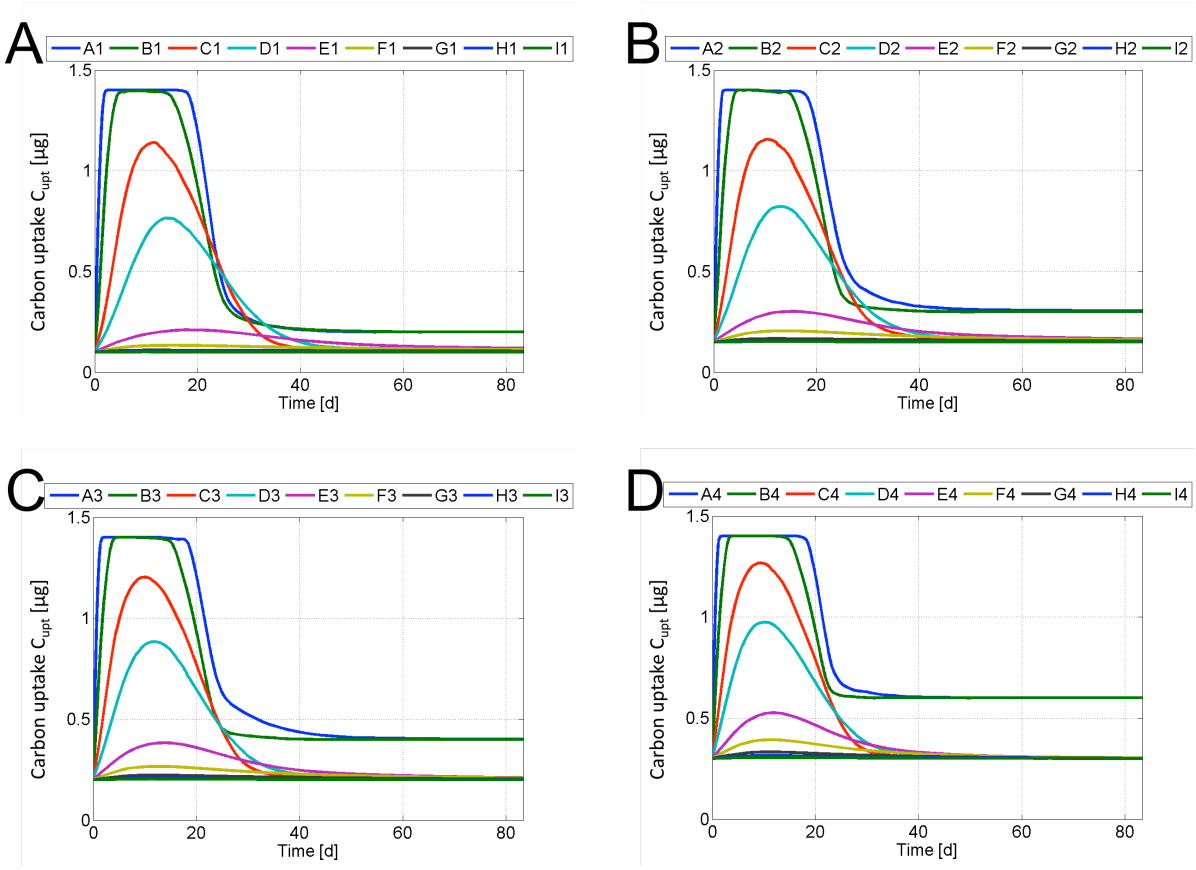

Figure 3-4: C uptake [µg] over time [d] for all simulated nutrient exchange strategies (see Table 1). A: C_{min} = 0.1 µg, B: C_{min} = 0.15 µg, C: C_{min} = 0.2µg and D: C_{min} = 0.3 µg.

For a broader overview, Figure 3-5 shows the mean C uptake rates as a function of K_m and C_{min}. Comparable with the corresponding plot of maximum fungal biomass (Figure 3-3),

rising K_m values result in dropping mean C uptake rates. But while maximum fungal biomass does not depend on C_{min} at low K_m values, the mean C uptake rate does depend on $C_{min.}$ This is because, after the growth phase, none of the strategies can maintain a high C uptake due to dropping P availability. Even strategies A and B suffer from P scarcity and allow their C uptake to drop to a lower value.

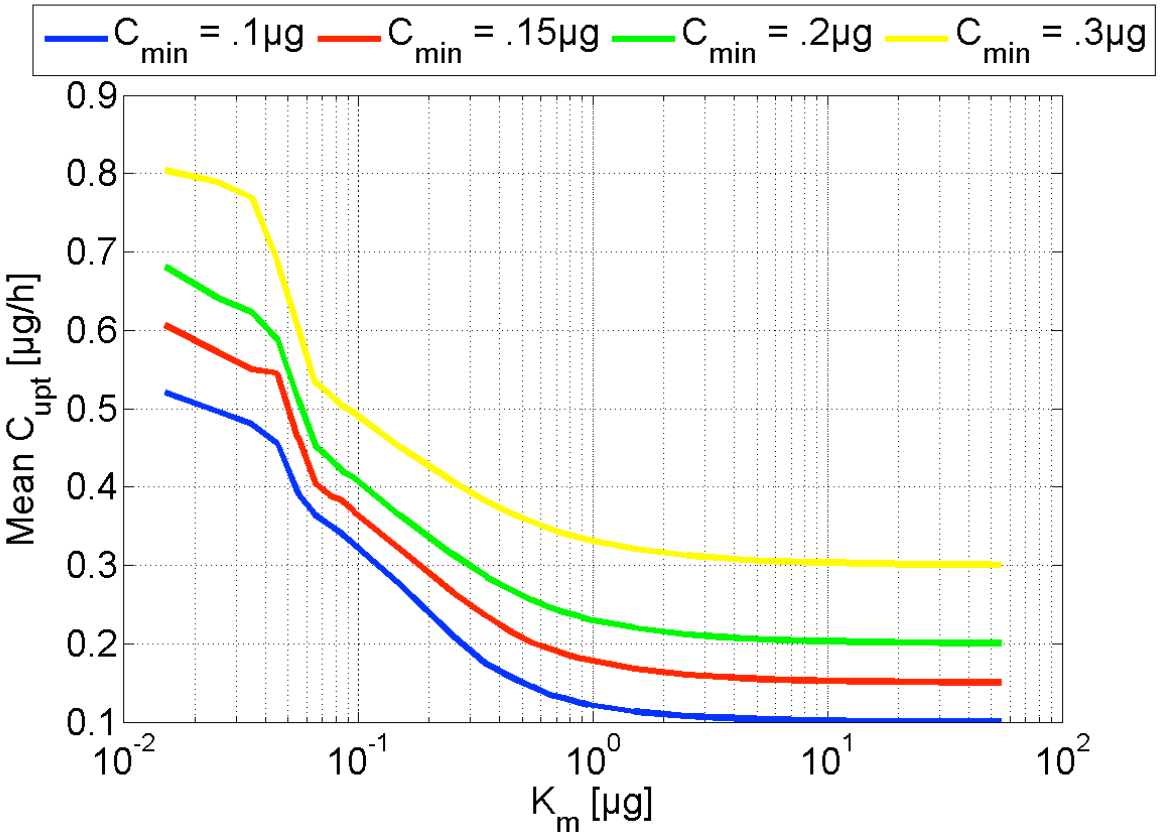

Figure 3-5: Mean C uptake rates [µg h^{-1}] over K_m for all C_{min} values.

Looking at P delivery, Figure 3-6 shows the mean P delivery rates over K_m for all simulated C_{min}. For low K_m values, the P delivery rates respond only marginally to changes in the C_{min} values. Like in the plot of maximum fungal biomass (cf. Figure 3), C_{min} gets only important for higher K_m. In this depiction, however, the functional responses of the P delivery rates to further changes in K_m strongly differ between the considered C_{min} values. For low C_{min}, the P delivery rates drop down with rising K_m to a level which coincides with that for a strongly parasitic strategy (e.g. low $K_m = 10^{-2}$), whereas P delivery rates can be maintained at the maximum level for high C_{min}. This can be explained by the slightly higher maximum fungal

biomass of the scenarios with high C_{min} (Figure 3-3), which results in higher P uptake rates for them and so in higher P delivery rates (Figure 3-6). However, even though these scenarios get more C and can deliver more P, they cannot profit from their higher P delivery rates in terms of C uptake as C uptake at high K_m is always as low as the corresponding C_{min} value (Figure 3-5).

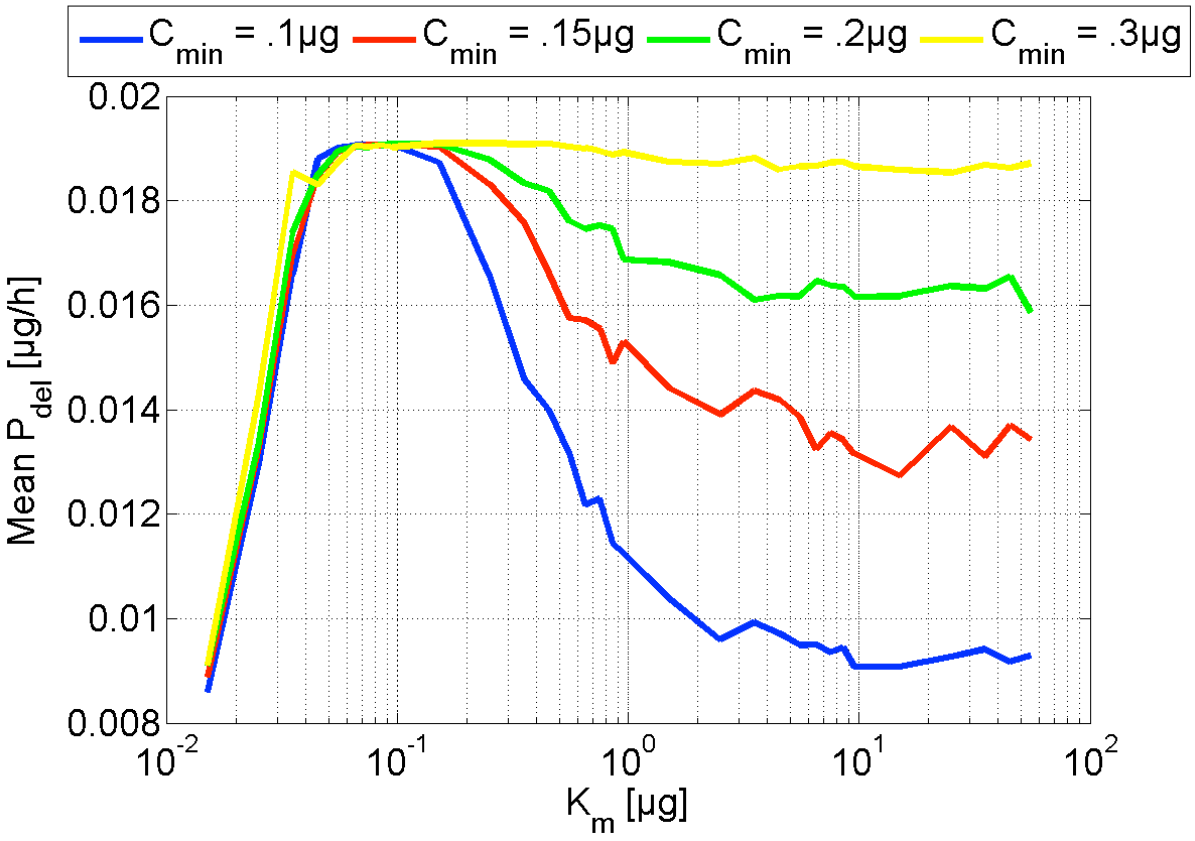

Figure 3-6: Mean P delivery rates [µg h^{-1}] to the plant over K_m for all C_{min} values.

To summarize, in our artificial AMF, the value of K_m strongly influences the development of fungal biomass, fungal C uptake rate and P delivery rate for all tested C_{min} values. The value of C_{min} itself gets only important at high K_m values. Figure 3-3, Figure ***3-5*** and Figure ***3-6*** show that, among all simulated nutrient exchange strategies, the more parasitic ones (low K_m values) perform best in terms of fungal biomass and C uptake rates but have low P delivery rates. Medium K_m values result in high P delivery, but in just medium fungal biomass and medium C uptake. High K_m values result in low fungal biomass and low C uptake. The P

delivery rates strongly increase with increasing C_{min}. The high P delivery at high C_{min} values that is particularly beneficial for the plant is mainly mediated through the assumption of infinite diffusion speed, which allows high P uptake rates even with low fungal biomass.

3.4 Discussion

The simulation model developed in the Methods Chapter 2 was able to reveal the consequences of different fungus-plant interaction strategies regarding the fungal nutrient exchange with the plant (C uptake for P delivery) for resulting fungal biomass growth, the P delivery dynamics from the fungus to the plant and the C uptake dynamics from the plant to the fungus. Evaluating the performance of the different simulated fungal nutrient exchange strategies (indicated by km and C_{min}) by the emerging maximum achievable fungal biomass, the C uptake rate and the P delivery rate, three functional types could be identified. These functional types are based on characteristic ranges of values for fungal biomass, C uptake rate and P delivery rate as a function of Km and C_{min} (Figure 3-3, Figure ***3-5*** and Figure ***3-6***). We could show that these ranges can be mainly classified along a single indicator: the K_m value of the nutrient exchange strategy.

The first functional type is characterized by low K_m up to about 3.5E-2 µg. Evidently, these fungi can achieve very high biomass (Figure 3-3), take up high amounts of C (Figure 3-5), but deliver almost no P to the plant (Figure 3-6). This means that the fungus profits from the plant in terms of C supply without delivering any substantial P amounts. Therefore, this first functional type of fungi can be seen as parasites and correspondingly we call the nutrient exchange strategy as 'parasitic'.

The second functional type characterized by K_m values between 3.5E-2 and 3E-1 was found to evolve fungal biomass and C uptake rates which are lower than in the functional type of parasitic exchange, whereas the evolved P delivery rates are around the maximum (reached at K_m = 1E-1 µg). Thus, the fungi profit from the plant in terms of C supply but have to deliver a substantial reward in form of P to the plant. Accordingly, this functional type of fungi can be seen as intermediate between pure parasites and pure mutualists and the nutrient exchange strategy was called as 'intermediate'.

The third functional group characterized by high Km values above 3E-1 µg evolves low fungal biomass and C uptake rates but strongly varying P delivery rates depending on the assumed

value of C_{min}. Hence, although fungi profit from the plant in terms of C supply they have to deliver a high reward in form of P to the plant. Therefore, this functional type of fungi mediates the strongest mutualistic interaction possible. This type can only build substantial biomass when minimum C delivery rates (C_{min}) are high. For K_m values above 5E-1 µg, the system crashes because fungi don't get enough C to grow a biomass that is sufficiently able to take up relevant amounts of P. Therefore, no further increase in mutualism is possible. Such plant-fungus interactions would not be able to exist in nature because fungi would not have enough energy to build relevant biomasses and reproduce.

The identification of these three AMF functional types is essential as it facilitates understanding of the relevance of the plant-fungus nutrient exchange strategy for the coupling of the C and P flux dynamics mediated by the artificial AMF considered in this study. It helps structuring the variety of possible exchange strategies (described by the parameter K_m) in terms of their impact on nutrient cycling and fungus biomass growth.

The identification of functional types is common in recent ecological research to reduce the complexity and variety of species in a specific ecosystem and so to get a better understanding of the system. The classification can be done using different indicators. Kazmierczak et al. (2015) used the response of plants to water stress as an indicator to identify two different plant functional types with different live strategies. Like in the present model, Kazmierczak et al. (2015) used only one parameter to determine the plant functional type. This simplicity is crucial to simulate the reaction of plants on different water regimes in larger models. Specifically, modelling tropical rain forests makes the use of plant functional types indispensable because of the infeasible number of different plant species. Köhler et al. (2000) used the successional status and the potential maximum height as parameters to indicate 15 different plant functional types in a tropical rain forest. Picard et al. (2012) found, while comparing five different classifications that tree species can be classified, using two almost completely independent axis (light requirement (at least at young stages) and potential size).

In the present study, we were able to reduce the complexity of different artificial AMF species to solely one trait (the nutrient exchange strategy). Torrecillas et al. (2012) have mentioned that different plant functional types were colonized by different strains of AMF and a different number of strains of AMF. Tinker et al. (1994) defined the symbiotic

efficiency as the surplus carbon gained by the plant as a response to AMF minus the amount of carbon invested for the symbiosis. However the response was found to depend on many biotic factors like community composition (e.g. Klironomos et al. 2000) and abiotic factors such as nutrient availability or humidity (e.g. Staddon et al.2003), even for the same fungus-plant combination (Burleigh et al. 2002, Smith et al. 2004). Since every arbuscular mycorrhizal association is a response to the different involved plants and fungi in the environment they inhabit (Feddermann et al. 2010), to our knowledge, no study tried to find functional types for AMF. Not only for plants, but also for animal species, grouping into functional types is possible, although less common (Blaum et al., 2011).

To parameterize the model and identify three functional types, the approach of pattern-oriented modelling (Grimm et al. 1996) was used. This approach (often also mentioned as inverse modeling) is widely used and accepted in environmental and especially ecological modelling (see e.g. Grimm et al. 2006, Wiegand, 2003). Its main idea is to utilize patterns that emerge at higher systems levels as basis for the parameterization of factors and processes on lower systems levels which are relevant for research question and model but are hard to determine directly or are sometimes even hidden. Following the proposal of Loreau (2010) of linking biodiversity and ecosystem research, it was possible to reduce this variety of plant-fungus interactions to three functional types characterized by three parameter ranges of K_m with typical biomass and nutrient dynamics. These three functional types describe parasitic, intermediate and mutualistic nutrient exchange strategies. This classification of the plant-fungus interaction by functional types can be used for further investigation of their performance in systems with temporally varying P availability and spatial heterogeneity since it shows the potential biomass of the different types and gives insight into the functioning of the coupled cycles of P and C.

In the following two chapters, we continue working with artificial AMF in the frame of a virtual lab approach. We systematically analyze implications of the three identified AMF functional types for the dynamics of fungal biomass and coupled C/P fluxes by taking into account temporal and spatial heterogeneity in the availability of P as scarce key resource.

3.5 References

Abott, L.K., Robson, A.D. and De Boer, G. 1984 The effect of phosphorus on the formation of hyphae in soil by the vesicular-arbuscular mycorrhizal fungus, Glomus fasciculatum. New Phytologist 97: 437-446.

Avio, L., Pellegrino, E., Bonari, E. and Giovannetti, M. 2006 Functional diversity of arbuscular mycorrhizal fungal isolates in relation to extraradical mycelial networks. New Phytologist 172: 347-357.

Blaum, N., Mosner, E., Schwager, M. and Jeltsch, F. 2011. How functional is functional? Ecological groupings in terrestrial animal ecology: towards an animal functional type approach. Biodivers.Conserv. 20: 2333-2345

Burleigh, S.H. Cavagnaro, T. and Jakobsen, I. 2002. Functional diversity of arbuscular mycorrhizas extends to the expression of plant genes involved in P nutrition. Journal of Experimental Botany 53: 1593-1601.

Feddermann, N., Finlay, R., Boller, T. and Elfstrand, M. 2010. Functional diversity in arbuscular mycorrhiza – the role of gene expression, phosphorus nutrition and symbiotic efficiency. Fungal Ecology 3: 1-8.

Grimm, V., Frank, K., Jeltsch, F., Brandl, R., Uchmański, J. and Wissel, C. 1996. Pattern-oriented modelling in population ecology. Science of the total environment 183: 151-166.

Grimm, V., Revilla, E. Berger, U., Jeltsch, F., Mooij, W.M., Railsback, S.F., Thulke, H.-H., Weiner, J., Wiegand, T. and DeAngelis, D.L. 2006. Pattern-oriented modeling of agent-based complex systems: Lessons from ecology. Science 310: 987-991.

Jansa, J., Mozafar, Ahmad and Frossard, E. 2005 Phosphorus acquisition strategies within arbuscular mycorrhizal fungal community of a single field site. Plant and Soil 276: 163-176.

Johnson, N.C., Graham, J.H. and Smith, F.A. 1997 Functioning of mycorrhizal associations along the mutualism–parasitism continuum. New Phytologist 135: 575–585.

Kazmierczak, M., Johst, K., and Huth, A. 2015. Conservatives and Gamblers: Interpreting plant functional response to water stress in terms of a single indicator. Ideas in Ecology and Evolution 8:29-41.

Klironomos, J.N., McCune, J., Hart, M. and Nevill, J. 2000. The influence of arbuscular mycorrhizae on the relationship between plant diversity and productivity. Ecology Letters 3: 137-141.

Köhler, P., Ditzer, T. and Huth, A. 2000. Concepts for the aggregation of tropical tree species into functional types and the application on Sabah's dipterocarp lowland rain forests. Journal of Tropical Ecology 16:591-602.

Loreau, M. 2010 Linking biodiversity and ecosystems: towards a unifying ecological theory. Philosophical Transactions of the Royal Society B 365: 49-60.

Marschner, H. and Dell, B. 1994. Nutrient uptake in mycorrhizal symbiosis. Plant and Soil 159: 89-102.

Picard, N., Köhler, P., Mortier, F. and Gourlet-Fleury, S. 2012. A comparison of five classifications of species into functional groups in tropical forests of French Guiana. Ecological Complexity 11: 75-83.

Smith, S.E., Smith, F.A. and Jakobsen, I. 2004. Functional diversity in arbuscular mycorrhizal (AM) symbioses: the contribution of the mycorrhizal P uptake pathway is not correlated with mycorrhizal responses in growth and total P uptake. New Phytologist 162: 511-524.

Staddon, P.I., Thompson, K., Jakobsen, I. Grime, J.P., Askew. A.P. and Alastair Fitter, A.H. 2003. Mycorrhizal fungal abundance is affected by long-term climatic manipulations in the field. Global Change Biology 9: 186-194.

Tinker, P.B., Durall, D.M. and Jones, M.D. 1994. Carbon use efficiency in mycorrhizas: theory and sample calculations. New Phytologist 128:115-122.

Torrecillas, E., Alguacil, M.M. and Roldán, A. 2012. Host preferences of arbuscular mycorrhizal fungi colonizing annual herbaceous plant species in semiarid Mediterranean prairies. Applied and Environmental Microbiology 78: 6180-6186.

Wiegand, T., Jeltsch, F., Hanski, I. and Grimm, V. 2003. Using pattern-oriented modeling for revealing hidden information: A key for reconciling ecological theory and application. OIKOS 100: 209-222

.

Chapter 4: Performance of AMF functional types in equalizing phosphorus pulses for plants

4.1 Introduction

Plant nutrients are in many cases not permanently available, because of their appearance depending on varying environmental factors. These can be precipitation, which itself can enter nutrients to the soil, or the resulting rise of soil water content can dissolve new mineral nutrients which, in this way, can become available to plants. Additionally, temperature variations can change the activity of soil microorganisms which are relevant for remineralization of organic matter or fixation of areal nitrogen. Even organic matter itself is not always available. Therefore, regular seasonal variations or irregular plant age and weather variations trigger the availabilities of plant nutrients in natural ecosystems. This results in fluctuating or pulsed resources for the plants (e.g. Craine 2009).

Thus, plants have to cope with times of nutrient scarcity alternating with times of high nutrient abundance. One way to cope with this insecurity in nutrient supply is to quickly utilize nutrient pulses to avoid losing them to ground or surface waters. Plant root systems, however, are not very flexible and thus are in most cases not able to react quickly enough (e.g. Lamb et al. 2012). Therefore, plants may cooperate with AMF to increase their root system and to exchange nutrients (e.g. P and C).

Furthermore, nutrient pulses may result in temporally varying conditions at a given place. Therefore, plants have to cope with varying nutrient availabilities. This may leave room for different strains of fungi with different fungal nutrient exchange strategies to be optimal at different nutrient conditions. Plants could use the diversity of available AMF to cope with temporal or spatial variability in nutrient availability.

Nutrient pulses are known to have large impacts on the fate of nutrients in ecosystems, but their importance has been found and forgotten several times in literature (Lodge et al. 1994). In tropical forests (Lodge et al. 1994), in temperate ecosystems (Hunt et al. 1989), but also in marine ecosystems (Shaffelke and Klumpp, 1998), nutrient pulses were found to have large impact on the microbial composition of the ecosystems. Lodge et al. (1994) have found that asynchrony of mineralization of nutrients and their use by plants can result in nutrient

loss from the system. Therefore, nutrient pulses play a critical role in maintaining the productivity of tropical forests. However, little is known about natural strategies of mitigating or utilizing nutrient pulses and whether AMF are able to fill this gap. In natural ecosystems, it is very hard to distinguish between individual fungi, which make it impossible to follow the path of nutrients from their pulsed appearance over their fungal uptake and transport to plants. Therefore this question cannot be answered without the use of simulation models. However, only few models for the simulation of arbuscular mycorrhiza exist. In existing models fungal growth usually depends only on carbohydrates, the extraradical mycelium of AMF is not modeled spatially explicit but as hyphae density and nutrient exchange between plants and fungi is ignored. Schnepf et al. (2008), e.g. did not consider nutrient exchange between fungi and plants or transport in the hypha and used density distributions for fungal mycelium. In a following study (Schnepf et al. 2011) they developed a mathematical model to simulate nutrient uptake by a single non growing hypha in soil. These models address interesting questions and help to get further understanding AMF, but cannot fully address the questions of plant benefit.

The model developed in this thesis (see Methods Chapter 2), for instance, simulates spatially explicit growth of individual hyphae depending on P and C availability, uptake of P from the surrounding of the fungi, transport of P to the plants and exchange for C. This makes it possible to follow P from its pulsed availability over the fungus to the plant on a very fine temporal and spatial scale. These properties are essential to investigate the question of AMF being able to equalize nutrient pulses for plants.

In this study, we investigate to what extent AMF are able to quickly respond to nutrient pulses and to transform these pulses into a continuous nutrient flow and supply to the plant. In particular, we examine the influence of the fungal nutrient exchange strategy and of the pulse regime on this transformation and equalization process. This is important as the capacity of the plant-fungus-interaction to buffer resource pulses may depend on both the exchange strategy and the pulse regime.

4.2 Methods

We use the simulation model developed in Chapter 2. but change the pattern of fungal P availability from a given amount fully available from the beginning of the simulation to a pulsed availability to become able to tackle the questions of consequences of nutrient

pulses. To examine the influence of the various fungal nutrient exchange strategies, we again vary K_m over the same spectrum like in Chapter 3 from parasitic to mutualistic interactions. In Chapter 3, we have found that C_{min} only becomes important when P is depleted, which gives rise to the hypothesis that C_{min} also becomes relevant in the case of regimes with very low P availability in the fungal compartment. In this study of P pulses, there are no regimes of permanent low P availability which would show a noticeable sensitivity to C_{min} variations. Therefore, we keep C_{min} constant in this study. To examine the impact of the pulse regime on the equalization effect of the AMF, two basically different pulse regimes are considered: regular small pulses versus irregular large pulses (see Table 4-1). A pulse is said to be regular or irregular if the time between two pulses is equal or very different respectively. Both regimes coincide in the total amount of P supplied over the simulated timespan, but in regime 1, there are 9 small equally strong, regular pulses, where in regime 2, there are 3 large equally strong, irregular pulses.

Table 4-1: Settings of two different pulse regimes

Parameter	Regular small Pulses	Irregular large Pulses
Number of Pulses in T_{max}:	9	3
Time between two Pulses:	33 h	33 h – 258 h
Amount of P per Pulse:	0.08 mg	0.24 mg
Total amount of P in T_{max}:	0.72 mg	0.72 mg

We simulated over T_{max}=350 h and made 50 replicates to minimize randomization artefacts.

4.3 Results

To check whether and how AMF equalize resource pulses for the plant, we first study the resulting nutrient dynamics for C and P as a function of the fungal nutrient exchange strategy under the two different pulse regimes. Figure 4-1 shows the C and P dynamics for the three AMF functional types identified in Chapter 3 with their characteristic nutrient exchange strategies (specified by respective K_m values) and the two pulse regimes (Table 4-1).

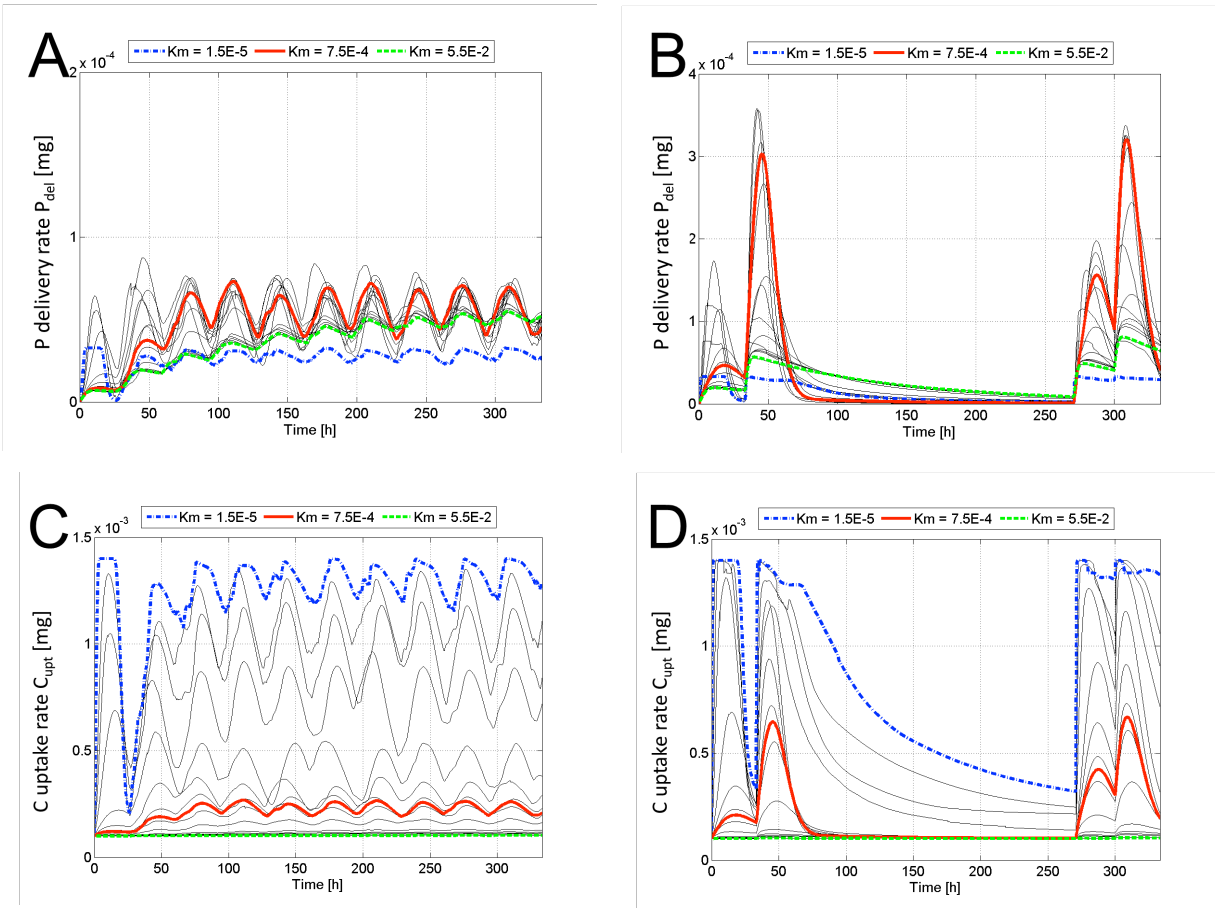

Figure 4-1: Nutrient dynamics for different K_m-values representing three AMF functional types with characteristic nutrient exchange strategies and the two P pulse regimes given in Table 4-1. (A and C): Regular P pulse regime; (B and D): Irregular P pulse regime; (A and B): P delivery to the plant P_{del}; (C and D) C uptake of the fungus C_{upt}. Colors exemplify K_m values of the parasitic (blue), the intermediate (red) and the mutualistic (green) AMF functional type. Grey lines show K_m values in-between.

The dynamics of P delivery over time (Figure 4-1 A and B) is strongly influenced by the K_m value of the AMF functional type and its nutrient exchange strategy. Accordingly, mean and variance in the corresponding P delivery curves strongly depend on the K_m value as well. Evidently, equalizing external P pulses seems to be best for high (green curve) and low (blue curve) K_m values and weak for intermediate values (red curve) in both pulse regimes.

The dynamics of fungal C uptake rates (Figure 4-1C and D) differs much more among the simulated K_m values than the dynamics of P delivery. It shows two characteristic responses that are common for both pulse regimes: (i) After a first maximum, there is an initial large

breakdown of the fungal C uptake rate C_{upt} which becomes stronger when Km decreases. This is a reflection of the higher P demand during fungal biomass growth. As a result, less amounts of P are available for delivery to the plants that, in turn, diminishes the return of C from the plant to the fungus (cf. Figure 4-1C and Figure ***4-1***D). (ii) Variance and mean of the pulse-induced fluctuations in the fungal C uptake rate decrease with increasing K_m. Since rising K_m values indicate more mutualistic fungi (cf. the discussion in Chapter 3), these fungi have a flatter nutrient exchange (C vs. P) function. So rising P delivery rates result in lower C uptake rates than for fungi with lower K_m values. This downsizes the entire C_{upt} curve with consequences for the respective mean and variance. To find a more objective measurement to compare the performances of the different AMF functional types in equalizing of the nutrient fluxes under the two pulse regimes, we plotted the standard deviations of the nutrient dynamics as a measure for the fungal equalization ability and the arithmetic means to characterize the amount of nutrients exchanged, over the corresponding K_m values (Figure 4-2). Low standard deviations indicate a good equalization ability of the fungal nutrient exchange strategy and high arithmetic means good delivery abilities.

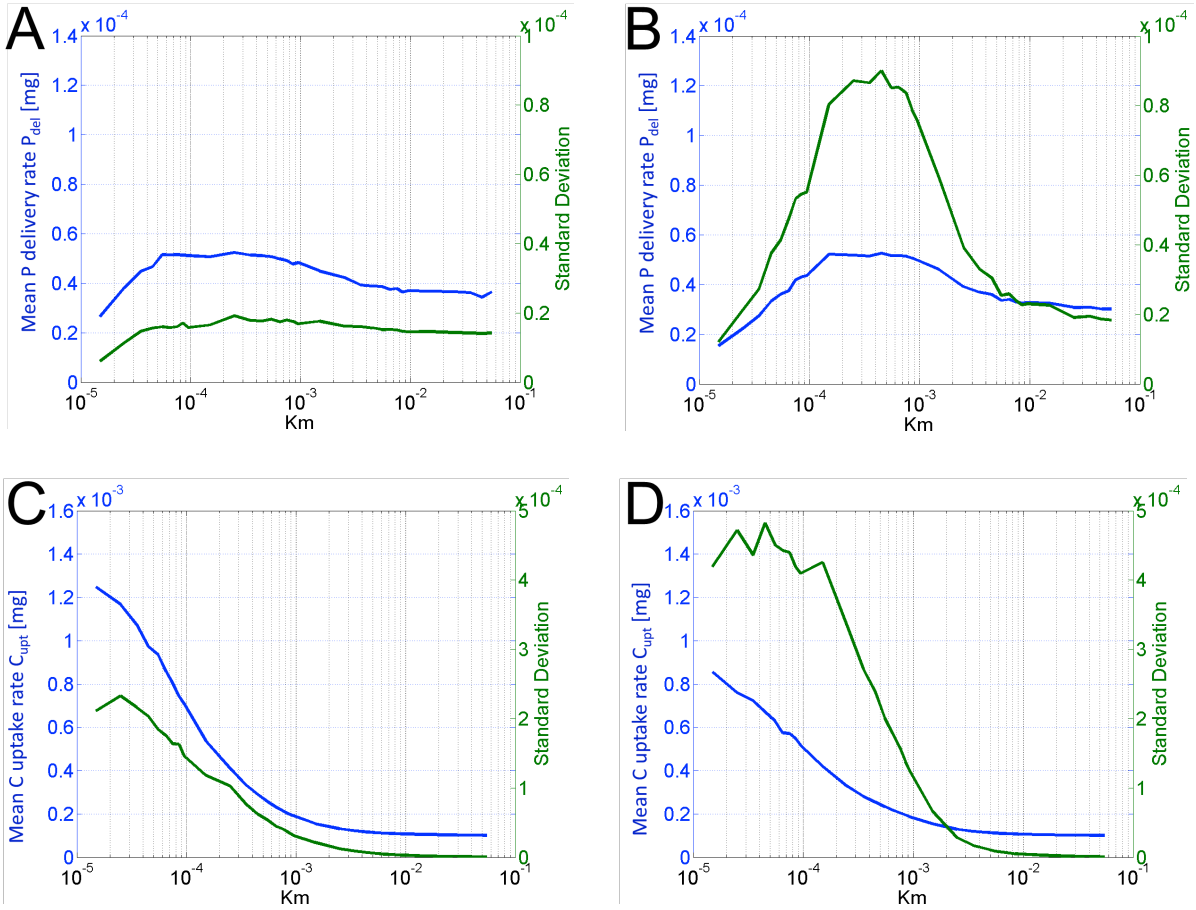

Figure 4-2: Mean (blue curves) and standard deviation (green curves) of the P delivery rate P_{del} (A, B) and fungal C uptake rate C_{upt} (C, D) over K_m. (A,C): Pulse regime 1; (B, D): pulse regime 2.

These plots show falling means and falling standard deviations for the C uptake rates for rising K_m values in both simulated pulse regimes (Figs. 2C and 2D). This clearly reflects knowledge from Chapter 3 about the fungal nutrient exchange strategies underlying the respective AMF functional types: low K_m values (parasitic type) cause high C uptake rates, whereas high K_m values (mutualistic type) cause low C uptake rates. Under pulse regime 1, the maximum C uptake rate is larger than under regime 2. Like we have expected from simulations of the temporal dynamics, low K_m values result in high standard deviations, which means, weak equalization. Moreover, standard deviations scatter a bit at this end of the range of simulated Km values, which can be explained by random artifacts. Standard deviations are in pulse regime 2 higher than in regime 1. This means that under the regime with large random pulses, fungi take up more C and uptake rates vary more over time.

Mean P delivery rates peak at medium K_m values, but standard deviations do so as well (Figure 4-2A and B). While the peak of standard deviations is small compared to that of the mean delivery rates under pulse regime 1, it is high under pulse regime 2.

Therefore, one could say that, under both pulse regimes, AMF can equalize externally induced P pulses. Under regime 1, the values of the standard deviation are generally low, regardless of the K_m values. In this case, the equalization capacity of the AFM is independent of the details of the fungal nutrient exchange strategy. In contrast, under regime 2, the equalization capacity strongly and nonlinearly depends on the K_m value and so on the nutrient exchange strategy. Equalization is strongest at very parasitic or very mutualistic interactions and weak in-between, which suggest the existence of two different equalizing mechanisms, which do not overlap at medium K_m.

As a last step of the study, we examine the dynamics of fungal biomass. Figure 4-3 shows the biomass at simulation end for all simulated K_m values.

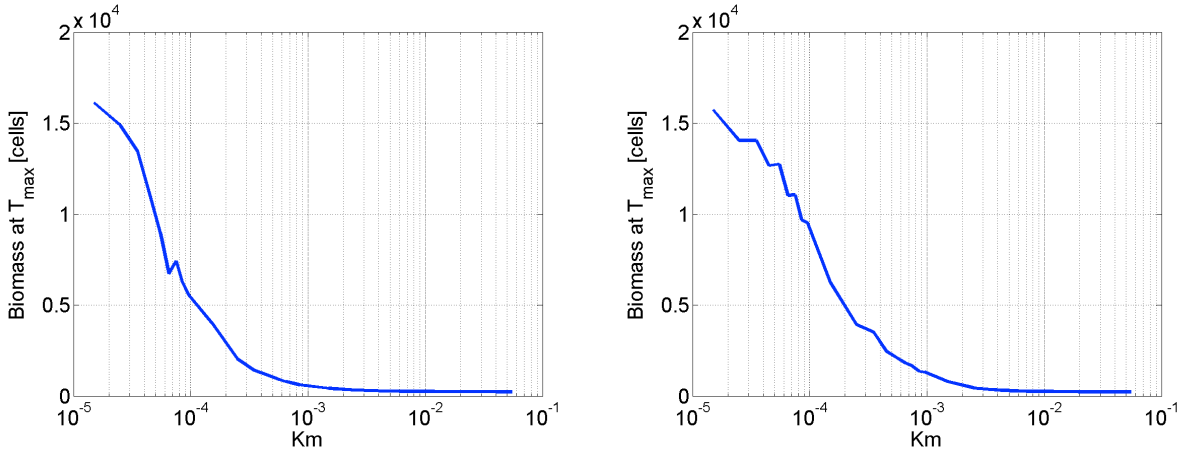

Figure 4-3: Fungal biomass at T_{max} over simulated K_m for pulse regime 1 (left) and pulse regime 2 (right).

Under both pulse regimes, rising K_m values result in drastically decreasing fungal biomasses. To fully understand the influence of fungal biomass on the C and P dynamics, Figure 4-4 shows the build-up of fungal biomass over time. It indicates almost no additional fungal growth after 50 hours. This is in line with P delivery and C uptake rates which do not show a trend over time (except for very high K_m values, which show slightly rising P delivery values over time in the regular pulse regime).

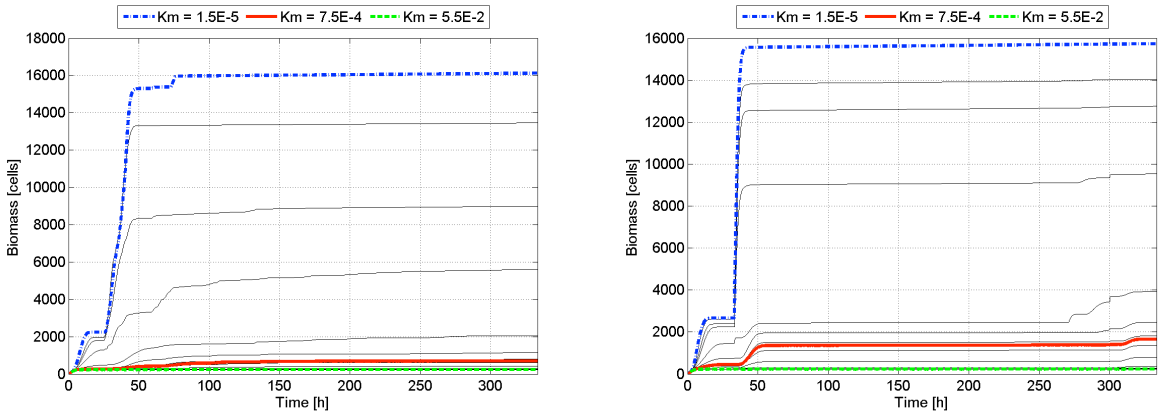

Figure 4-4: Fungal biomass over time for all simulated K_m values in pulse regime 1 (left) and pulse regime 2 (right).

4.4 Discussion

We studied the capacity of AMFs to equalize the effects of nutrient pulses in a plant-fungus-interaction. In particular, we investigated whether and how the different AMF functional types with their characteristic nutrient exchange strategies (identified in Chapter 3) are able to equalize temporal P pulses by transforming them into a continuous P flux delivered to the plant. We found that only the parasitic and the mutualistic nutrient exchange strategies are able to equalize irregular P pulses, but not the intermediate strategy. For regular P pulses, in contrast, the equalization capacity is similar over the complete spectrum of simulated K_m values regardless of the details of the fungal nutrient exchange strategy.

Both, the C and P dynamics, emerging from the model, were found to be strongly dependent on the K_m values and so the nutrient exchange strategy. In our simulated time span, a high equalization capacity for the P dynamics only evolved either for low or for high K_m-values, i.e. purely parasitic or purely mutualistic AMF. Both cases, however, are characterized by low P delivery rates. Therefore, equalization seems to require low P delivery to the plant. This effect can be explained by three different model processes (c.f. Chapter 2). (1) C scarcity can reduce the fungal P uptake from the surrounding medium that results in a reduced fungal P delivery to the plant. (2) Since P is needed to build fungal biomass, fungal growth can deplete the P pool and so also influence the P delivery to the plant. (3) The exchange from P to C has a finite capacity. When this capacity is reached by the high rates of fungal C uptake

C_{upt} in systems with very parasitic fungi, P delivery is also kept at that level. As shown for the dynamics of fungal biomass (Figure 4-4), (2) seems to be not plausible, because fungal growth finds almost exclusively place at the beginning of the simulation, but the effect of reduced P delivery can be seen during the whole simulation period.

Therefore, a reduced fungal P uptake from the surrounding medium or high fungal carbon uptake rates from the plant remains possible explanations. These two equalizing mechanisms act each in a particular functional type as follows:

Mutualistic AMF with their high K_m values can build only very low fungal biomass (Figure 4-3) and accordingly exhibit a low P uptake and delivery which in turn comes along with very low C uptake from the plant. This indicates a strong C scarcity for mutualistic fungi, and so a substantial risk of collapse of the system. This means, the good equalization capacity of the mutualistic fungi results from very low fungal P uptake rates because of the lack of C and biomass. So P cannot be stored inside the fungus, but stays in the surrounding medium and is taken up very slowly and transported to the plant.

In contrast, parasitic AMF with their low K_m can build very high biomass (Figure 4-3) and accordingly exhibit high P uptake. These fungi use the whole capacity of the plant-fungus interface and have therefore the maximum possible carbon uptake rates. Thus, the good equalization capacity of the parasitic fungi is due to the quick P uptake from the surrounding but the resulting high P amount is not needed completely for C exchange and therefore is stored inside the fungus. This is the mechanism one would expect for a buffer and indicates a functioning system.

In both fungal nutrient exchange strategies, the mean P delivery rate is found to decline to zero after a long period without a P pulse because, in these pulse-free periods, very parasitic and very mutualistic fungi can live on the stored or not yet taken up P, while medium K_m fungi cannot deliver anything.

Studying the nutrient and biomass dynamics resulting from the resource pulses, we were able to identify two basic mechanisms that are able to equalize the effects of nutrient pulses in our simulated plant-fungus-interaction system. The first equalization mechanism which we call ‘internal equalizing’ is relevant for fungi with parasitic nutrient exchange strategies. The second one which we call ‘external equalizing’ relates to fungi with mutualistic nutrient

exchange strategies. None of these mechanisms works for fungi with intermediate exchange strategies.

Functioning of the internal equalization mechanism

The parasitic AMF functional type (i.e. fungi with very low K_m values) realizes high C uptake rates and can therefore quickly build fungal biomass and take up P from the surrounding medium. It then stores this P internally. This stored P can be used to obtain C even in periods without P in the surrounding medium.

Functioning of the external equalization mechanism

The mutualistic AMF functional type (i.e. fungi with high K_m values) results in low C uptake rates, slow building of biomass and so very slow uptake of surrounding P. Because the C uptake rate of these fungi hardly exceeds the minimum rate C_{min}, they can retain their very low P uptake rate until they have taken up all surrounding P and have delivered it to the plant. Due to the very low P uptake rate, P is depleted very slowly in soil, thus working as a buffer mechanism.

The intermediate AMF functional type (i.e. fungi with medium K_m values) results in C uptake that is high enough for large biomass and therefore quick P uptake, but the maximum C uptake rate is never reached. Therefore, P is not stored, but always completely exchanged for C. This means, the buffer mechanisms do not work here because no internal storage of P takes place (everything is immediately exchanged for C) and no external storage takes place (quick P uptake because of a large biomass and C availability). So P pulses are taken up by fungi, transported quickly to the plant and exchanged for carbon. The buffering capacity of these fungi is therefore very low.

After this study, we have to rethink our nomenclature of fungal nutrient exchange strategies. Of course, parasitic fungi deliver just low amounts of P in phases of high external P availability shortly after the P pulse. Thus, they require lots of C at just low reward, but in times of external P scarcity (long time after the pulse), they still can deliver P from their high internal storage, when other fungi with more mutualistic strategies have no P stored. In this way, the fungi with (seemingly) ‘parasitic’ nutrient exchange strategies can also be seen as insurance for times of scarcity/shortage.

The most mutualistic fungi, in contrast, have to deliver quite high amounts of P to the plants but get almost no C back from them. This in turn results in low fungal biomass growth. Low biomass, however, results in a low spatial presence limiting the access to P in systems with low diffusion rates thus impeding P uptake. So, the observed external equalization mechanism is based on the assumption that P diffusion is infinite. In explicit, the dynamics of fungi with very large K_m values show the beginning of the collapse of the system. Looking back on the entry question, this external buffering would anyway make little sense, because the related nutrients would be stored in soil. If this would be desirable, plants could take them up directly without giving any carbon to a fungus. Therefore the external storage of these fungi is neither a feature, but the beginning of the failure of the system.

Insights into reasons for the high AMF diversity in nature

This study can also contribute to the question why there is such a high AMF biodiversity in nature. While it is hard to explain why plants tolerate AMF with different P delivery abilities and different C requirements, we showed that the parasitic AMF functional type which obtains high C input at low reward (low P delivery) can become important for plants in times of nutrient scarcity/shortage (because the internal storage mechanism can work). AMF which obtain C input at higher reward (substantial P delivery), in contrast, can be beneficial for the plants in times where nutrients are not limiting because they also develop a sufficiently large biomass and can deliver high amounts of P from far larger distances than plant roots could for relatively low amounts of C as reward.

Unfortunately (to our knowledge) no laboratory or field study investigated the performance of different fungal strains in different conditions in a way which founds the different roles of these fungi for plants and different equalization mechanisms. However, Kiers et al. (2011) found different fungal strains delivering different amounts of nutrients. Although they also reward better performing strains with higher C transfer, they accept less performing fungi and deliver C to them. This may result in the assumption that plants trust more in a larger biodiversity than in a monoculture of best performers as insurance for changing conditions. Additionally, Birhane et al. (2012) investigated colonization with AMF and development of plants under pulsed and regular water availability. They found that under pulsed water availability, plants were colonized with AMF to a larger extent than under regular water availability. Additionally, plants with AMF are known to develop more biomass than plants

without AMF. This also points into the direction that plants use AMF as an insurance against adverse conditions, droughts in this study. The finding that AMF colonization rates are higher in the irregular water pulse regime than in the regular one also fits perfectly to our result that AMF are much more relevant in these regimes.

Asghari and Cavagnaro (2011) investigated the role of AMF for the exploitation and leaching of the nutrients N and P in pulse-based microcosm systems. They found a better exploitation and less leaching in the microcosms with AMF than in those without. This finding clearly points into the direction that AMF can quickly take up nutrient pulses and transport them to their plant partner. Although it does not say anything about equalization, it leaves no room for external equalization mechanism.

This simulation study impressively illustrates how important it is to explicitly consider all relevant nutrient fluxes and exchanges between plants and AMF including the resulting nutrient and biomass dynamics and so to link biodiversity to ecosystem functioning (like proposed by Loreau 2010). If we would have ignored only one of the observed factors (carbon uptake, phosphorus delivery and biomass development) it would not have been possible to draw the right conclusions. Additionally, this study shows the importance of spatial explicitness. We set P diffusion aside, because in the petri dish system the assumption of infinite P diffusion speed was good, but for the transition of our results to field level, we have to leave this assumption and start to simulate realistic P diffusion. This will be done in the next chapter.

4.5 References

Asghari, H.R. and Cavagnaro, T.R. 2011. Arbuscular mycorrhizas enhance plant interception of leached nutrients Functional Plant Biology 38: 219-226.

Birhane, E., Sterck, F.J., Fetene, M., Bongers, F. and Kuyper, T.W. 2012. Arbuscular mycorrhizal fungi enhance photosynthesis, water use efficiency, and growth of frankincense seedlings under pulsed water availability conditions. Oecologia 169: 895-904.

Craine, J.M. 2009 Resource Strategies of wild plants. Princeton University Press, UK. 330 pages.

Hunt, H.W., Elliott, E.T. and Walter, D.E. 1989. Inferring trophic transfers from pulse-dynamics in detrital food webs. Plant and Soil 115: 247-259.

Kiers, E.T., Duhamel, M., Beesetty, Y., Mensah, J.A., Franken, O., Verbruggen, E., Fellbaum, C.R., Kowalchuk, G.A., Hart, M.M., Bago, A., Palmer, T.M., West, S.A., Vandenkoornhuyse, P., Jansa, J. and Bücking, H. 2011. Reciprocal Rewards Stabilize Cooperation in the Mycorrhizal Symbiosis. Science 333: 880-882.

Lamb, E.G., Stewart, A.C. and Cahill, J.F. Jr. 2012 Root system size determines plant performance following short-term soil nutrient pulses. Plant Ecology 213:1803-1812.

Lodge, D.J., McDowell, W.H. and McSwiney, C.P. 1994. The importance of nutrient pulses in tropical forests. Tree 9: 384-387.

Loreau, M. 2010 Linking biodiversity and ecosystems: towards a unifying ecological theory. Philosophical Transactions of the Royal Society B 365: 49-60.

Schaffelke, B. and Klumpp, D.W. 1998. Short-term nutrient pulses enhance growth and photosynthesis of the coral reef macroalga *Sargassum baccularia*. Marine ecology progess series. 170: 95-105.

Schnepf, A., Roose, T. and Schweiger, P. 2008 Impact of growth and uptake patterns of arbuscular mycorrhizal fungi on plant phosphorus uptake – a modelling study. Plant Soil 312: 85-99.

Schnepf, A., Jones, D. and Roose, T. 2011 Modelling Nutrient Uptake by Individual Hyphae of Arbuscular Mycorrhizal Fungi: Temporal and Spatial Scales for an Experimental Design. Bulletin of Mathematical Biology 73: 2175-2200.

Chapter 5: Relevance of the interaction for efficient P use in heterogeneous environments

5.1 Introduction

Major sources of phosphorus (P) in soil are minerals, like apatite, and organic matter. Both are spatially heterogeneously distributed. Mineral compounds are quite insoluble in water and organic matter needs to be mineralized by microorganisms to become bioavailable. The spatial P distribution is therefore very heterogeneous. Because of the low diffusion rates of P in soil, P depletion zones evolve very quickly around plant roots (Marschner and Dell, 1994). Therefore, plants have either to cope with very low P uptake rates, or to continuously explore their surroundings for new P sources by generating new roots. Because both possibilities are very energy demanding and a continuous growth of roots to explore the surrounding soil for P brings a high risk of building useless roots, a symbiosis with fungi might be very promising. This means, the exploration risk would be 'sourced out' from plants to fungi which are rewarded with carbohydrates. These are mostly delivered from the plants in exchange for nutrients (Smith and Read 2008, Marschner, 2012). Fungi can very quickly build new hyphae and dismiss hyphae which are no longer needed. This makes fungi more effective in finding nutrient sources than plants.

In the previous two chapters, we investigated the coupled dynamics of the two nutrient pools P and C and the fungal biomass under different strategies for nutrient exchange between fungus and plant. Based on ranges of coupling parameters (e.g. K_m and C_{min}) in which nutrient and biomass dynamics behave qualitatively similarly, we have identified three different functional types of fungi (parasitic, intermediate, mutualistic). We have shown that these functional types have different capacities to equalize the effect of temporal variability in form of P pulses. In both studies, however, P was assumed to be spatially homogeneously distributed with an infinite diffusion rate, which was a good assumption for the petri dish system on which our model simulations were based. As a next step to realism, we now relax this assumption and investigate the implications (e.g. benefits, costs) of AFM for plants in systems with different spatially heterogeneous P distributions and finite diffusion rates. As the AMF functional type (parasitic, intermediate, mutualistic) was

found to have a strong influence on the results of the previous studies, we investigate the impacts of spatial heterogeneity and finite diffusion rates of P on the functioning of the plant-fungus interaction system and the implications of different fungal nutrient exchange strategies. In homogeneous environments with infinite diffusion rates, fungal biomass was found to be less important for P uptake (since the whole P pool was accessible from every point in the simulated area). For heterogeneous environments with finite P diffusion, however, we expect an increase of its importance. Fungi with little biomass and slow growth have access to a much smaller pool of P than fast growing fungi with large biomass. Thus, slowly growing fungi are expected to suffer from both C scarcity (because of low C delivery from the plant) and P scarcity (because P depletion zones evolve around the fungal tips due to both slow diffusion of P to the fungus and slow fungal growth to P richer areas). This is especially expected when P diffusion which helps to access more P from a colonized place and fungal growth which is needed to colonize new places with P are slower than P uptake.

Additionally, sporulation may become an important process in this scenario. In the previous chapters, sporulation started for the whole mycelium at the same time when the P concentration in the medium fell under the limit for P uptake (see Chapter 2). In environments with a finite P diffusion rate, every part of the mycelium senses a different P concentration and will, therefore, stop P uptake and transform its branched absorbing structures (BAS) to spores at an individual time point (see Chapter 2). Since spores don't need energy in form of C, this process may serve as a resilience mechanism and become relevant for the fungal ability to explore space.

The impact of spatial heterogeneity has been investigated in many different fields. For example, a higher structural and functional diversity have been observed in more heterogeneous habitats. Hu et al. (2014) found this relationship at multiple scales from 10x10 m to 50x50 m in a subtropical evergreen broad leaved forest. De Souza Júnior et al. (2014) used a simulation model to investigate the effects of spatial heterogeneity on the diversity of ecosystems and found a unimodal relationship between both. In a grassland bird community, Hovick et al (2015) found bird diversity positively correlated with landscape heterogeneity across seven landscapes. Thus, spatial heterogeneity can become an important determinant for ecosystem functioning. Therefore, we investigate how spatial heterogeneity in the P resource distribution affects the biomass and nutrient dynamics in

the plant-fungus interaction system. We assume different initial distributions of P and a finite P diffusion rate and study how they affect fungal growth and the fungal ability to deliver P to the plant for different functional types (parasitic and mutualistic) of fungi. In particular, we test the hypothesis that sporulation can work as a resilience mechanism.

5.2 Methods

Like in the chapters before, we used the simulation model developed in Chapter 2. Now, however, we change the assumptions on the spatial distribution and diffusion coefficient for P. Based on the results of the previous chapters, we change the range of investigated K_m values. The previously addressed AMF functional type with a mutualistic fungal nutrient exchange strategy (large K_m-values) resulted in very low fungal biomass and thus very low P uptake and delivery rates. In an environment with heterogeneous P distribution and a finite P diffusion rate, fungal biomass is expected to become more important, since P uptake can only stay on a high level if new P sources are constantly explored. This is biomass-, P- and C-demanding. Therefore, AMF of the mutualistic function type with their low C availability are expected to grow not quickly enough to constantly explore new P sources, and growth to become even slower in response to the C-induced P-scarcity. Since these strains show no ability to quickly explore large areas and to transport reached P over large distances to plants, we do not investigate them in this chapter. AMF with intermediate fungal nutrient exchange strategies (moderate K_m-values) studied in the previous chapters show no equalization capacity. Moreover, they only build biomass which has low potential for a quick adaption to different spatial conditions and are expected to even reduce biomass growth due to a lower P availability in heterogeneous environments. Therefore, two K_m values from the previously called parasitic end of the range of the nutrient exchange strategies are investigated in this study.

Based on a model Petri dish, three different initial P distributions are considered (Figure 5-1). Like in the previous chapters, simulations are conducted in a Petri dish which is divided in two compartments. The left compartment (black half in Figure 5-1) represents the compartment in which plants and fungi grow together. This compartment is not simulated explicitly. Simulations start at the time point where one fungal hypha manages to grow over the barrier between the two compartments. This point is simulated as the place of P/C exchange. The right compartment (colored half in Figure 5-1) shows the simulated

compartment where fungi grow. Colors indicate the P concentration at the beginning of the simulation. Red means no P available, blue indicates high P availability. Like in the previous chapters, no fungal hyphae are present in the simulated compartment at simulation start. The first, artificial half-circle-like P distribution (Figure 5-1A) is a reference to investigate the influence of the so-called initial internal P-pool which is the amount of P *inside* the initial fungal cells available for growth and exchange at the beginning of the simulation in a P-free environment. Therefore, it is only important at the beginning of the simulation, when fungi cannot take up P from their surroundings (because there is no P; see Figure 5-1). To find an initial internal P-pool large enough to enable fungi to build enough biomass to reach new external P sources, the initial internal P-pool was varied in this scenario. The radius of the half circle was chosen in a way to reflect the distance to the first P source in Distribution II (Figure 5-1C) which is much longer than in Distribution I (Figure 5-1B). These two distributions are used to investigate the influence of spatial P distribution on the C- and P-dynamics and on biomass growth. The total amounts of P are the same in all three distributions.

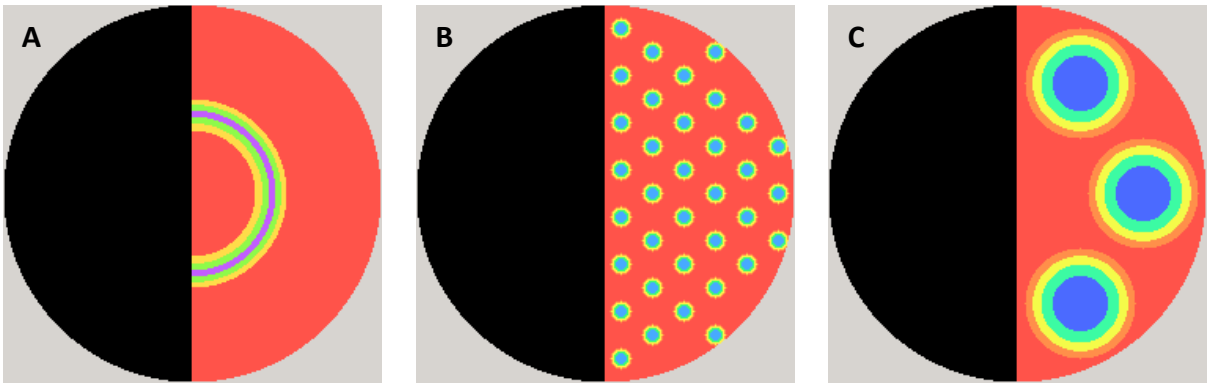

Figure 5-1: Initial P distribution in a model petri dish. Red: no P, blue: high P concentration, green and yellow intermediate availabilities, black: area not simulated plant compartment.

We varied different parameters, which are: (1) K_m (a low K_m–value corresponds to a very parasitic fungal nutrient exchange with the plant and a higher K_m–value to a less parasitic exchange (cf. Chapter 3), (2) the P diffusion coefficient D_s and (3) only in the reference scenario (Figure 5-1A), the initial internal P-pool P_{ini} to find a suitable amount of initial internal P which allows the fungi to reach the distant external P source of Distribution II (Figure 5-1C). Table 5-1 shows the parameterizations of all simulated scenarios.

*Table 5-1: Parameterizations of the simulated scenarios in the reference analysis (*Figure 5-1*A). K_m characterizes the plant fungus nutrient exchange strategy (low K_m, very parasitic strategy, higher K_m, less parasitic strategy). D_s is the P diffusion coefficient. $P_{int}(t=0)$ is the initial internal P-pool.*

Scenario	K_m [mg]	D_s [mm² d^{-1}]	P_{ini} [mg]
Scen1	10^{-5}	0.001	10^{-6}
Scen2	10^{-5}	0.001	10^{-5}
Scen3	10^{-5}	0.001	10^{-3}
Scen4	10^{-5}	0.01	10^{-6}
Scen5	10^{-5}	0.01	10^{-5}
Scen6	10^{-5}	0.01	10^{-3}
Scen7	10^{-3}	0.001	10^{-6}
Scen8	10^{-3}	0.001	10^{-5}
Scen9	10^{-3}	0.001	10^{-3}
Scen10	10^{-3}	0.01	10^{-6}
Scen11	10^{-3}	0.01	10^{-5}
Scen12	10^{-3}	0.01	10^{-3}

All scenarios are simulated over a period of 960 h (40 d). This time span is much larger than in the previous chapters since the finite P diffusion rate slows down fungal P uptake. Therefore, fungal exploration of space and exploitation of P needs more time. For all scenarios, we made 20 replicates to minimize artefacts due to random effects.

5.3 Results

5.3.1 Preliminary Test with the Reference Scenario

Spatially explicit fungal growth and external P depletion are shown in Figure 5-2 for scenario 12 as an example. The black half of the circle is not simulated and represents the compartment of the Petri-dish in which plants and fungi grow together. Fungal growth starts in the middle of the black-red dividing line. With its initial internal P-pool P_{int}, and only one little fungal hypha (Figure 5-2A), the fungus manages to grow and reach the half circle-shaped external P source P_{ext} (Figure 5-2B) and explores the whole compartment with its mycelium (Figure 5-2C). External P is taken up by the fungus and diffuses into the direction

of lower concentration (Figure 5-2D to F). While the borders between the zone of P availability and no P availability at the simulation start (Figure 5-2) are very sharp, diffusion leads to more and more washed out borders (Figure 5-2E and F). Figure 5-2E shows that P depletion zones develop around fungal hyphae. We found that sporulation takes place in fungal hyphae in places with low P availability. A larger overview showing the fungal hypha in detail is presented in Figure 5-3.

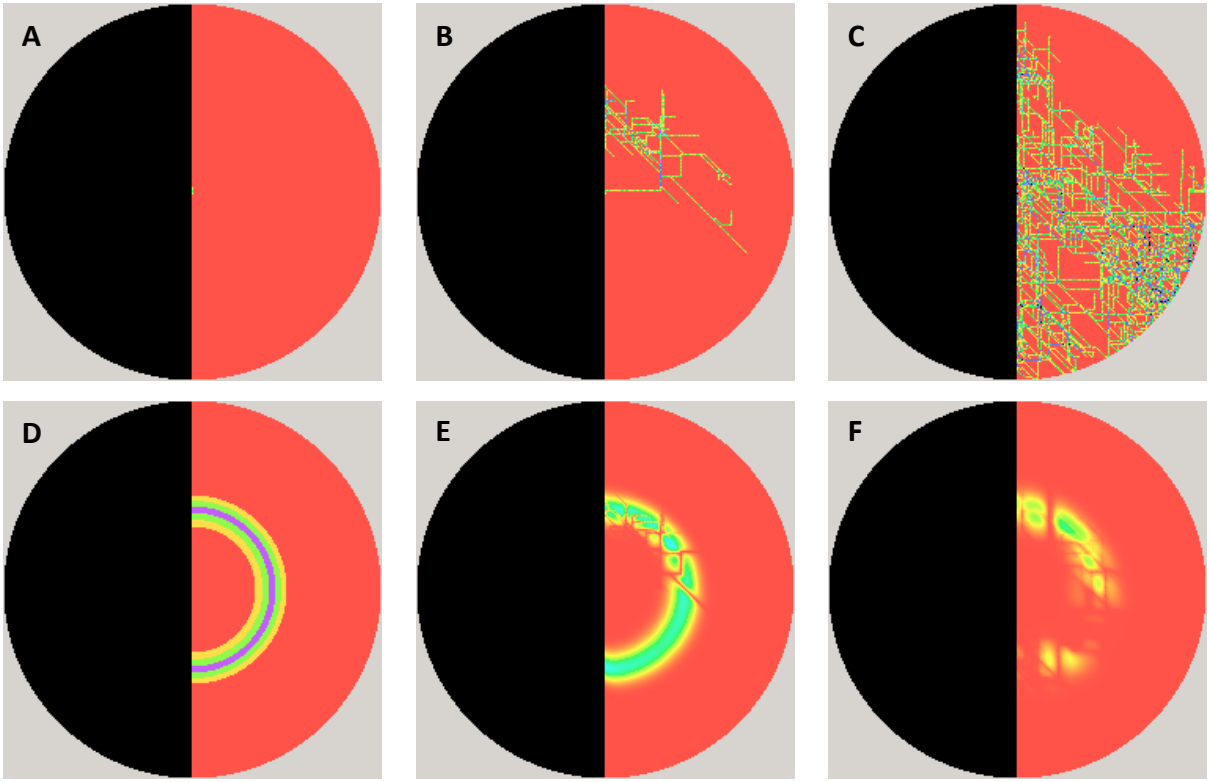

Figure 5-2: Mycelia development (A-C) and spatial distribution of the external P availability (D-F) at t=0h (A, D), t=100h (B, E), and t=250h (C, F) in the reference distribution with Scenario (12).Fungal hyphae are shown in yellow, hyphae with BAS are green and hyphae with spores are indicated by purple color. The red surrounding means there are no hyphae.

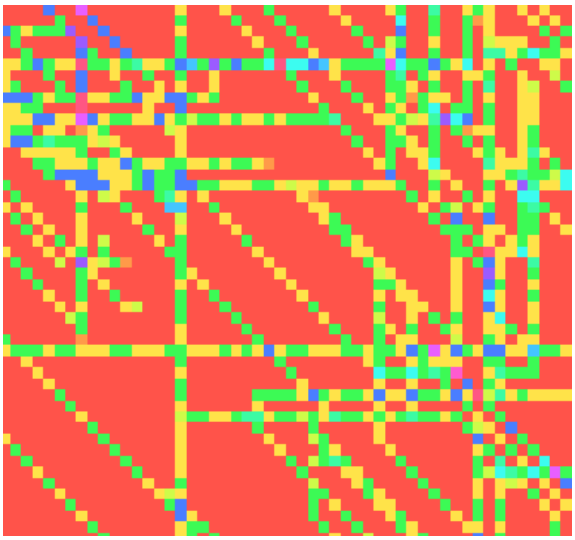

Figure 5-3. Detailed overview of the fungal hypha. Fungal hyphae are shown in a scale from yellow to blue with yellow meaning only one hypha in a grid cell, and more hypha over green to turquois and blue. BAS count the same as one unit of hypha in a cell. Hyphae with spores are indicated by purple color. The red surrounding means there are no hyphae.

To find out how long it takes for the fungus to grow to the external P source, we decided to calculate the time until the fungus has taken up 5% of the initial external P pool ($P_{ext}(t=0)$). In Figure 5-4, this indicator is plotted against the assumed diffusion coefficient (D_s) for all simulated scenarios. In four of these reference scenarios, the fungus was not able to take up this 5% of the initial P_{ext} during simulation time because the P_{ini} was too low to enable the fungi to cover the distance between the starting point of fungal growth and the next P source. So these scenarios are missing in this figure. K_m is found to have no influence on this indicator, whereas P_{ini} showed high impact. Furthermore, the diffusion coefficient D_s shows high influence on the simulated time until 5% initial P_{ext} uptake that is noticeably shortened, but mainly on scenarios with lower initial internal values P_{ini}. This suggests that the corresponding fungi do not manage to reach the initial external P sources P_{ext} by growth, but wait until P_{ext} reached the fungus by diffusion. So these fungi have clearly not enough P_{ini} to reach and uptake P sources.

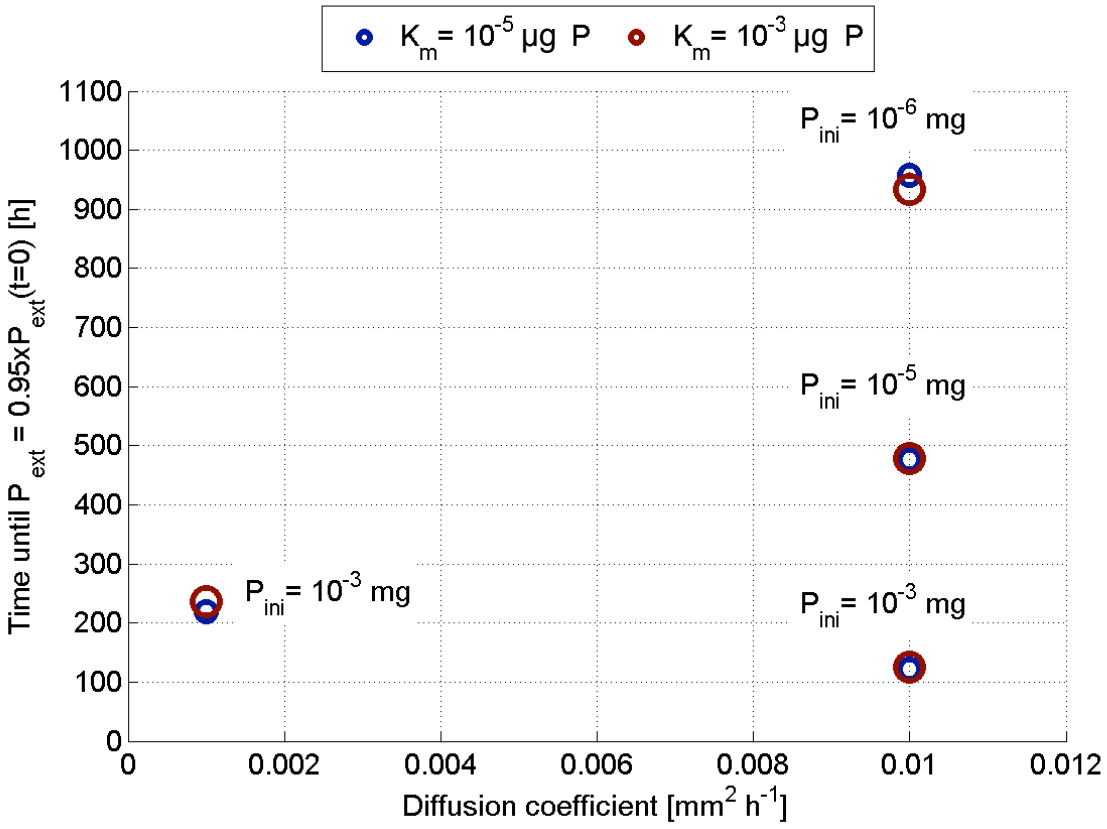

Figure 5-4: Time until 5% of the initial external P source $P_{ext}(t=0)$ is taken up by fungi for all simulated scenarios over the diffusion coefficient D_s for different initial values of the internal P pool $P_{int}(t=0)$. Missing values indicate that 5% uptake could not be reached until simulation end. Different marker sizes represent the two simulated K_m-values

To be more precise about the plants' benefits of this symbiosis, we look at the plants' C delivery to the fungus until this time point (Figure 5-5). For fungi, which do not manage to take up 5% of the initial external P pool $P_{ext}(t=0)$ during simulation time, we plot the overall C delivery. Even here, the influence of the K_m value is very low. Only for the scenarios with high initial P P_{ini}, differences can be seen. The simulations with low initial internal P pool (P_{ini} = 10^{-6} and 10^{-5} mg) show the same amounts of C delivery by the plant for both nutrient exchange strategies (K_m = 10^{-5} and 10^{-3}). This suggests that these fungi get the minimum C uptake C_{min} during the whole simulation time because otherwise the more parasitic fungus (K_m = 10^{-5}) would have got more C than the less parasitic one (Km = 10^{-3}). The amounts of C delivery in the simulations with the highest amounts of initial P_{ini} result in different P deliveries which imply that the C delivery rate is higher than the minimum for this fungi.

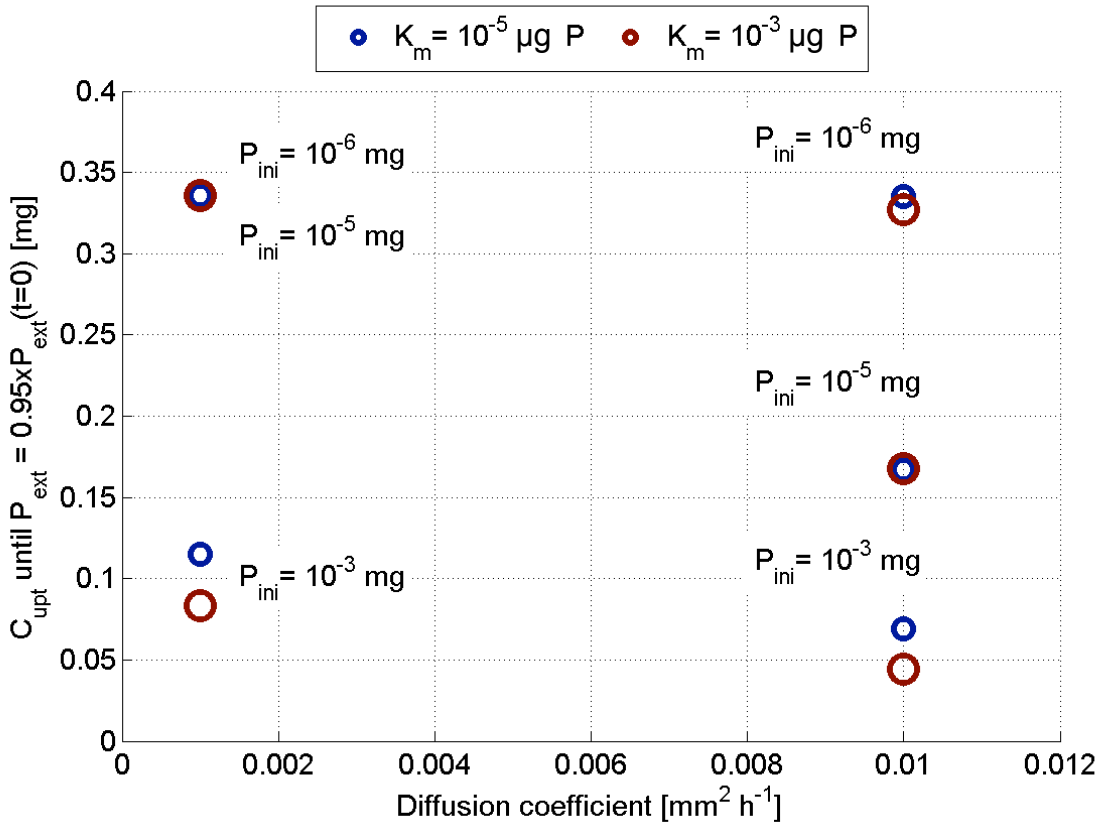

Figure 5-5: C uptake of the fungus until 5% of the initial external P source P_{ext} is taken up by fungi for all simulated scenarios over the diffusion coefficient D_s. For scenarios in which fungi did not manage to take up 5% of initial $P_{ext,}$ the fungal C uptake until simulation end was plotted. Since $P_{ini}=10^{-6}$ and $P_{ini}=10^{-5}$ did not manage to take up 5% of the initial P_{ext} for D_s = 0.001, the values for these scenarios are identical. Different marker sizes represent the two simulated K_m-values.

Because only the scenarios with highest initial P_{ini} values show fungal biomass growth large enough to explore even remote areas like in Distribution II, we decided to simulate only these scenarios for the two P Distributions I and II in Figure 5-1. Although this does not automatically mean that fungi can reach the P source in these scenarios, but they are the most promising.

5.3.2 Heterogeneous external P Distributions I and II

One example of the spatially explicit dynamics of external P depletion is shown in Figure 5-6. In the P_{ext} Distribution I (Figure 5-6A-F), diagonal stripes of P seem to emerge. These stripes

arise from the projection of the hexagonal grid on quadratic pixels with the neighborhood rule of hexagon and are therefore only an artefact of visualization and do not influence fungal growth and C/P dynamics. Diffusion of course is equally simulated in every direction.

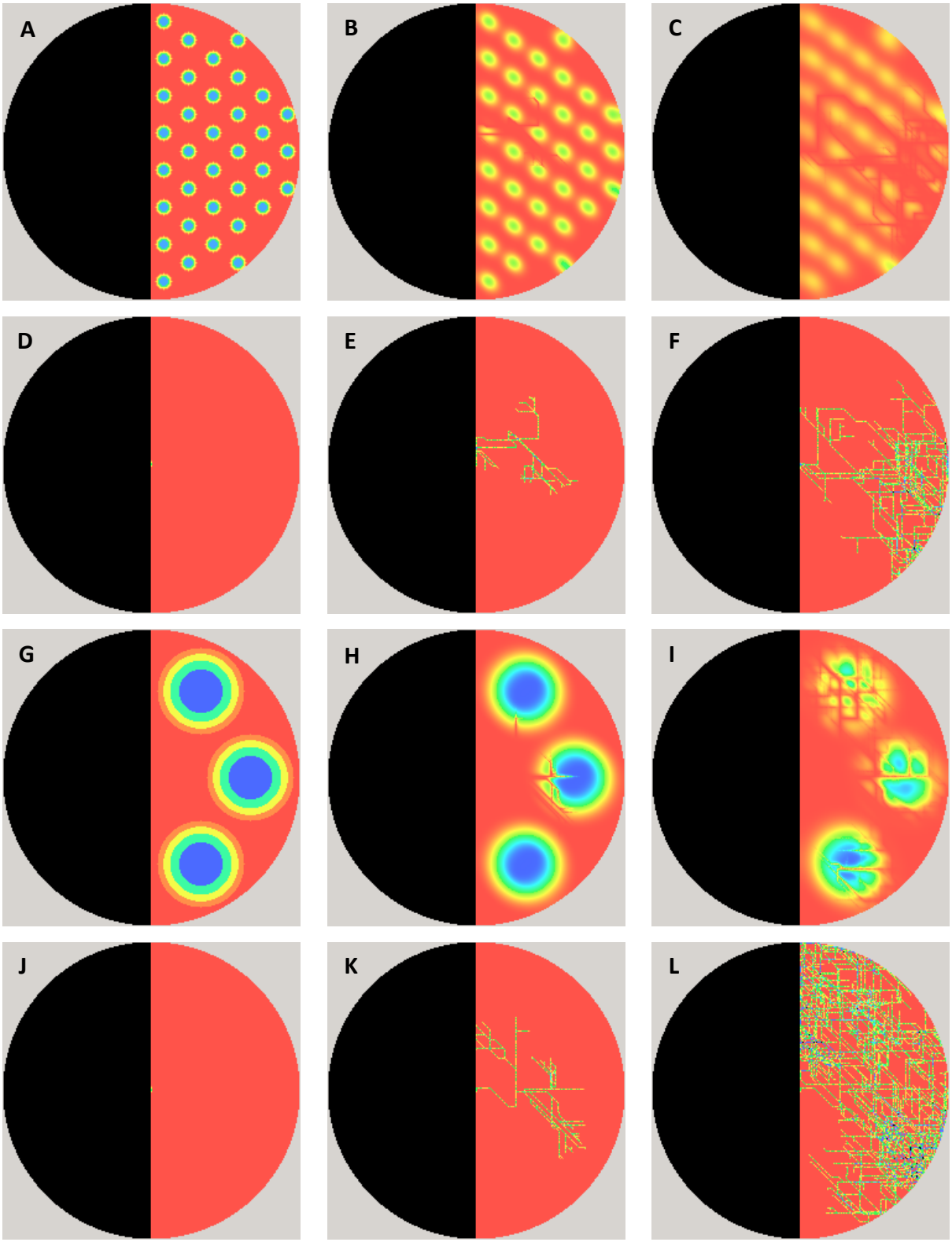

Figure 5-6: External P depletion dynamics in P_{ext} Distribution I (A-C) and P_{ext} Distribution II (G-I) and corresponding fungal mycelium of Distribution I (D-F) and Distribution II (J-L) at t=0h (A and D) t=100h (B and E) and t=250h (C and F) for Scenario (12). Fungal hyphae are shown in yellow, hyphae with BAS are green and hyphae with spores are indicated by purple color.

To explore the plant benefit of the symbiosis, Figure 5-7 shows the cumulative P delivery from the fungus to the plant for all simulated parameterizations (Table 5-1). In all scenarios and distributions, P delivery is high at the beginning of the simulations. These high P delivery rates result from the relatively high initial internal P pool P_{int} of the fungus that cannot only be used for fungal biomass growth, but also for exchange with the plant to gain C. So these high P delivery rates at the beginning are not an indicator for good spatial exploration which we searched for. Even less, a well exploring fungus would use this P for growth and exchange only that much for C to meet its needs. This means, only P delivery rates after the first 'jump' are really interesting. In the P Distribution I, the parameter scenarios Scen3 and Scen6, which represent the functional type of very parasitic fungi, show good P delivery rates. Interestingly, higher P diffusion rates D_s bring a major advantage, which can be seen in Scen6 compared to Scen3. This advantage is even larger for Scen12 compared to Scen9 which represent the functional type of the less parasitic fungi. Both of them deliver very few P after the initial delivery, but with the high P diffusion rate of Scen12, the fungus gets in contact with P and can deliver high rates at some point, whereas the fungus of Scen9 retains very low rates during the whole simulation period. Looking on P Distribution II, the observed effects increase. The less parasitic functional types (Scen9 and Scen12) show very high initial P delivery rates, but very low rates afterwards. Additionally, while, in Distribution I, Scen9 delivers least P and Scen12 is the best P deliverer, in Distribution II, Scen9 and Scen12 are almost identical. This can be explained by the fact that, in Distribution I, Scen12 (high P diffusion) is able to reach a P source while Scen9 (high P diffusion) is not. In Distribution II, even in the high P diffusion scenario (Scen12), the fungi do not get in contact with a P source. Therefore, both scenarios are almost identical. The more parasitic functional types of Scen3 and Scen6 show smaller initial deliveries, and can therefore use more of their initial P_{int} for growth. In Scen6, the high P diffusion coefficient enables the fungus to reach the P sources and it can start to deliver this P. In Scen3, the lower P diffusion coefficient hinders the fungus to reach the P sources during simulation time and the fungus delivers very few P to the plant. However, in Distribution II, fungi deliver much less P during the simulation period than in Distribution I (please mind the different scales) because of the longer distances to the next P source.

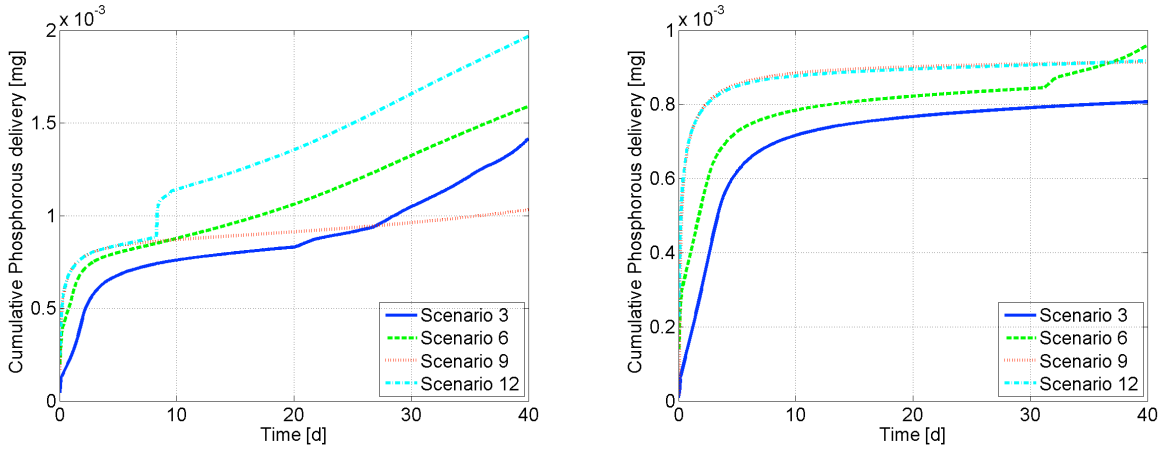

Figure 5-7: Cumulative P delivery from the fungus to the plant [mg] over time [d] for all simulated scenarios for P Distribution I (A) and P Distribution II ((B). Please note the different y-axis.

This difference in P delivery clearly shows the influence of the spatial distribution of the external P source P_{ext} on the coupled dynamics of C and P.

To get a better insight into the fungal P uptake, Figure 5-8 shows the cumulative fungal P uptake over time for all simulated parameterizations. Like expected from Figure 5-7, the scenarios with higher P diffusion coefficients D_s (green and cyan blue) perform much better than the scenarios with lower P diffusion coefficients D_s (red and blue). But comparing here different fungal nutrient exchange strategies, the very parasitic (green and blue) fungi perform better than the less parasitic ones (cyan blue and red).

So, very parasitic fungi perform much better in P uptake, but deliver less P to the plant (compare Figure 5-4 and Figure 5-7). This means, they either store it in their mycelium (which is a relevant mechanism also for P pulses, see Chapter 4), use more P for growth, or their higher biomass leads to longer transport ways which delays delivery. Like shown in Figure 5-7, relevant P delivery rates after the initial 'jump', start after about eight days for scenario Scen12, after ten days for scenario Scen6 and after 20 days for scenario Sscen3 in Distribution I and after more than 30 days in scenario Scen6 in Distribution II. All other scenarios do not deliver relevant amounts of P in the simulation time. P uptake, however, already starts after about two days in all scenarios in Distribution I and after about eight days in Distribution II. This means, P uptake starts in most cases much faster than P delivery to the plant. The reason is that fungi need P not only for exchange with C, but also use it

themselves for growth. Fungal growth only takes place at the fungal tip, where potentially most external P is available for uptake, since new P sources are first discovered there. So, only the fraction of P which is not used for growth is transported away from the fungal tip and available for exchange at the beginning of the simulation when no older hyphae are available which do not need P for themselves but directly transport it to the plant to exchange it for C. As a result, P delivery can only take place, when P uptake takes place not only directly around the fungal tip from where it is used for growth, but also in older hypha from where it is transported to the plant.

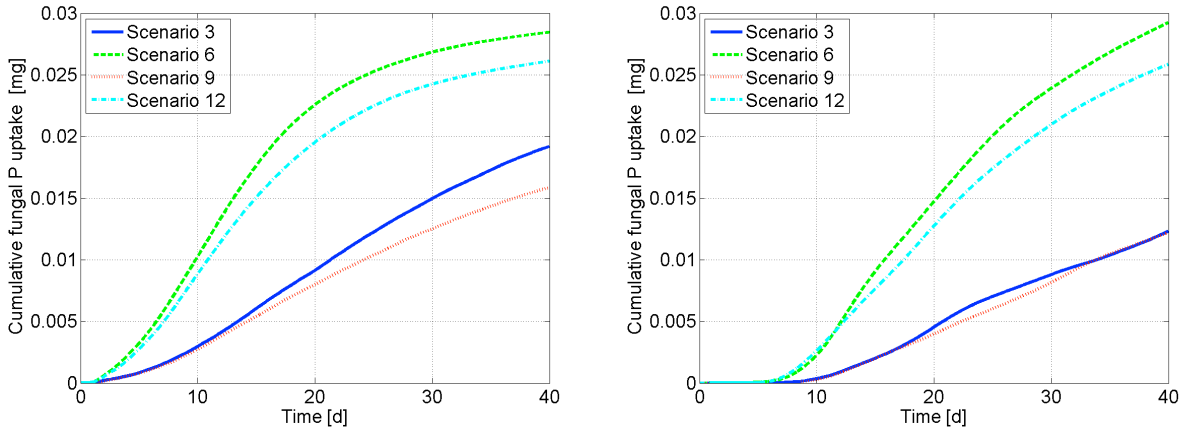

Figure 5-8: Cumulative fungal P uptake [mg] over time [d] for all simulated scenarios for P Distribution I (A) and P Distribution II (B).

Plant benefit is not only determined by fungal P delivery but also how much reward it has to invest in terms of C delivery to the fungus. Therefore, cumulative fungal C uptake over time is plotted in Figure 5-9 for all simulated scenarios. The fungal C uptake rates vary little between the different P distributions. Because of the higher P diffusion, Scen12 delivers more P than Scen3 (cf. Figure 5-8), but as the less parasitic fungus, it gains less C per P. So both fungi come out with almost the same C uptake. The very parasitic fungus with high P diffusion of Scen6 and the less parasitic P delivering fungi with low P diffusion of Scen9 are the extremes. The results of the different P distributions (I and II) differ only during the first quarter of the simulation. Both high diffusion scenarios (Scen6 and Scen12) can benefit from high C uptake rates right from the beginning in Distribution I, whereas in Distribution II, there is a delay.

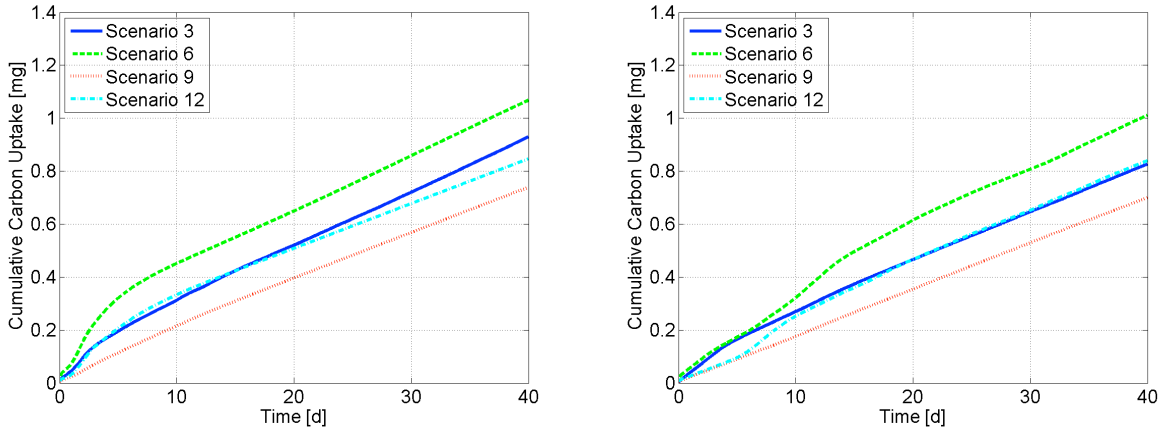

Figure 5-9: Cumulative fungal C uptake [mg] over time [d] for all simulated scenarios for P Distribution I (A) and P Distribution II (B).

Looking at the fugal biomass for Distribution I in Figure 5-10A, the scenarios with worse performance in P uptake and delivery and the scenarios with very low P diffusion rates (blue and red) develop most biomass. This seems to be inconsistent, but looking at the sporulation rates in Figure 5-10C, sporulation is also highest in these fungi. The mechanism behind this pattern is the process which triggers sporulation. Fungal hyphae start sporulation when the P uptake rates drop down. As sporulation means that Branched Absorbing Structures, which need C for maintenance, are transformed to spores, which do not belong to the fungal mycelia any more (Chapter 2), the corresponding fungus can use the saved maintenance cost to grow new hypha. In simulations with lower P diffusion rates, P depletion zones develop around fungal hypha (see Figure 5-2 E and F and Figure 5-6), which cannot be filled quickly enough by diffusion. This triggers sporulation. In simulation with higher P diffusion coefficients Ds, this depletion zones evolve much later (data not shown), since concentration gradients are quicker equalized by quicker diffusion. So fungi can exploit their surrounding quicker, with less biomass. With further exploitation, these depletion zones evolve even with higher diffusion rates, and fungi would start to sporulate then, but have no more P for growth left.

In comparison, Distribution II looks very different. In the scenarios with the higher diffusion coefficient (Scen3) and (Scen12), more biomass is built, but sporulation is similar in all scenarios. But comparing the dynamics of Distribution II with the one of the period 0 to 15 h

of Distribution I, they look quite similar. This suggests that the large area without P in Distribution II (Figure 5-1) protracts fungal growth and sporulation.

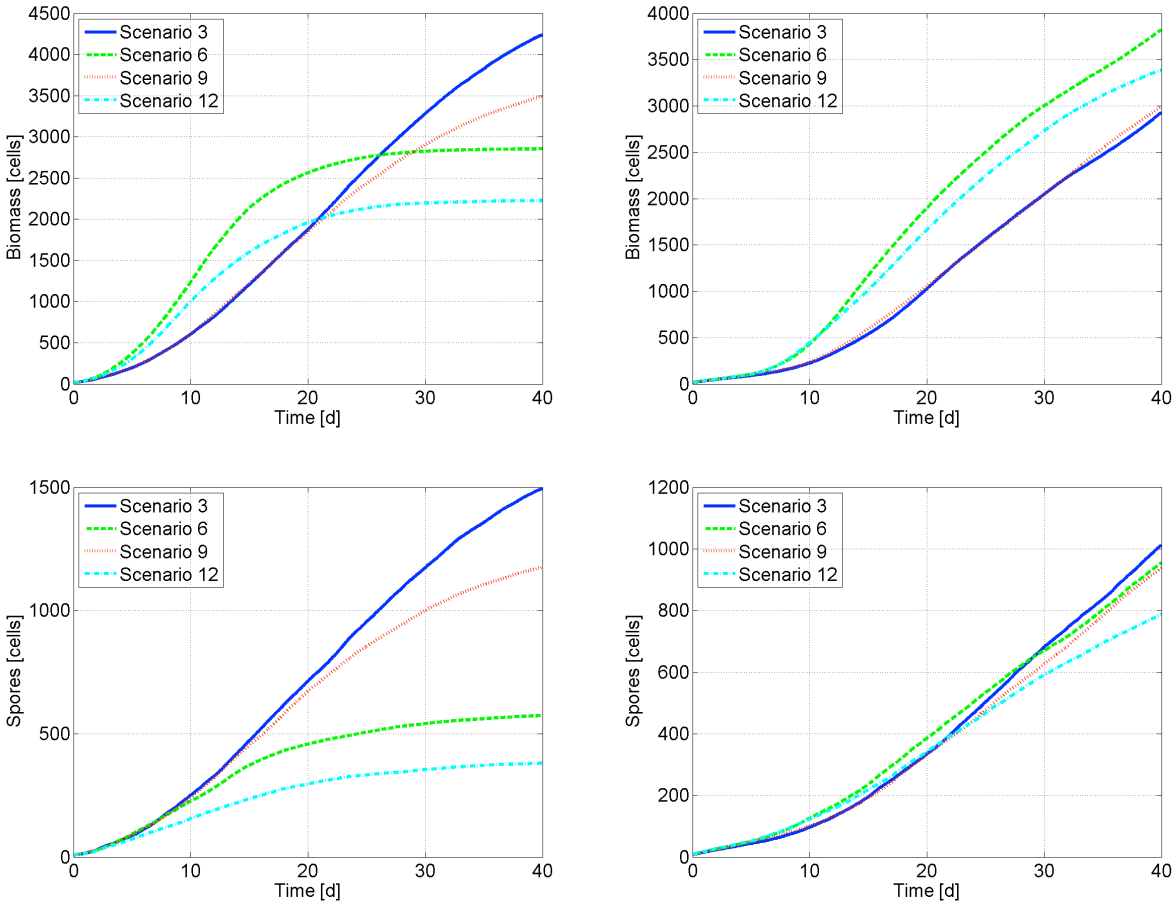

Figure 5-10: Fungal biomass and amount of spores [cells] over time [d] for all simulated scenarios for P Distribution I (A) and P Distribution II (B Please, note the slightly different y-axes.

5.4 Discussion

Fungi can be very effective in exploring and exploiting areas for P and in delivering it to plants to exchange it for C. The plants' benefit is determined by the amount of P delivered by the fungi compared to the amount of C they have to pay. Therefore, both C delivery from the plant and P delivery to the plant have been studied as a function of the spatial distribution and diffusion ability of P in the soil. We compare here only two nutrient exchange strategies from the parasitic end (very parasitic and less parasitic strategy) because, in heterogeneous environments with finite P diffusion, fungal P uptake from soil is assumed to be highly dependent on fungal biomass. Since only parasitic fungi were found to

develop large biomasses in the previous chapters, we focused on these fungi. This means, plants have to invest large amounts of C in fungi to get the required P in heterogeneous natural environments.

In our study, we could show that the plants' benefit depends strongly on the P diffusion coefficient, and less on the fungal nutrient exchange strategy. Although very parasitic fungi still got more C from the plant, differences were small and P delivery to the plant was similar because both fungi belonged to the parasitic type and developed similar amounts of biomass. Nevertheless, biomass of the very parasitic fungi was slightly larger than that of the less parasitic ones at the same diffusion rate. This means that the pattern shown for homogenous environments and pulsed resources in the previous chapters, i.e. the less parasitic (higher K_m) the fungi become, the less biomass they can develop, is also valid in heterogeneous environments with finite diffusion. On the other hand, this suggests that mutualistic strategies cannot persist in heterogeneous environments as their fungal biomass was too low to explore relevant areas and the system would collapse. This effect was also observed in the homogenous environments of the previous chapters, but because of the infinite diffusion rates, the collapse occurred at much higher K_m values (i.e. at very mutualistic strategies).

In distributions with many small P sources (cf. Distribution I), exploitation starts quickly and needs few fungal biomass, while in distributions with few large P sources (cf. Distribution II), fungi need due to the longer distance to the next P source a longer development time and more biomass until exploitation can begin. This leads to lower P delivery rates to the plant, because of the higher demand of phosphorus for the growth of biomass.

In general, we can say that (i) low P diffusion coefficients and (ii) high spatial aggregation of P sources lead to the development of more fungal biomass and lower P delivery rates (at least during and directly after the establishment of the fungus. It would be interesting to check in a future study if this pattern persists in heterogeneous environments with pulsed P supply. Fungi which built up large biomasses should be able to quickly reply to nutrient pulses, however, the nutrient scarcity between nutrient pulses reduces fungal growth dramatically. Therefore successful fungi need to very quickly respond to nutrient pules and grow large biomasses to take up and store nutrient pulses. The quick respond is supposed to

depend very much on the distance of the fungus to the nutrient and the diffusion coefficient of the nutrient.

Our simulations reveal how fungi can optimize their biomass for P uptake depending on external P availability and P diffusion. In scenarios with higher P diffusion coefficient, the internally stored P is used for exchange for C which itself is used to support a small but effective mycelium with a large number of BAS. In scenarios with very low P diffusion coefficients, fungi use a large amount of the external P source to develop huge biomass and quickly transform their BAS to spores when P uptake drops below a certain level at the specific place (see Chapter 2).

We found that sporulation is the key model rule for this adaption of biomass to the spatial availability of P. It allows the fungus to transform BAS into spores when the P uptake rates drop down. These spores do not need C for maintenance. Thus, the fungus can use the saved maintenance cost to grow new hypha for further exploration of the environment. This mechanism leads to the fungal ability to adapt its biomass to its requirement and so to an efficient resource use. This finding demonstrates the importance of considering sporulation as a process when simulating fungal growth although it has not been found important in the previous chapters. For AMF, sporulation therefore works as resilience strategy to adapt its mycelium to the heterogeneity of its environment.

In a future study, one could combine temporal resource heterogeneity of Chapter 4 and spatial heterogeneity of this study to investigate the ability of fungi to smooth resource pulses which are spatially heterogeneous and considering limited P diffusion ability.

Our results suggest that AMF have the ability to deliver nutrients over large distances to the plant and can adapt their biomass by sporulation to different spatial conditions. With these new insights, the classification in parasitic, intermediate and mutualistic interactions in the previous chapters was a bit misleading. Although mutualistic fungi deliver P to the plant with very little C invest by the plant in spatially homogeneous environments, those fungi would not be able to deliver any P in spatially heterogeneous environments because of the very small biomass and therefore their inability to flexibly adapt their biomass to varying conditions. This suggests that a higher C invest by the plant pays back; maybe not in the short term, when P is highly available, but for sure in the long term when P is locally or temporally not available.

Our results also perfectly fit in the findings of functional ecology with higher diversity in heterogeneous environments (e.g. de Souza Júnior et al., 2014; Hu et al., 2014; Hovick et al., 2015). The utility of fungal strains from the more mutualistic AMF functional types have been shown in the previous chapters for homogeneous environments (Chapter 3) and environments with pulsed P supply (Chapter 4). This Chapter 5 even demonstrates the usefulness of fungal strains from the very parasitic functional type. Therefore, in natural environments with a variety of abiotic conditions different fungal strains from the entire spectrum of inspected functional types are beneficial for plants. Furthermore, In sum, our results indicate that AMF are an efficient symbiont for plants for an effective exploration and exploitation of nutrients in heterogeneous environments and can be seen as a nature-based solution for higher P use efficiency in times of increasing P shortage.

5.5 References

De Souza Júnior, M.B., Ferreira, F.F. and de Oliveira, V.M. Effects of the spatial heterogeneity on the diversity of ecosystems with resource competition. Physica A: Statistical mechanics and its applications 393: 312-319.

Hovick, T.J., Elmore, R.D., Fuhlendorf, S.D., Engle, D.M. and Hamilton, R.G. Spatial heterogeneity increases diversity and stability in grassland bird communities. Ecological applications 25: 662-672

Hu, G., Jin, Y. Liu, J. and Yu. M. 2014. Functional diversity versus species diversity: relationships with habitat heterogeneity at multiple scales in a subtropical evergreen broad-leaved forest. Ecological research 29: 897-903.

Marschner, H. and Dell, B. 1994. Nutrient uptake in mycorrhizal symbiosis. Plant and Soil 159: 89-102.

Marschner, P. 2012 Mineral nutrition of higher plants, 3rd ed. San Diego, USA: Academic Press. 651p.

Smith, S.E. and Read, D.J. 2008 Mycorrhizal symbiosis, 3rd ed. San Diego, USA: Academic Press. 800p.

Chapter 6: General discussion

6.1 Lessons learnt – Model structure

To investigate the role of arbuscular mycorrhizal fungi (AMF) on the dynamics of key nutrients such as phosphorus (P) and carbon (C), different model structures are in use in the literature. Landis and Frasier (2007), for instance, have developed a model for C- and P-transfer in AMF in which they have simulated the growth of plant and AMF biomass in a fixed volume of soil. However, since they found it counterproductive to simulate biomass spatially explicitly without modelling soil structure and texture for their purpose, they kept AMF and plant biomass without spatial information. In contrast, Schnepf et al. (2008) have developed a model for AMF with spatial information for fungal biomass. However, they have not considered nutrient exchange between fungi and plants or transport in the hypha and have used density distributions for fungal mycelium. In a later study (Schnepf et al. 2011), they have developed a mathematical model to simulate nutrient uptake by a single hypha in soil.

Since we wanted to simulate the coupled dynamics of C and P on a fine spatial scale, all these models were structurally inadequate for our purpose. However, spatially explicit models of fungi (no mycorrhiza) were available from Boswell et al. (2007). They have expanded a previous model of fungi (Boswell et al. 2003) to simulate fungal growth in a complex environment and have included spatially explicit growth of fungal hypha. This structure for fungal growth seemed to be most promising for our purpose. However, many modifications and extensions were necessary to simulate fungal growth in 3 dimensions in the form of vertical layers to consider the growth of hypha above and below each other, and with more than one limiting nutrient. Therefore, we developed a spatially explicit model to simulate growth of AMF based on their nutrient uptake in form of P from the surrounding and their exchange of P to C from a plant. To parameterize the model, we used the approach of pattern-oriented modelling (Grimm et al. 2006). Therefore, we performed laboratory experiments in Petri-dishes and used the results to calibrate the model output. Speed of fungal growth was identified by multiple laboratory measurements where Petri-dish systems with AMF were investigated with binoculars. The model was able to simulate fungal growth

with the same speed. We were able to fit model output on P and C dynamic results from further laboratory experiments. Unfortunately, our temporal and monetary conditions did not allow us to conduct any more laboratory experiments to further boost the confidence of several parameters and validate model output fully quantitatively. However, as our study was organized like a virtual laboratory, the qualitative results provided important insights into key factors and mechanisms of the functioning of artificial AMF as base of hypotheses for exploring real AMF.

6.2 Lessons learnt - Identification of AMF functional types

The structure of the model developed in this thesis and the analysis of the resulting AMF biomass growth and P-C dynamics allowed us to identify and discover different functional types in the variety of artificial AMF which are indicated by their strategy of exchange of P for C with their plant partner. This strategy in turn can be characterized by a single indicator – the K_m value of the corresponding P/C exchange function (see Table 2-2 in Chapter 2). We dedicated AMF with a K_m-value below 3.5E-2 to the type of parasitic fungi, strategies with a K_m-value between 3.5E-2 and 3E-1 to the type of intermediate and strategies with a K_m-value above 3E-1 to the type of mutualistic fungi. This functional grouping was only possible as we considered and compared three emerging dynamic processes (AMF biomass growth, its P delivery dynamics to the plant and its C uptake dynamics from the plant). The functional types reduce the variety of plant-fungus interactions and are characterized by typical biomass and nutrient dynamics within certain parameter ranges of K_m .

Our model results have also shown that the AMF functional type (characterized by the K_m value) has implications for the entire system dynamics, not only for the nutrient exchange per se (which is directly affected by the chosen K_m value), but also for the buffer capacity of the system against temporal variability of P availability (see Chapter 4) and the spatial exploitation of P (spatial heterogeneity of P availability; see Chapter 5). ***Table 6-1*** shows the implications of different functional types (in terms of K_m ranges) for nutrient cycling and buffer capacity of the fungus-plant interaction.

Table 6-1. Properties of different fungal functional types.

	Parasitic (K_m <3.5E-2)	Intermediate (K_m 3.5E-2 – 3E-1)	Mutualistic (K_m > 3E-1)
C taken from plant	Very much	Medium	Little
P transported to plant	Little	Medium	Very much
P pulse equalization	Good	Bad	Good
P cluster equalization	Good	Medium	Bad
P storage ability	Fungus	None	Soil
Fungal biomass	Very large	Medium	Very small

These implications additionally give rise to the hypothesis that fungal strains which belong to the same AMF functional type also coincide in the qualitative behavior of the C- and P-dynamics they induce. Further laboratory experiments are necessary to investigate this hypothesis. This is also a good example how models and experiments can interact and that the collaboration of modelers and experimenters can be fruitful. Experiments are an important source during model development. However, models can later on be used to develop new hypotheses and result in ideas for new experiments to prove model outcome (see e.g. also Banitz 2011).

6.3 Lessons learnt – Coupling nutrient cycles by AMF-related species interactions

The nutrient cycles of C and P are coupled by the interaction of two different species (AMF and plants). In the presented model, this is operationalized using the P-C-exchange strategy of the AMF (see previous section). Our model results on artificial AMF have shown that the nutrient exchange strategy (parasitic, intermediate, mutualistic) is crucial for the resulting C- and P-dynamics. This exemplifies the need of further cooperation of the two scientific disciplines ecosystem and biodiversity research, as was already underpinned by Loreau (2010). Without the inclusion of two species interacting on a temporal and spatial scale, the cycles of C and P would have been very different. On the other hand, the interactions of both species could not have been described on a certain temporal and spatial scale without

referring to the C- and P-cycles. This means, many questions in ecology can simply not be answered without combining the knowledge of matter fluxes such as nutrient cycles from ecosystem research with the organismic knowledge of how different species interact from biodiversity research. As has been shown in this study, the methods of ecological modelling and our approach to create species interactions by the use of nutrient cycles can be a good link between both fields. However, this sets high demands on the modeler. He/she ought not only to be familiar with modeling and programming techniques to find a suitable model structure, build the model, implement it and use adequate methods for parameterization of the model and analysis of model output, he/she must also have (or be willing to gain) at least basic knowledge of the two scientific fields which shell be linked. The last part of this list is not only important to act as a link between two specialist researchers but also to identify processes necessary for the model. Therefore, it is desirable that the methods of ecological modeling get more space in the training of young biologists, and environmental scientists. Like in every modelling project, it is very important for such a link to develop an explicit question, which shell be addressed by the model. It's the purpose of the modeler, to be very certain about that point with the collaborating researchers from the other disciplines, since the question determines the relevant processes. In the current project, e.g. the necessity of the process of sporulation was discussed very intensively and seemed useless in the first chapters. However, in the last study (see Chapter 5), this process turned out to be crucial for the systems behavior. But when not paying attention to the relevance of a certain process/factor during the model development, the amount of processes can get overwhelming which can make the entire model useless, at least from the point of view of understanding.

6.4 Lessons learnt – P-use efficiency and buffer capacity mediated by AMF-plant-interaction

Phosphorus is nowadays used in many ecosystems as a fertilizer to promote plant growth. However, in many cases, it is also a fossil resource that will be depleted someday (cf. Wijkman and Rockström, 2012). Therefore, options to promote P-use efficiency are assessed and investigated throughout science and technology (e.g. Rengel 2013). Regarding this

question, also possibilities and limitations of using mycorrhiza as bio-fertilizer are highly under discussion (Berruti et al. 2015, Carvajal-Muñoz and Carmona-Garcia 2012). The results of this study point in the direction that AMF have the potential to largely enhance the efficiency of P-use because of two different mechanisms.

In ecosystems with pulsed P availability, AMF are potentially able to quickly take-up P-pulses in a way that reduces the loss of P due to leaching into ground- or surface waters. However, this mechanism largely depends on the AMF functional type. While AMF of the parasitic and intermediate functional type are very quick in P-uptake, those of the mutualistic functional type are not because of their slow C-supply. Therefore, AMF might help to reduce the loss of P-pulses imported into ecosystems. Depending on the AMF functional type, these pulses can be directly transported to the plant (intermediate functional type) or stored inside the fungal mycelium and converted into a steady flow of P to the plant (parasitic functional type). While this equalization might be desirable in natural habitats, it would be a problem in most agricultural systems, where high P availability at a specific time point is needed for crop development. If these functional types detected in the variety of artificial AMF would also be found in nature, the presented results would become very relevant for the development of biofertilizers. The selection of AMF could then be made in such a way that its functional type fits to the need of the system.

The second mechanism of AMF helping to promote P-use efficiency is an improved spatial exploitation of P in heterogeneous environments. With sporulation as a senescence mechanism, AMF are able to adapt their mycelium to the spatial and temporal conditions of the P distribution. So plants can use larger parts of the nutrients in their (below-ground) environment to develop above-ground biomass.

In conclusion, our model results indicate that AMF have the potential to largely enhance P-use efficiency by helping to reduce the leaching of P (and potentially other nutrients) into ground- and surface waters (quick uptake and storage of nutrient pulses) and by a very good spatial exploitation of P which might reduce the necessary application of the fertilizer.

6.5 References

Banitz, T. 2011. Modelling bacterial growth, dispersal and biodegradation: an experiment-based modelling study of the spatiotemporal dynamics of bacterial colonies, their

responses to dispersal networks, and their performance in degrading organic contaminants. Phd-Thesis, University of Osnabrück Germany 111 pp.

Berruti, A., Lumini, E., Balestrini, R. and Bianciotto, V. 2015. Arbuscular mycorrhizal fungi as natural biofertilizers: Let's benefit from past successes. Frontiers in Microbiology 6: 1559.

Boswell, G.P., Jacobs, H., Davidson, F.A., Gadd, G.M. and Ritz, K. 2003 Growth and Function of Fungal Mycelia in Heterogeneous Environments. Bulletin of Mathematical Biology 65: 447-477.

Boswell, G.P., Jacobs, H., Ritz, K., Gadd, G.M., and Davidson, F.A. 2007 The Development of Fungal Networks in Complex Environments. Bulletin of Mathematical Biology 69: 605-634.

Carvajal-Muñoz, J.S. and Carmona-Garcia, C.E. 2012. Benefits and limitations of biofertilization in agricultural practices. Livestock Research for Rural Development 24.

Grimm, V., Revilla, E. Berger, U., Jeltsch, F., Mooij, W.M., Railsback, S.F., Thulke, H.-H., Weiner, J., Wiegand, T. and DeAngelis, D.L. 2006. Pattern-oriented modeling of agent-based complex systems: Lessons from ecology. Science 310: 987-991.

Landis, F.C. and Frasier, L.H. 2007. A new model of carbon and phosphorus transfers in arbuscular mycorrhizas. New Phytologist 177:466-497.

Loreau, M. 2010 Linking biodiversity and ecosystems: towards a unifying ecological theory. Philosophical Transactions of the Royal Society B 365: 49-60.

Rengel, Z. 2013. Improving water and nutrient-use efficiency in food production systems. Wiley-Blackwell 320 pp.

Schnepf, A., Roose, T. and Schweiger, P. 2008 Impact of growth and uptake patterns of arbuscular mycorrhizal fungi on plant phosphorus uptake – a modelling study. Plant Soil 312: 85-99.

Schnepf, A., Jones, D. and Roose, T. 2011 Modelling Nutrient Uptake by Individual Hyphae of Arbuscular Mycorrhizal Fungi: Temporal and Spatial Scales for an Experimental Design. Bulletin of Mathematical Biology 73: 2175-2200.

Wijkman, A. and Rockström, J. 2012. Bankrupting nature – Denying our planetary boundaries. Routledge London and New York. 224pp.

Glossary

AMF	Arbuscular Mycorrhizal Fungi
C	Carbon
P	Phosphorus
BAS	Branched Absorbing Structures
C/P exchange strategy	Fungal strategy of nutrient exchange. A parasitic strategy is determined by low P delivery to the plant but high C uptake, a mutualistic strategy in return shows high P delivery with low C reward.
C/P exchange function	The function determining the C/P exchange strategy. A flat saturating function for mutualistic strategies and a steep saturating function for parasitic strategies.
C/P interface	The place at which the C/P exchange finds place. I.e. the place where the fungi growths into the plant.
K_m	The half saturation constant of the function determining the C/P exchange strategy. A low value results in a parasitic strategy, a high value in a mutualistic one.
C_{min}	The minimum rate of fungal C uptake, even without P delivery to the plant.
T_{max}	Time of simulation end.
C_{upt}	Fungal C uptake from the plant
P_{del}	Fungal P delivery to the plant

Figures

Tables

Acknowledgements

Nach einer Promotionszeit, die deutlich länger dauerte als ich erwartet hatte, möchte ich nun all jenen danken, die mich in dieser Zeit wissenschaftlich aber auch menschlich unterstützt haben.

Mein Dank gilt natürlich zu aller erst meinen Betreuerinnen Karin Frank und Karin Johst aus der ökologischen Modellierung und meinem mikrobiologischen Betreuer Thomas Fester. Karin Johst hat mit Ihrem unermüdlichen wissenschaftlichen Ideenreichtum und viel Enthusiasmus zum Entstehen dieser Arbeit beigetragen. Durch viele intensive Diskussionen und Hilfestellungen bei kleineren und größeren Problemen hat sie mich während meiner Promotionszeit immer unterstützt. Auch als ich schon lange nicht mehr am UFZ war hat sie mich durch kontinuierliches Nachhaken dazu gebracht, weiter an der Dissertation zu arbeiten. Vielen Dank dafür. Auch Karin Frank hat mich mit ihrer wissenschaftlichen Expertise immer unterstützt und das Entstehen dieser Arbeit durch viele Richtungsweisende Diskussionen voran gebracht. Selbst als ganz zum Ende meiner Arbeit, als ich das UFZ schon zwei Jahre verlassen hatte, mein Laptop den Geist aufgab haben sie mich von Leipzig aus unterstützt und mir dringend benötigtes Equipment zugeschickt. Beiden auch vielen Dank für das Korrekturlesen meiner Dissertation. Die konstruktive Kritik und vielen Verbesserungsvorschläge haben mir sehr geholfen.

Thomas Fester hat mir mit seiner mikrobiologischen Expertise vor allem während der Modellentwicklung sehr geholfen. Durch die Laborarbeiten die von Frank Zielinsky geplant und mit Hilfe von Sybille Mothes und Elke Schulz in seiner Arbeitsgruppe umgesetzt wurden konnte ich viele Erkenntnisse während der Modellentwicklung ziehen.

Herzlich danken möchte ich auch Andreas Thiele, für seinen Einsatz als Retter in der Not, als mein Laptop aufgab und viele Daten schon verloren schienen. Weiterhin danke ich Gabriele Nagel für ihre administrative Unterstützung, Michael Müller für seine Unterstützung während der Modellentwicklung und für viel Spaß bei mehreren Winterschulen in Leipzig und Sevilla sowie allen Mitarbeitern der Abteilung Ökologische Systemanalyse des UFZ, vor Allem Rico, Sebastian, Franziska und Thomas für ihre Gesellschaft während der Arbeit und das Teilen der Höhen und Tiefen im Leben eines Doktoranden.

Zum Schluss geht mein Dank natürlich an meine Frau und meine Kinder, die vor allem nachdem ich das UFZ verlassen habe viel zu oft auf ihren Mann und Papa verzichten mussten damit diese Arbeit fertig werden konnte. Ich danke euch dafür dass ihr meine Launen ertragen habt, mir den Blick auf das wirklich wichtige im Leben gelenkt habt und mich immer wieder motiviert habt weiter zu machen. Auch danke ich meinen Eltern und Geschwistern die mich immer unterstützt und an mich geglaubt haben. Nur damit mein Vater endlich aufhört mich mit seiner Flasche „Barolo“ zu nerven ist diese Dissertation überhaupt fertig geworden.